A Three-Dimensional Model of the Light Regime in an Avocado Orchard

Research Thesis

Submitted in Partial Fulfillment of the Requirements for the Degree
of Master of Science of Agricultural Engineering
(Water, Soil and Environmental Engineering)

Matan Hadari

Submitted to the Senate of the Technion – Israel Institute of Technology
Shvat, 5765 Haifa October, 2004

The Research was done under the Supervision of Dr. David M. Broday and Prof. Benjamin Zur from the Faculty of Civil and Environmental Engineering, and Dr. Guedi Capluto from the Faculty of Architecture and Town Planning.

The guidance and assistance of Dr.Gad-Ish Am is Gratefully Acknowledged

The Generous Financial Help of the Technion is Gratefully Acknowledged

Table of Contents

Figures list

Tables:

Abstract

One of the major limiting factors in agricultural production in general, and in Avocado orchard in particular, is the availability of solar radiation in the wavelengths relevant to photosynthesis (400-700nm) at different canopy regions. The dense and vigorously growing Avocado canopy, if not managed correctly, results in large sized trees that tend to shade themselves and the neighboring trees. Insufficient light in Avocado orchards has been observed to reduce fruit yield, deteriorate its quality, and allocate it at the top of the trees. Various canopy management strategies were devised during the years, based mainly on the growers intuition and on 'thumb rules' adopted from work done on apples during the 70`s and the 80`s. Most of these practices, however, were not supported by quantitative measurements or simulation models. The progress in computer software and hardware enables us to inspect the dynamics of solar radiation, and to calculate light interception and penetration for a large variety of canopy management strategies. The model presented here uses the state of the science illumination software 'Radiance', complimented by an additional code enabling simulation results (radiation readings) to be collected and analyzed over the whole growing season. Since 'Radiance' is originally meant for architectural purposes (mainly for internal illumination), it holds the ability to deal with complex shape models produced by commercial software (AutoCAD, 3DMax, etc.).

Field measurements of light intensity were conducted in a commercial Avocado CV. 'Hass' orchard in kibbutz 'Shomrat', Israel. The measurements were found in good agreement with model predictions of light intercepted at the canopy surface, and used for calibrating the code regarding the extinction of light within the canopy. In particular, a large number of measurements was conducted in order to gain better understanding of the attenuation of light as it penetrates into the Avocado canopy. Numerous orchard models were tested in order to examine various agrotechnical practices that can effect light interception. We aimed at three major goals: maximizing the total intercepted radiation, maximizing light intensity (PPF), and maximizing the total radiation at the lower 2 m of the canopy. For that purposes, results indicate that the tree height should be reduced and that trees should be pruned at a sharp angle. However, the intercepted light does not provide clear cutting outcomes as for which practice is superior, and a new concept – the

‘potentially productive canopy volume’ (PPCV), was introduced. The PPCV is defined as the volume maintaining a threshold level radiation for a given exposure time. The extinction coefficient measured in the field has been adopted for use by the software by means of a material (‘mist’) with favorable extinction properties. Thus, it enabled us to analyze the penetration of solar radiation into the canopy. The results of the PPCV analysis indicate that maintaining high PPCV for long times is possible in the high density small-tree orchard.

According to our simulation results, high density planting seems to be a promising practice for maintaining most of the canopy potentially productive for long times, thus producing fruits (income) at high efficiency.

Symbols:

ρ_f- Foliage density [m^2 leaf*m^{-3} canopy]

h- Planck constant [$6.626*10^{-34}$J*s]

C - Speed of light [$3*10^8$ m/s]

E – Energy carried by a photon of light [J]

I - Transmitted light intensity [μmole/m^2/s or W/m^2]

I_o - Incident light intensity [μmole/m^2/s or W/m^2]

k – Radiation Extinction coefficient [1/meter]

K_c – LAI coefficient [-]

$K_{Radiance}$- Light extinction coefficient minimizing the RMSE between 'Radiance' simulations and field data

L - Leaf area index [m^2 canopy/m^2 land]

N_0 – Avogadro number [$6.02*10^{23}$ molecules/mole]

PAR - Photosynthetically active radiation (Radiation with wave length of 400-700nm) [μmole/m^2/s or W/m^2]

PPF- Photosynthetic photon flux [μmole/m^2/s]

S – Distance the photons travel through the canopy [m]

α - Absorptivity of individual leaves for the specific waveband of interest [%]

λ – Wave length [m]

τ - Transmisivity, relative light intensity [I/I_0]

Terms:

Azimuth –α [degree] –The angle between the projection of the normal of a surface onto the horizontal and true north. Measured clockwise

CIE Clear Sky A clear sky assumes that the Sun is visible, resulting in a very non-uniform luminance distribution where the area around the Sun is much brighter than any other area. The CIE Clear Sky model relates the irradiance (I) at any point in the sky vault with the zenith luminance (Iz)

$$\frac{I}{Iz} = \frac{(0.91 + 10.0 \cdot e^{-3k} + 0.45 \cdot \cos 2(k))\,(1 - e^{-0.32\sec(z)})}{(0.91 + 10.0\, e^{-3zs} + 0.45 \cdot \cos 2(zs))\,(1 - e^{-0.32})}$$

where *k* is the angle (in radians) between the point with luminance *I* and the Sun, *z* is the zenith angle of the point and *zs* is the zenith angle of the Sun.

ELADP-Ellipsoidal leaf angle distribution parameter.

Elevation angle - γ [degree] –The altitude angle above the horizon of a point in the sky hemisphere.

Irradiance - [W/m^2] - Quotient of the radiant flux ($d\phi_\varepsilon$) incident on an area element of the surface (dA).

Latitude [degree] -The angular distance north or south from the earth's equator measured through 90 degrees. The latitude is taken positive in the northern hemisphere.

Longitude [degree] - The arc or portion of the earth's equator intersected between the meridian of a given place and a reference meridian (usually the one from Greenwich, England). The longitude is taken positive east of the Greenwich meridian and negative west of the Greenwich meridian.

Radiant flux $-\phi_\varepsilon$ [W] – The power emitted, transmitted or received in the form of radiation.

Reflectance – The ratio of the reflected radiant to the incident flux in the given conditions. The reflectance is also called the albedo for a radiant flux.

Zenith angle - z [degree] – The angle between a point in the hemisphere and the vertical $z=\pi/2-\gamma$.

1 Literature review

1.1 Light interception and photosynthesis of tree canopy

The connection between increased light interception and yield has been studied intensively, especially in apple orchards. Dry matter production as well as various parameters dealing with quality and quantity of fruits were reported to have an empirical relationship with the amount of light falling on the orchard (Barritt, 1989; Barritt et al., 1991; Wunsche et al., 1996). However, the agreement was better for the primary biomass production than for the fruit yield, due to the additional parameters affecting the yield (Palmer, 1999).

Full canopies of orchard crops intercept only 65% to 70% of the available radiant energy, thereby creating an upper limit to the production potential (Jackson, 1980). It appears that maximum photosynthetic rate occurs when leaves are exposed to at least 0.3 of the full sunlight intensity (Heinecke, 1966). The fraction of the total sunlight intensity mentioned above is evidently not always adequate for the normal development of vegetative and reproductive buds. Palmer (1977) found that flower-bud differentiation in apple trees is more sensitive to shading than vegetative growth. Heinecke (1966) reported insufficient coloring of apples when the light intensity was below 0.4 and when it was lower than 0.5 fruit size was adversely affected. Jackson (1978) confirms that high light interception is a prerequisite for maximal yield, whereas shading causes a reduction in flower-bud formation, fruit size, and fruit color. In Florida, rejuvenation of crowded Avocado orchards as a result of topping and tree removal, proved to be successful. Although the orchard was less dense (130 trees ha^{-1} instead of 276 trees ha^{-1}) and the tree height was reduced to 4.8m, the yield increased from 6.9 t ha^{-1} to 19.8 t ha^{-1} (Crane et al., 1992). The result from this experiment emphasized the great importance of light interception, since it is the main reason for the increase in yield.

Reports from South African Avocado pruning trials (Stassen et al., 1999) showed improvement in the yield from pruned hedgerows. The yield response to pyramid shaping and lowering of the tree height was considerable. Both practices aimed at increasing the light intercepted by the hedgerow. The pyramidal shape improved canopy-sun grazing angle and the height lowering prevented inter-row shading. In a pruning trial aimed at testing the effect of lowering the height of Avocado trees (Thorp and Stowell, 2001),

trees were pruned down to 4 and 6 meters and fruit yield was collected from various heights. Reducing tree height resulted in a shift in the location of most of the Avocado fruits. The same amount of fruit previously found in the 4-6 m height layer in the 6m high trees was found in the 2-4 m height layer in trees pruned to 4 m height. In a research done in New Zealand the harvest quality of fruit exposed to sun was compared with that of completely shaded fruit. Significant differences were found between the two fruit types and between the different sides of fruits exposed to sun. Namely, fruits exposed to sun had higher dry matter and higher levels of potassium, calcium, magnesium and oil (Woolf et al., 1999).

1.2 The Avocado's response to light

Due to its rain forest origin, characterized by competition for light, the Avocado (*Persea americana* Mill.) tree have a natural vegetative bias towards greater allocation of photo-assimilates to shoot growth than to reproductive organs (Schaffer and whiley, 2002). This vegetative bias results in rapid production of short-lived leaves and increased shading of the canopy, thus reducing the number of well-lit terminal shoots capable of flowering (Schaffer and Whiley, 2003). The growth of Avocado reproductive organs consumes large amounts of energy, which is then being stored. Indeed, CV. Fuerte fruits with 17% oil content and a flesh-to-seed ratio of 4:1 (fresh mass) store Energy equivalent value of 8 GJ ton^{-1} compared to 2.9 GJ ton^{-1} for Valencia oranges and 2.6 GJ ton^{-1} for apples. The leaves can also store large amounts of carbohydrates and minerals, with episodic growth flushes resulting in leaves of varying age and photosynthetic efficiency (Wolstenholme, 1987). It is generally agreed that the low yielding potential of Avocado orchards is due to two main factors: the high oil content of the fruit (oil is 2-3 times more energy-expensive than carbohydrate) and the large seed with its concentrated food reserves (Wolstenholme, 1987).

1.3 Light measurements in Avocado leaves and trees

PAR (photosynthetically active radiation) is defined as the radiation in the 400 to 700 nm waveband, representing the portion of the spectrum that plants use for photosynthesis.

Within the plant canopy, radiation levels can vary from full sun to almost no direct light within few centimeters. Therefore, reliable measurement of PAR requires many samples at different locations within the canopy. The photosynthetic active radiation (PAR) is defined in terms of photon (quantum) flux, i.e. the number of moles of photons in the radiant energy between 400 nm and 700 nm. The reason for using quantum rather then energy flux results from the greater importance of the amount of photons intercepted rather than the total energy, in the photosynthetic reaction equations. The *Photosynthetic Photon Flux* (PPF) - the photon irradiance - is expressed in moles per square meter per second. One mole of photons is also known as an *Einstein*.

1.3.1 Photosynthetic response curve

Though not many experiments were conducted trying to find directly the relationship between light interception and penetration and the tree yield, due to the difficulties involved, a few experiments were held in order to create the *photosynthetic response curve* of the Avocado. This curve depicts the photosynthetic response to varying intensities of light, as measured by CO_2 consumption. The photosynthetic response curve is a 'second order curve'. First, the rate of photosynthesis is determined from the linear section of the CO_2 concentration vs. time curve. Then, rates corresponding to different light intensities are used to plot the photosynthesis vs. light intensity curve. The assimilation rate is measured under a range of light intensities, with the latter being changed by incorporating filters or shading nets.

1.3.1.1 Light saturation point

At a particular light intensity, the so-called *light saturation point*, the rate of CO_2 assimilation levels off. Any further increase in the amount of incident light does not cause an increase in the rate of photosynthesis. Therefore, as light intensity increases beyond the saturation level, light is no longer the limiting factor in the overall photosynthetic process. Above the light saturation point the photochemical reactions produce more ATP and NADPH than can be used by the (non-photochemical) fixation of CO_2. The *saturation point* is typical mostly to illuminated leaves. Shaded old leaves stay below that level of light most of the day. They also have a different photosynthetic potential due to the difference in their thickness and the amount of chloroplasts. The light

saturation point is defined in terms of the saturation light intensity (PPF_{max}) or the maximal CO_2 assimilation rate - A_{max}.

The light saturation point of single leaves from container grown 'Fuerte' trees (Scholefield et al., 1980) was found at PPF_{max} = 400-500 μmole $m^{-2}s^{-1}$. For full container-grown trees a saturation point of PPF_{max} = 660 μmole $m^{-2}s^{-1}$, or 33% of full sun light on clear sky sunny day in Israel, has been reported (Bower, 1978). The higher saturation level of full trees is the result of the fact that as light intensity increases, more and more shaded leaves approach their saturation point. Field measurements in an Australian orchard (Whiley, 1994) revealed a saturation point of PPF = 1100 μmole $m^{-2}s^{-1}$. This high value may represent a higher fraction of shaded leaves. Moreover, it was suggested that the higher light saturation point observed in field-grown trees may have been a result of root restriction in container-grown trees, which limited net photosynthesis to about 7 μmol CO_2 $m^{-2}s^{-1}$ as compared to 23 μmol CO_2 $m^{-2}s^{-1}$ for orchard trees (Wolstenholme and Whiley, 1999).

1.3.1.2 Light compensation point

When extrapolated to lower intensities, the light response curve does not pass through the origin. The light intensity through which the curve intercepts the *x* axis is called the *light compensation point*. At light levels below this value there is no net CO_2 assimilation. Processes, such as cellular respiration, cause uptake of O_2 from the air, yet under sufficient light conditions the rate of photosynthesis greatly exceeds that of O_2 uptake and a net release of O_2 to the atmosphere is evident. However, under very low light conditions the amount of O_2 consumed exceeds that produced by photosynthesis and no net O_2 formation is evident. The light compensation point measured in Avocado leaves is very low. Values of 10 μmol $m^{-2}s^{-1}$ were measured in a 'Hass' orchard (Whiley, 1994). In another work (Wolstenholme and Whiley, 1995) the compensation point was determined at 30 μmole $m^{-2}s^{-1}$. These low values are indicative of shade tolerance characteristics, an important feature in the Avocado's native origin as gap-colonizer in dense forests (Scholefield et al., 1980). In an orchard environment, however, the low compensation point can be a disadvantage, since less-productive leaves, sustained at low light levels, may increase the overall shading (Wolstenholme and Whiley, 1999).

1.4 Planting strategies in Avocado

The basic idea behind any orchard design is harvesting the sun in the most effective way to produce economic yield. The design of an orchard should optimize light interception over the crop life span, and maximize yields and yield stability (Whiley, 2002). The planting strategy depends largely on factors such as land value, topography, drainage and availability, and cost of labor and machinery. Square planting of Avocado orchards was normally practiced until very recently. Large spacing of 10m x 8m and 12m x 9m (92-120 trees/ha) was practiced where land was not limited. This planting method results in large trees with small fruits. Medium density orchards of 7m x 6m (238 trees/ha) are practiced with timely removal of a diagonal row, preventing the orchard from closure (Whiley, 2002). Another technique for reducing the orchard's self-shading is 'stag-horning' or the reduction of the trees to 1m height when they reach a height of 10m. These methods of thinning the orchard work for a short time, after which the trees fill the gaps and diminish the effect of thinning or stag-horning (Snijder et al., 2000).

1.4.1 Hedgerow planting

The use of mechanical pruning equipment and the practice gained from other orchard crops (apple, mango) lead to the establishment of the hedgerow method in Avocado orchards. The planting method became rectangular over the years, giving the hedgerow a distinct direction, preferably a North-South direction. The space in between the hedgerows is maintained in order to enable spraying, pruning and picking activities as well as improved light interception. The hedgerow is mechanically pruned, at least twice a year, and re-growth is delayed through the use of growth retardants. The constant annual pruning of the row can create a 'solid' opaque wall, and therefore periodic strategic limb removal is needed (Whiley, 2002). Snijder et al. (2000) showed that Avocado trees could be trained into a *central leader*, giving the hedgerow a pyramidal geometry. These trees give rise to higher initial yields, since tree size and light interception and penetration into the tree could easily be maintained. A set of pruning strategies for different canopy crowding scenarios was also suggested. The single leader pruning practice can allow a higher planting density as recommended by Stassen (1999, see Table 1).

Table 1- Recommended plant spacing for Avocados under normal management situations (Stassen, 1999).

Cultivar	Spacing	Trees per hectare
Fuerte	7.0 m x 3.5 m	408 trees/ha
Hass	6.0 m x 3.0 m	556 trees/ha
Pinkerton	5.0 m x 2.5m	800 trees/ha
Ryan	5.5 m x 3.0 m	607 trees/ha
Edranol	5.0 m x 2.5 m	800 trees/ha

Razeto et al. (1992) studied the effect of planting density on Avocado yield. In their field trials three planting densities were tested: 6x6m, 5.5x3m, and 4x2m (corresponding to 278, 606 and 1250 trees/ha, respectively). Yield per tree was proportionally affected by the planting density. However, yield per hectare grew as the density increased. The yield per tree as well as other factors such as individual fruit weight and oil content was higher as the spacihng between the rows increased.

1.4.2 Ultra high density planting

A new method for increasing yield, practiced in growing number of locations, is the ultra high density planting method. This practice takes advantage of the appearance of precocity (early bearing) and juvenile vigor of young Avocado trees (Hofshi, 1998). Under this practice trees are 2-3m tall and are trained to a single central leader, creating cylindrical or conical tree geometry. Hofshi's recommendations for planting density are 2.25m x 2.25m (1975 trees/ha) for upright varieties such as 'Reed', 'Lamb Hass', and 'Gwen', and 3m x 3m (1111 trees/ha) for 'Hass' (Hofshi, 1999a). This square planting is favorable especially in hilly terrains due to drainage and irrigation restrictions. Another motivation for keeping the trees small is the savings in picking labor and machinery costs.

A hedgerow version of high density planting, 1.5m x 4m (1667 trees/ha), was demonstrated by Stassen (1999) in S. Africa. The ultra high density orchard is expected to close down within 7-10 years, and therefore there is a need for continuous canopy

management to keep the tree in its cylindrical shape, and for selective tree removal after the orchard becomes overcrowded (Hofshi, 1999a). Stassen (1999) claims that when well managed and pruned, the high yield potential of ultra high-density orchard can be maintained for 20 years or more.

1.4.3 Pruning

The development of pruning and canopy management is a relatively new field in Avocado growing. The first stages of its development were done on the basis of trial and error. For many years, growers assumed that the Avocado tree does not need a systematic annual pruning. Intervention in the vigorous healthy growth cycle of fruit bearring material seemed unnecessary and harmful. Shape-giving pruning was used mainly in seedlings, to get more branching in types with distinct axial growth (“Reed”, “Bacon”, “Etinger”), or to prevent over branching in cultivars with no axial growth (“Wurtz”, ”Fuerte”) (Bergh and Lahav, 1996). In pruning trials done in Israel (Lahav et al., 1971), it was found that by controlled pruning rejuvenation and enlarged fruit sizes can be achieved in mature trees and branches. The continuous increase in canopy volume and the gradual canopy closure in 20-30 year old orchards, and the trees' growth to considerable heights, made picking and spraying difficult, costly, and even dangerous at times (Hofshi, 1999b). The overcrowding of the canopy created a dense closed orchard, with limited light interception. There are a number of citations in the literature suggesting that light deficiency typical to overcrowded canopies caused reduced yields and a tendency of the fruits to be located at the top of the tree (Bender and Faber, 1999; Thorpe, 1999; Zilberstaine and Kalusky, 1999; Whiley, 2002). Mechanical pruning came hand in hand with the hedgerow planting development. The relatively cheap and fast mechanical pruning proved useful in maintaining the hedgerow confounded to a preplanned geometry, and also created rejuvenation in the canopy. One disadvantage of this method is the creation of a near opaque ‘walls’ limiting light penetration into the canopy. South African pruning trials (Stassen et al., 1999) demonstrated increased yields in hedgerows pruned to pyramid geometries and reduced tree height.

Another way of changing the vegetative bias of Avocados is by using growth regulators such as paclobutrazol (Adato, 1990), which control the vegetative growth while fruit retention may increase. In established orchards, application of paclobutrazol

could delay crowding whereby tree removal is postponed and production per hectare increased (Kohne and Kremer-Kohne, 1987). Stassen et al. (1999) concluded that there is a need for a combination of canopy management practices (selective and mechanical pruning, cincturing, and growth inhibitors) in order to maintain a high yielding pyramidal shaped high-density orchard. A method of gradual selective leaders removal has been devised in Israel (Zilberstaine and Kalusky, 1999; Thorp and Stowell, 2001), which is based on removal of a limb every 1-2 years after picking and clearing the working line. The removal of the limb enables better light penetration into the midst of the canopy and promotes juvenility. The disadvantage of this method is the need (and cost) of professional and experienced pruning personal.

1.5 Light interception models

The dependence of agricultural productivity on solar radiation is being investigated since the beginning of modern agricultural research. Several books (Monteith, 1973; Ross, 1981; Myneni et al., 1989) and review articles (Jackson, 1980) have been published. Most of the work done during the 70`s and 80`s dealt with field crops, which can be represented by a continuous two-dimensional geometry. For field crops, much attention was given to light penetration into the canopy. The leaf area index (LAI) concept, i.e. the ratio between the total one-sided leaf area and the ground covered by the canopy, was introduced in order to facilitate the use of the Beer-Lambert law of exponential dissipation of radiation through resistive media. The basic equation, still in use in many models, is (Monsi and Saeki, 1953)

$$I = I_0 \exp(-k \cdot L) \qquad (1)$$

where I and I_o are the transmitted and incident light intensities, respectively, L is the leaf area index, and k is the extinction coefficient. Since the canopy in orchards is discontinuous and therefore three-dimensional, the integrated vertical LAI concept used in filed crops is not applicable for orchards. For example, a very tall columnar tree could have high vertically summed LAI but the light at different points within its canopy will be more dependent on the path length from its envelope than from its top, i.e. the vertically summed LAI (Jackson, 1980).

Various attempts to model and mimic the radiation balance in apple orchards were done over the years (Jackson and Palmer, 1972; Palmer, 1977; Palmer and Jackson, 1977; Palmer, 1980). These models used a range of opaque hedgerows models to examine different tree geometries in various configurations (Cain, 1972; Jackson and Palmer, 1972). These solid models showed that light interception is largely dependent on the proportion between the ground directly covered by the canopy, and the height of the hedge. The conclusions from these studies were that slanted hedgerow surfaces could give a better distribution of light along the canopy surface than in a vertical hedgerow. In fact, Cain (1972) predicted that optimal light distribution would be achieved in a hedgerow trimmed at 20^0 with a tree height twice the width of the clear alley. In addition, for N-S planted rows the distribution of intercepted light would be better than that of E-W planted rows. Palmer and Jackson (1972) predicted an increase in light interception with increasing height of pyramidal tree geometry. Other issues examined were the change in time of growth parameters, such as LAI (Palmer and Jackson, 1977) and shape factors, such as spacing and row orientation (Palmer 1980), on light interception. These studies are the basis of modern orchard training systems, but due to the limits in computation power at the time, these models were based on numerous simplifications, such as neglecting ground reflections, etc. Palmer's studies were extended to include a growth model, predicting the transformation of light interception into total biomass production. Results of this model suggested that solar radiation is the main limiting factor in canopy growth (Friday and Fownes 2001).

A computerized model mimicking the structure of a peach tree showed a great sensitivity of photosynthetic activity to shading and to the canopy density (Genard et al., 2000). A model for light penetration into canopies of citrus trees was developed in Israel (Cohen et al., 1987). The model accounts for various parameters, such as leaf inclination distribution, LAI distribution, gap frequency, and growth model. The rows of trees in the model were divided into small cells for which light intensity has been calculated. The intensity of photosynthetic activity has also been modeled. The researchers concluded that: (1) the highest photosynthetic activity would occur for maximal LAI, (2) rows with slanted "walls" did not show the highest overall photosynthetic activity but had better light penetration, (3) little effect of row orientation was observed, but there was an

advantage to N-S rows in light distribution, and (4) significant water saving can be achieved by reducing the orchards height to a value as low as 3 meters.

A two-dimensional model for estimating solar radiation interception and penetration was presented by Annandale et al. (2004). The model simulates solar interception by representing the trees as ellipsoids standing on bare stems, and so the morphological data needed to model the tree are the ellipsoid parameters, the bare stem height, and the leaf area density. The authors report good agreement between model results and field measurements. The model uses a revision of the Beer- Lambert law for light penetration into canopies

$$\tau = e^{-0.5\rho_f S\sqrt{\alpha}} \qquad (2)$$

where S is the depth the radiation travels through the canopy, ρ_f is the foliage density (m^2 leaf m^{-3} canopy), and α is the absorptivity of individual leaves for the specific waveband of interest. Assuming constant foliage density and constant absorptivity, the extinction of light is exponential with the penetration width. This concept is utilized in our model as well. The limitations of these elaborate and sophisticated models is in the complexity regarding their operation and the parameters needed to be inputted, many of them are difficult to acquire. This limits the practical implementation of these models.

1.6 Summary

Increasing interest in canopy management and its implications on 'light harvesting' is evident in the Avocado scientific and applied literature over the last decades. Most of the practices and orchard management philosophies are based on the extensive work done on apples from the early 70`s by researchers like Jackson, Palmer, Lakso, and others. Though general in their nature, studies on light management in apples take into account practices and constrains relevant to apples. In general, most of the work on canopy management of orchards dealt with planting density and direction and with tree geometries. An increase in the overall light interception was predicted with the increase in planting density, but insufficient data made it impossible to quantify the relationship. Much less attention was given to the fate of the intercepted radiation as it penetrates into the canopy volume. In addition, very limited information is available in the literature

regarding the relationship between the distribution of the penetrating radiation and the total yield of Avocado fruits. Simulation models mimicking interactions between canopy management parameters, intercepted radiation, light penetration, and yield components could contribute to an improved design and practices of light management in Avocado plantations.

1.7 Objective

The general objective of this project is to develop a simulation tool capable of mimicking the dynamics of the light regime in an Avocado orchard as a function of canopy-light interaction parameters and agronomic practices. This model is to be used for the design of new orchard architectures and for evaluation of new and existing tree geometry, planting density, and row orientation for a range of geographical locations, seasons, and time of the day. Thus, the model needs to be modular and to support complicated geometries imported from standard commercial drawing software.

Specific objectives include:

1. Construction of the model.
2. Study the effect of various geometric parameters, such as tree height-to-row width ratio, pruning angle etc, on light interception.
3. Investigation of light penetration into the Avocado canopy, in selected orchard geometries.
4. Drawing of general recommendations for canopy management to improve light interception, penetration, and distribution.

2 Methods & Materials

2.1 Field measurements

Light intensity measurements were taken in two separate occasions: in the beginning (June) and the end (September) of the Israeli growing season. These measurements are the basis of our modeling and understanding of the light behavior in Avocado canopies.

2.1.1 The measuring system

Light intensity was measured using the "SunScan" system (Delta-T, Cambridge, UK). This system is made up of 3 elements:

1. ***SunScan probe*** - A linear array of 3 probes, each is 1 meter long and contains 64 equally spaced photodiodes - resulting in a 3 meter long probe with 192 sensors. The probe handle contains batteries and electronics for converting the photodiode outputs into digital photosynthetic active radiation (PAR) readings, which are sent to the Data Collection Terminal via a RS232 link.
2. ***Beam Fraction sensor*** - The Beam Fraction sensor (BFS) measures PAR levels and is used to monitor the incidence angle of the light on the canopy boundaries. The BFS incorporates two photodiodes. One can be shaded from the direct solar radiation by a shade ring, which allows the direct and diffuse components of the PAR to be measured simultaneously. This is necessary for the computation of the leaf area index (LAI). The BFS uses an array of photodiodes with a unique computer-generated shading pattern to measure incident solar radiation. A microprocessor calculates the global and diffuse components of the radiation and determines the radiation levels. Two analogue voltage outputs are provided for the global and diffuse radiation.
3. ***Data Collection Terminal*** - To observe and store readings from the SunScan probe, a Data Collection Terminal (a Psion Workabout) is used. The Workabout is a lightweight, robust field unit with a full alphabetic keyboard for the annotation of readings.

Figure 1 - The beam fraction sensor (left), and the ‘grid pole’ held by Prof. Zur (right).

Figure 2 – The BFS held by Dr. Broday coupled with the SunScan probe (left) during measurements of light intensity in different heights, using a ‘cherry picker’.

2.1.2 Canopy and ground reflectance

One of the basic parameters in the model is the canopy and ground reflectance. The reflectance was measured by measuring the incoming solar radiation by leveling the measuring pole on top of the canopy at about the solar noon, and then measuring the outgoing radiation by leveling the pole at the same point facing the canopy. The ratio between the incoming and outgoing PAR is the reflectance. At each point 3-5 measurements were averaged.

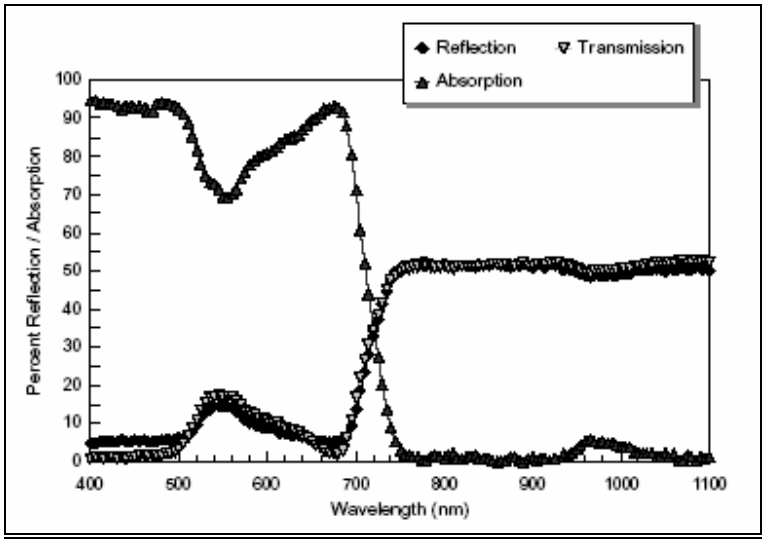

Figure 3 – Reflection, absorption and transmittance at various wavelengths for Avocado leaves (Heath et al., 2001).

2.1.3 Intercepted light measurement

An incremental measurement of light along the outer boundaries of the canopy were taken in a well pruned row during the 15th of September 2003 and the 8th of June 2004, in order to evaluate the numerical results of the simulation and to parameterized the code to closely match the true conditions found in the field. Accuracy requirements for different parameters used by the model, such as ambient conditions, geographical information, etc., were assessed.

Light interception over the canopy envelope was measured at kibbutz Shomrat orchard by positioning the 3-meter long measuring pole (see figure 4) along the canopy's outer envelope (the hedgerow outer "skirt"), starting at a height of 1m. The measurements were taken in 10-20 minutes intervals between 10:00 and 14:00, allowing

the probe to be exposed to both direct and diffused sun light. In parallel, we simulated light interception under conditions similar to the orchard design and after implementing in the code the reflectance of the Avocado canopy, obtained as described above. The measurements were averaged along the pole, and compared to the simulation results.

Figure 4– The intercepted light measurement set up (‘Shomrat’ orchard; cv. Hass).

2.1.1 Light penetration into the canopy

In order to better understand the behavior of light penetrating into the canopy, light intensity measurements were taken in the depth of the canopy. The measuring method was based on a method devised by a team lead by Dr. Moshe Meron (Meron et al., 2001). The measurements were taken on June and September 2004 at a full grown (6-7m height) ‘Hass’ Avocado orchard, planted at N-S hedgerows in a 7x6m grid and pruned at various strategies. Measurements were done using the SunScan probe coupled with the BFS and connected to the data collection terminal. A 7.5 m pole with shoulders evenly spaced every 0.5 meters (see Figure 1) created the measuring grid, enabling a measurement at fixed intervals. The pole was placed close to the morphological center of the tree and the SunScan probe was placed on its shoulders so that its tip is at the row center. The probe was then leveled and a reading was taken and logged on the data logger. The measurements were taken from bottom to top, thus yielding a ‘half-tree-cross section’.

This procedure was repeated every 1 meter along the row, and on both sides of the hedgerow.

At the analysis stage, the results were normalized by dividing them by the total solar radiation measured by the BFS - yielding the fraction of solar energy at each sensor. Readings from each sensor were multiplied by a specific calibrating factor. The calibration factor was obtained by taking 3 consecutive readings in a fully exposed area by a perfectly leveled measuring pole and comparing the average (per sensor) with a benchmark reading, obtained by the external BFS sensor. Data were exported to a PC and iso-luminance contours were plotted using Surfer v.8 (Golden Software, Golden, CO) by applying the "*natural neighbor*" interpolation method. The *natural neighbor* interpolation algorithm uses a distance-weighted average of the neighboring observations, but does not extrapolate contours beyond the convex hull of the data locations. The contour of the 95% level of the external radiation was considered the tree outer contour.

2.1.4 Evaluating the physical extinction coefficient

The extinction coefficient *k* was evaluated according to the following method:

- Measurements around the solar noon at the central 50 cm of each tree's cross section were selected (see Figure 5).
- The results were aligned, in order to create a rectangular array.
- A graph of relative transmitted light vs. distance was plotted per day and per tree face. A regression was performed on the data points for the various days and canopy architecture, from which extinction coefficients were extracted.

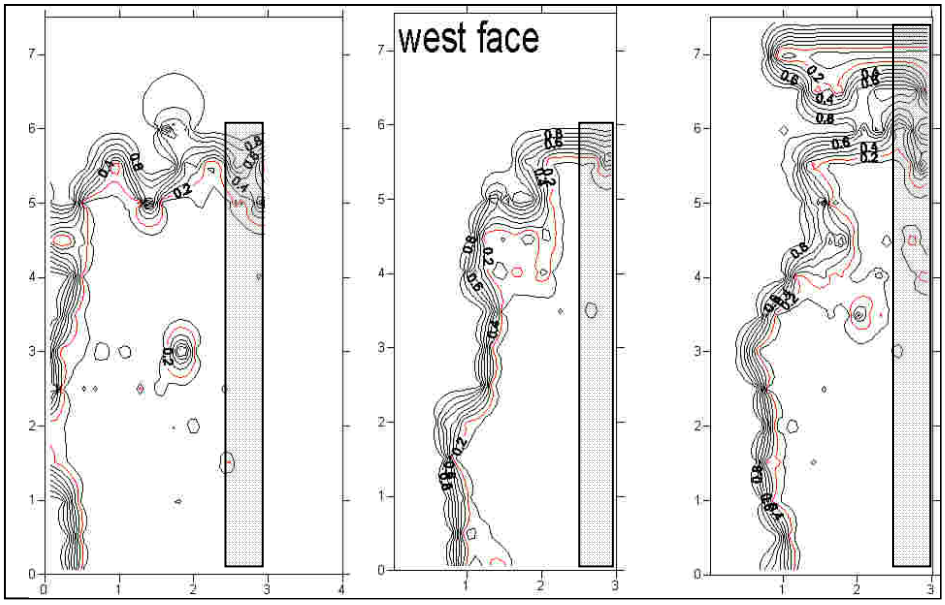

Figure 5 – Canopy cross section with the part used to obtain the "$K_{physical}$ "

The extinction coefficient was calculated using the Beer-Lambert model. In this study we use a simplification of Norman and Campbell's (1983) model, which was evaluated in the field (Annandale et al. 2004). Thus, assuming a constant foliage density and constant absorptivity, eq. 2 can be written as

$$\tau = e^{(-k' \cdot S)} \tag{3}$$

where S is the width the radiation travels through the canopy, and $k`$ is the extinction coefficient. In this form, the extinction coefficient can be used as a parameter of light scattering within "Radiance".

2.1.5 The Potentially productive canopy volume concept

Assessing the light falling on the tree envelope may be valuable, but can be misleading as well. The amount of radiation intercepted on the envelope of the top canopy layer of a pyramidal shaped hedgerow, for example, would be higher than that intercepted by the lower parts, but would hold less canopy volume behind it. It is reasonable to assume that due to the high energetic requirements of fruit bearing in Avocado, fruits would be located in canopy volumes exposed to high levels of PAR for relatively long daily hours. This assumption is supported by the observations of fruit location at the tree tops. Furthermore tree canopy is not an opaque matter but transmits light through gaps in canopy or as a result of leaf movement in the wind. This transmittance enables leaves not lying at the tree outer envelope to be photosynthetically active, and should be taken in consideration when yield optimization is sought.

This calls for modeling of light extinction through the canopy - from the external level down to a level where the light intensity is not enough to produce substantial photosynthetic response. The goal of maximizing the canopy volume which is above the light saturation point for prudoctive photosynthesis was presented in a few works in the past (Wolstenholme and Whiley, 1999; Whiley, 2002; Schaffer and Whiley, 2003). Assuming that most of the fruit production is located at the volume of canopy receiving PAR at a level above the saturation level for photosynthesis enables us to refer to this volume here as the *Potentially Productive Canopy Volume (PPCV)*.

The correlation between greater radiation levels and greater yield was discussed above. Hence, a greater potentially productive volume per orchard area is a proxy of greater yield per area, which is the ultimate goal of crop growing. Clearly, this is true as long as light is the only limiting factor and other factors, such as irrigation, nutrient supply etc. are fulfilled. Similarly, this work is not aimed at investigating the physiological affect of various pruning methods apart from its contribution to light interception. Assessing the potentially productive canopy volume can point to those parts of the tree which are expected to be non-productive. These parts do not take part, or take a small part, in the photosynthetic process (maintaining at most respiration and growth) and can be referred to as "parasitic" with respect to fruit bearing - taking valuable inputs such as water and nutrients but not contributing to considerable valuable dry matter production.

2.1.6 Assessing the canopy LAI

A by product of measuring the dissipation of light as it penetrates the canopy is an estimation of the cumulative LAI (expressed in m^2 leaves area/m^2 of covered ground). Though stated by the measuring pole manufacturers as dubious for orchard plantations (because of phenomena such as leaf clumping, large woody structure, etc.), the lack of such values for Avocado canopies in the literature makes it worthwhile to asses the LAI. We used an equation developed by Campbell (Campbell 1986, Potter 1996), who assessed the extinction coefficient K_c from the relative direct radiation, using an ellipsoidal distribution function for the leaves' orientation (ELADP). This distribution was measured by counting inclination of leaves (method taken from the 'sun-scan' manual), yielding an ELADP parameter of 2.3. The formula devised by Campbell is:

$$\tau = K_c(x,z) \cdot LAI \tag{4}$$

$$K_c(x,z) = \frac{\sqrt{x^2 + tg^2(z)}}{x + 1.702(x+1.12)^{-0.708}} \tag{5}$$

where x is the ELADP, z is the sun zenith angle, Kc the extinction coefficient, LAI is the cumulative overlying leaf area index, and τ is the relative direct radiation. The LAI was extracted in a similar manner to the physical extinction coefficient, using the central 50 cm around the solar noon. In the same way that light penetration contours were drawn, the cumulative LAI was cast into a two-dimensional half cross section. Again, as stated in the measuring device manual, these contours may be not accurate for absolute values of LAI, but may show valid trends.

2.1.7 Fruit counting

Fruits counting per height group were done on November 2003 and November 2004, about a week prior to their picking. The tree height was divided into three sections: low (0-2m), medium (2-4m) and high (above 4m). Due to the great variability in the fruit number per tree (some trees had more then 300 fruits compared with trees with 3 or even no fruits), great fruit drop due to winds, and inadequate canopy management, the results did not prove statistically viable as for the contribution of different treatments to lowering the location of fruits. Results are presented in the appendix.

2.2 Computer Modeling - The 'Radiance' software

Radiance is a computer software package developed by the Lighting Systems Research group at Lawrence Berkeley National Laboratory, University of California, under the direction of Greg Ward (Ward and Shakespeare, 1998). It is a research tool for accurately calculating and predicting the distribution of visible radiation by using a combination of ray-tracing and radiosity techniques. The program uses three dimensional (3D) geometric models as input to generate spectral radiance values in the form of photo realistic images and numerical tables.

2.2.1 The 'Radiance' light evaluation method

In the physical world, photons are emitted from a light source (the sun in our case) and bounce between surfaces (i.e. reflected) until being absorbed or transmitted by a surface. A small number of them reach the point of view or measurement device and create an image or a light reading/signal (see Figure 6a). Mimicking this process by a computer software can be done with forward ray-tracing, namely sending numerous rays in all directions, following their path, and creating an image out of those reaching the view point. This process is incredibly time consuming and inefficient, since the majority of the rays never hit the view point. *Radiance* uses a backwards light-rays tracing method. This method involves tracing rays backwards from the view point in arbitrary directions (according to the 'Monte Carlo' method) and 'splitting' the ray in every intersection, again in an arbitrary method (see Figure 6b). This process ends when the ray hits a direct or diffused source or after a preset number of bounces have occurred. The result is mathematically equivalent to following light forward from the source. The basic radiance equation used in the software is:

$$\underbrace{L_r(\theta_r,\Phi_r)}_{\substack{\text{raditation at}\\ \text{the point}}} = \underbrace{L_e}_{\substack{\textit{emitted}\\ \textit{.radiation}}} + \underbrace{\iint L_i(\theta_i,\Phi_i) f_r(\theta_i,\Phi_i;\theta_r,\Phi_r)\left|\cos\theta_i\right|\sin\theta_i d\theta_i d\Phi_i}_{\textit{reflected radiation}} \qquad (6)$$

where L is the radiance, f is the reflectance/transmittance function, and θ and ϕ are spherical angles. Subscript i is incident, r is reflected and e is emitted.

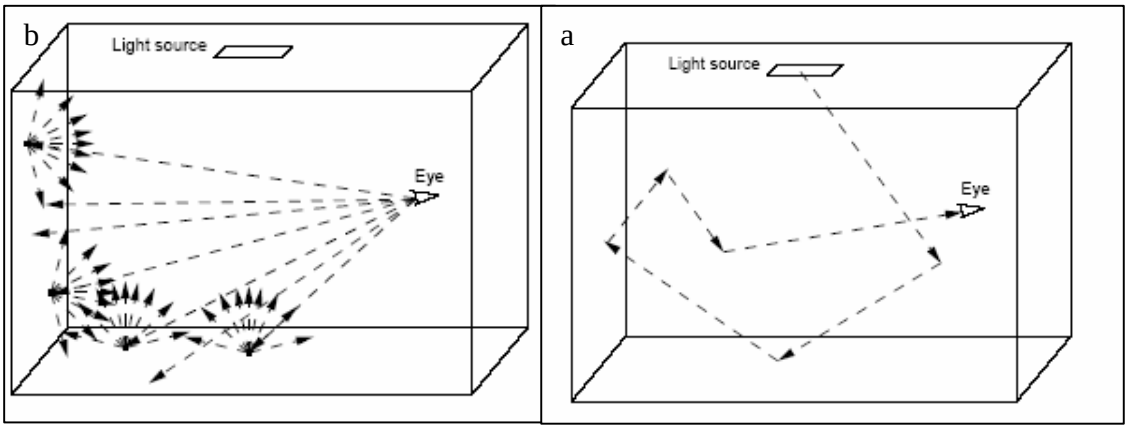

Figure 6 – Direct ray tracing from an object to the eye (a) and back – ray tracing (b) (http://radsite.lbl.gov/radiance/refer/backgrnd.pdf).

The main difficulty in ray tracing software is their inability to account for diffuse inter-reflections between objects, which is generally approximated by a constant ambient value. Indirect lighting is particularly difficult to render. Radiosity calculates the radiation caused by reflected light from nearby objects. This is called inter-object diffuse radiation. The essential difference between the implementation of the two methods is that ray tracing traces rays from pixels in the scene back to the light sources, while radiosity follows light from light sources through the scene as patch-to-patch diffuse interaction. Unlike ray tracing, which works best for highly reflective scenes, radiosity takes into account the distribution of light throughout the scene and is best suited for images containing mostly matte surfaces and indirect lighting. *Radiance* overcomes this shortcoming using an efficient algorithm for computing and caching *indirect irradiance* values over surfaces, while also providing more accurate and realistic light sources and surface materials (Ward and Shakespeare, 1998).

2.2.2 Building a 'Radiance' scene

Figure 7 depicts a flow chart of the processes taking place in our use of '*Radiance*' (though many more features are available). The boxes describe processes and the ovals describe data. The first step in creating a radiance scene is building a geometrical model

of the physical world. The geometric input is created by an AutoCAD model that is transformed into *Radiance* description. The *Radiance* software supports elaborate models and has translators for many design software. Another part of the scene description is the definition and application of materials for the objects in the scene. Material spectral properties include their color, reflective properties, and transmittance properties. In our case, we are using for the trees the material "mist" - a semi transmitting material whose properties will be described later. The third part of the scene is the sky description, created by the 'gensky' generator. *Gensky* produces a *Radiance* scene description for the CIE (Commission Internationale de L`eclairage) standard sky distribution at the given month, day and time for any given geographical location.

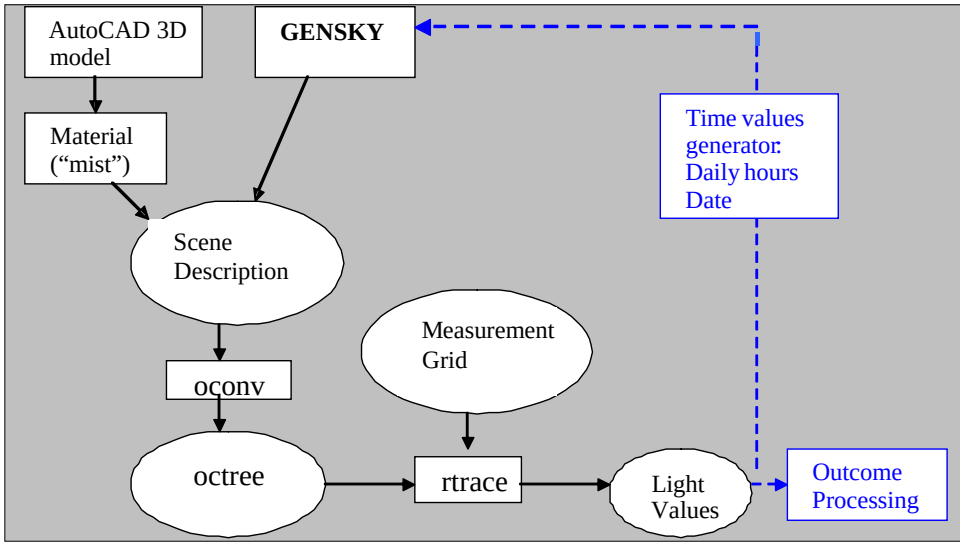

Figure 7 – Flow chart of the 'Radiance' simulation method used in this model. Rectangles represent processes and ovals represent data (adapted from Ward, 1994).

This scene description is then translated by the generator 'oconv' into a *Radiance* description file - the octree. The scene is then processed by the 'rtace' program which produces numerical results. Along with the scene, the measurement grid on which radiation is calculated and used as input for the 'rtrace' program (it should be mentioned that programs such as 'rpict' and 'rview' can give us also visual images of the rendered scene). In order to evaluate light properties along the growing season, we programmed a script that creates a time varying environment and sum/average the outcomes (dotted line in Figure 7).

2.2.3 ‘‘Radiance” features used in this model

2.2.3.1 Mist

Mist is a virtual material used to delineate a volume of participating media. Mist surfaces are used to enclose volumes within which a given light source or sources show significant scattering. A list of important light sources may be given, along with an extinction coefficient, a scattering albedo, and a scattering eccentricity parameter. The extinction coefficient is added to the global coefficient. Extinction is in units of m^{-1} and indicates the proportional loss of radiance over one width unit. The extinction coefficient was extracted by correlating the field data with *Radiance* simulations (as explained in 2.1.4). The scattering albedo, if present, overrides the global setting within the volume. An albedo of (0, 0, 0) means a perfectly absorbing medium and an albedo of (1, 1, 1) means a perfectly scattering medium (no absorption). The scattering albedo was extracted from spectral response curve of ‘Hass’ Avocado leaves (Heath et al., 2001).

2.2.3.2 Gensky

Gensky produces a *Radiance* scene description for the CIE standard sky distribution at the given month, day and time. The output sky distribution is given as a brightness function, *skyfunc.* Its value is in W steradian^{-1} meter^{-2}. The *x*-axis points east, the *y*-axis points north, and the *z*-axis corresponds to the zenith. The CIE model used was sunny clear sky (<30% cloud coverage), the location coordinates were 32.55N:35.04E and the time, the day and the month were given by the script.

2.2.3.3 Rtrace

Rtrace traces rays from the standard input through the *Radiance* scene given by *octree* and sends the results to the standard output. Rtrace operators used in this model are:

-I : A Boolean switch to compute irradiance rather than radiance, with the input origin and direction interpreted instead as the measurement point and orientation.

-Ab *N :* Sets the number of ambient bounces to *N.* This is the maximum number of diffuse bounces computed by the indirect calculation. A value of zero implies no indirect calculation.

-ar *res* : Sets the ambient resolution to *res.* This number will determine the maximum density of ambient values used in the interpolation. Error will start to increase on surfaces spaced closer than the scene size divided by the ambient resolution. The maximum ambient value density is the scene size times the ambient accuracy (see the *-aa* option below) divided by the ambient resolution.

-aa *acc*- Set the ambient accuracy to *acc.* This value will approximately equal the error from the interpolation of indirect radiation. A value of zero implies no interpolation.

-ad *N* : Sets the number of ambient divisions to *N.* The error in the Monte Carlo calculation of indirect irradiance is inversely proportional to the square root of this number. A value of zero implies no indirect calculation.

-as *N* : Sets the number of ambient super-samples to *N.* Super-samples are applied only to those ambient divisions that show a significant change.

Table 2 – Recommended values for ‘rtrace’ parameters used in our model (Ward and Shakespeare, 1998).

Parameter	Description	Min	Fast	Accurate	Max
-ab	ambient bounces	0	0	2	8
-aa	ambient accuracy	0.5	0.2	0.15	0
-ar	ambient resolution	8	32	128	0
-ad	ambient divisions	0	32	512	4096
-as	ambient super-samples	0	32	256	1024

Table 2 shows the values recommended by ‘Radiance’ developers for fast or accurate performance of the ‘rtrace’ program. In the calculation reported here we used the values recommended for accurate computation.

2.2.4 Finding “RADIANCE” extinction coefficient

In order to evaluate the software’s simulation results, a root mean square error (RMSE) between the field measurements and the ’Radiance’ simulation results has been calculated. The extinction coefficient implemented in “Radiance" as a material property of "Mist" is the one minimizing the discrepancy between the physical light extinction and the ‘Radiance’ simulation results. To achieve this goal, iso-radiation contours of the field measurements were calculated using natural neighbor interpolation. The tree contour was assumed to be that of 95% radiation, thus overlooking local self shading (since adjacent rows were not shading each other during the measurements). This contour was extracted into a row with which a model of the orchard was built. A grid of virtual sensors was designed at the exact same points where field measurements were performed (192 sensors over 3 meters, with vertical spacing of 0.5meters from the ground up to a height of 7.5 meters). This grid was simulated in “Radiance” for the same geographical and time data of the field measurements, and various extinction coefficients were tested. Each simulation point on the virtual grid was compared to the result of the field measurement in the exact same position, and the RMSE between them calculated.

2.2.5 Evaluation of the average intercepted radiation

In evaluating the intercepted radiation (IR) over the canopy envelope, the following steps were taken:

- Models of the various canopy architectures (as described above) were drawn in AutoCAD (ver. 14) and “Radiance” shape files were extracted.
- A grid of virtual light meters was introduced, with spacing of 10cm x 10cm between the nodes. The grid was placed on the canopy outer skirt (see Figure 8). Two rows from each side of the tested row were accounted for. Adding more rows proved to be redundant (see for example the trapezoidal hedgerow simulation layout).

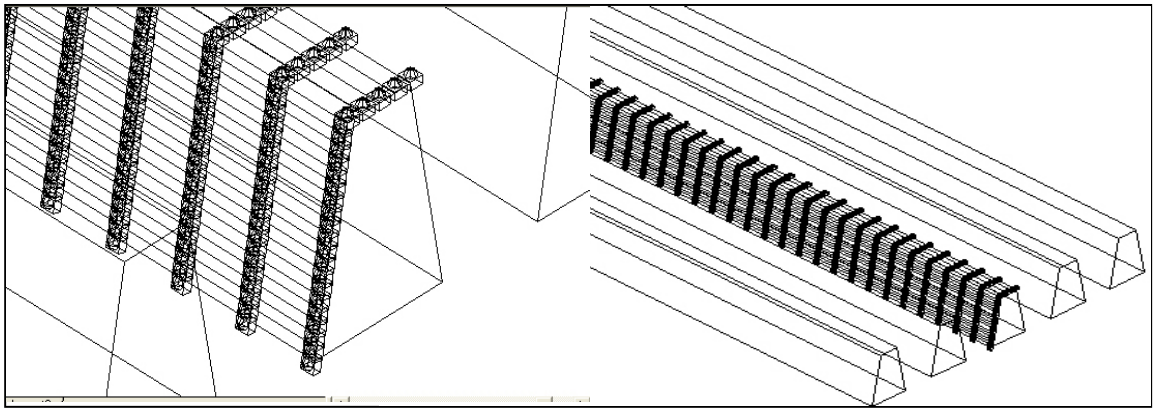

Figure 8 – 'Radiance' model of trapezoidal cross section hedgerow and the virtual light sensors positioning.

"Radiance " parameters used include:

- Canopy reflectivity - 8%
- Ground reflectivity - 8%
- Site coordinates – 32.55N:35.04E
- Number of ambient bounces (reflections) - 3

- A C^{++} routine was developed to sum and average automatically the light intensity. Readings were taken from each virtual "sensor" (grid point) in a one hour interval from 5:30 to 19:30, thus accounting for all the light hours in the period the measurements refer to. The simulations were done for the 15th of each month between April and October - the relevant seasons for growth. Readings were taken at the photosynthetic wave band (400-700nm)

Model results were processed to give two outcomes:

- Averaging the results gives an average radiant flux expressed in Wm^{-2}. The transformation into photosynthetic photon flux density (PPFD) in μmole $m^{-2}s^{-1}$, the common unit used by in the literature, reads

$$PPF = \frac{I(\frac{W}{m^2})}{E(J)} \cdot \frac{1}{N_0(\frac{1}{mole})} = \frac{I(\frac{J}{m^2 \cdot s})}{\frac{C(\frac{m}{s}) \cdot \hbar(J \cdot s)}{\lambda(m)}} \cdot \frac{1}{N_0(\frac{1}{mole})} = \tag{7}$$

$$3.76(\lambda = 450nm) \cdot I \leftrightarrow 4.59(\lambda = 550nm) \cdot I \leftrightarrow 5.43(\lambda = 650nm) \cdot I$$

The representative wave length for Avocado canopy was extracted From Figure 3 and found to be about 550nm.

- Summing the readings taken along the season and multiplying them by the surface area per hectare and by the time interval the measurements refer to yields the total seasonal energy intercepted by the canopy.

2.2.6 Evaluation of the PPCV

In evaluating the potentially productive canopy volume (PPCV) over the canopy envelope, the same 'Radiance' model supplemented by a C^{++} routine that was used for assessing the intercepted radiation was used. A grid of virtual light meters was introduced, with spacing of 10cm x 10cm between the nodes. The grid was placed vertically in the middle of a row (see Figure 9).

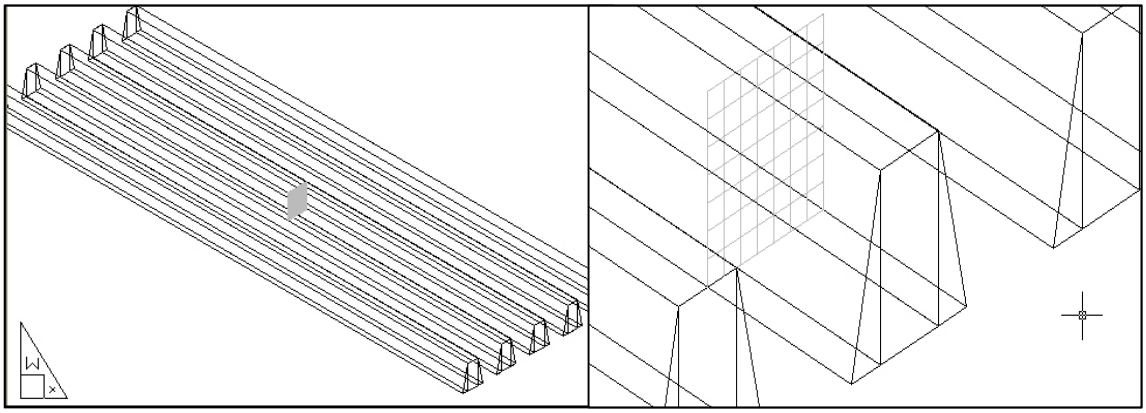

Figure 9 – 'Radiance' model of trapezoidal cross section hedgerow and the virtual light sensors positioning.

The new parameter introduced into "Radiance" was a "mist" coefficient of 1.5. A C++ routine was developed to sum and average automatically the potentially productive points. Readings were taken from each virtual "sensor" (grid point) in a one hour interval from 5:30 to 19:30, thus accounting for all the light hours in the period the measurements refer to. The simulations were done for the 15^{th} of each month between April and October - the relevant seasons for growth.

Each point was assessed whether it is potentially productive or not. The decision rule was as follows: a point that was illuminated at a level of at least 100 W/m^2 (PPF=~500 μmol $m^{-2}s^{-1}$) for the given exposure time was considered "*Potentially*

productive". These parameters were chosen from the photosynthetic activity curves. From these curves we can see that the activity threshold chosen is close to the beginning of the plateau – the maximal photosynthetic efficiency. This value also corresponds to findings by (Heinicke, 1963), proposing that 30% of full sun light is the lower light limit for photosynthetic activity in apples. The time limit chosen is short enough to let all parts of the canopy receiving light for only a short time to still be considered potentially productive while, on the same time, being long enough not to let a point that was only irradiated for a short time to be considered potentially productive. The points were summed at three different height levels: 0-2 m, 2-4 m, and >4 m. The potentially productive fraction of the cross section was calculated and multiplied by the total canopy volume per unit area.

2.2.7 Geometric properties of the orchard design

2.2.7.1 High density planting

Trees in high density planting were modeled as 2 m height cylinders or cones with a base radius of 0.75 m, planted in a 2.5m x 2.5m planting grid.

2.2.7.2 Trapezoidal hedgerow:

A trapezoidal cross section hedgerow that includes two slanted pruned walls and a "top" roof was considered. The trees were "planted" on a 7m x 6m grid with a tree height of 5.5 m and a canopy "skirt" of 4 m.

2.2.7.2.1 Pruning angle

An important parameter, which can be controlled by the farmer is the pruning angle. Changing the angle is just a question of how the blades of the pruning machine are set. For a given planting strategy, a smaller pruning angle (measure from the horizontal) gives a better grazing angle but reduces the overall tree volume. In order to investigate this interplay, various pruning angles were examined. The basic shape was trapezoidal with a 4 m base and 5.5 m high (See figure 10).

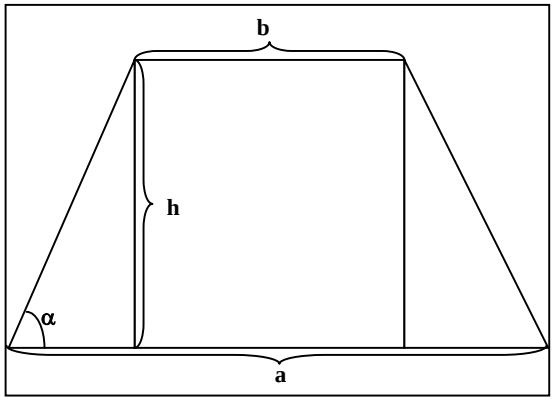

Figure 10- Basic dimensions of the trapezoidal hedgerow modeled when testing the pruning angle.

Table 3 – Dimensions, of the models used to inspect pruning angles.

α	h	a	b
[deg]	[m]	[m]	[m]
72	5.5	4	0.5
75	5.5	4	1
79	5.5	4	2
84	5.5	4	3.5

2.2.7.2.2 The tree height to-row width ratio

An important and widely used parameter of orchard planting is the tree height-to-row separation width ratio. The rule of thumb value widely used for it is 0.8. The intercepted radiation and the photosynthetically potentially productive volume were tested at five different ratios, as described in Table 4. The basic tree had a trapezoidal cross section and the ratio was changed either by keeping the row geometry fixed and changing the width between the rows or by keeping the inter-row separation width fixed and changing the tree height. The height was changed by ‘slicing’ the upper meter of a 7.5 m trapezoidal hedgerow with the same pruning angle as the one in the first method.

2.2.7.3 Additional models

Two additional models were added in order to account for practiced canopy management techniques. The first was a representation of the actual situation in many closed up orchards (TrBig). The tree was modeled as 7.5 m high trapezoidal hedgerow, planted at row width of 7 m and skirt width of 6 m. The second model, representing a South-African approach (Kohne and Kremer-Kohne, 1990; Stassen ,1999), is a higher density hedgerow with 4 m height (Tr4_dens).

Table 4 - Geometrical properties of models used in simulations.

Investigated Aspect [representative model name]	Tree Height [m]	pruning angle [deg]	Planting grid [mxm]	Tree height to row width ratio [R]	Surface Area [m^2/ha]	Canopy Volume [m^3/ha]
Pruning Angle						
Tr72	5.5	72	7x6	0.79	17,200	17,678
	5.5	75	7x6	0.79	17,714	19,642
Tr55	5.5	79	7x6	0.79	18,829	23,571
	5.5	84	7x6	0.79	20,779	29,464
R- tree height changed						
	7.5	79	7x6	1.07	23,537	28,017
	6.5	79	7x6	0.93	20,976	25,396
	5.5	79	7x6	0.79	18,826	23,571
	4.5	79	7x6	0.64	16,439	20,443
	3.5	79	7x6	0.5	14,063	16,825
R – row dist. changed						
	5.5	79	9x6	0.61	33,000	26,360
	5.5	79	8x6	0.69	27,500	21,966
	5.5	79	7x6	0.79	23,571	18,828
	5.5	79	6x6	0.92	20,625	16,475
	5.5	79	5x6	1.1	18,333	14,644
Additional tree models						
TrBig	7.5	81	7x6	1.1	27,332	53,570
Tr4_dens	4	79	5x3	0.8	19,300	18,000
Individual Trees [2m height]	Base diameter – top diameter					
Cylinderical	1.5- 1.5	90	2.5x2.5	0.79	15,990	5655
Conical	1.5 - 1	83	2.5x2.5	0.79	13,480	3980
	1.5 - 0.5	76	2.5x2.5	0.79	10,370	2720
	2 – 1	76	2.5x2.5	0.79	16,335	5864

3 Results & Discussion

3.1 Intercepted light

3.1.1 Experimental results

3.1.1.1 Canopy and ground reflectance

Results of canopy and ground reflectance measurements in the experimental site are presented in Table 11. Each result represents an average of 3-5 measurements in each direction. The canopy reflectance was found to be: 0.081 ± 0.051 (n=7). The ground reflectance was found to be: 0.070 ± 0.014 (n=3).

3.1.1.2 Comparison between measurements of intercepted light and results form 'Radiance' simulations

Figure 11 (Appendix) presents measured and simulated light readings between 10:40 and 14:10 on the 14th of September 2003 in kibbutz Shomrat orchard. A good agreement is apparent during most hours of measurement. Exceptions are apparent at 11:50 and 13:05, mainly because of the appearance of clouds. At these times, the coming PAR, as measured by the BFS, was only 16% and 23%, respectively, of the average level of the PAR during the measurements. The RMSE between the measured and simulated values was about 99 μmole m^{-2} s^{-1}, or 6% of the average PAR. Similar measurements were taken 9 months later, on the 8th of June 2004, following the spring pruning. Results of the measured and simulated readings are presented in Figure 12. During the early hours (10:00-10:30) the measured radiation is higher then the simulated values, whereas the opposite is true after the solar noon. The higher experimental values in the morning may suggest that light penetrating through gaps in the neighboring row have reached the measuring pole, a source of light which was not accounted for in the simulation model. On the other hand, the higher simulated values after the solar noon probably reflect the fact that temporary changes in cloudiness and atmospheric turbidity were not included in the simulations. The average RMSE between the measured and simulated incident PAR is 214 μmole m^{-2} s^{-1}, or 11% of the average light intensity during the measuring period.

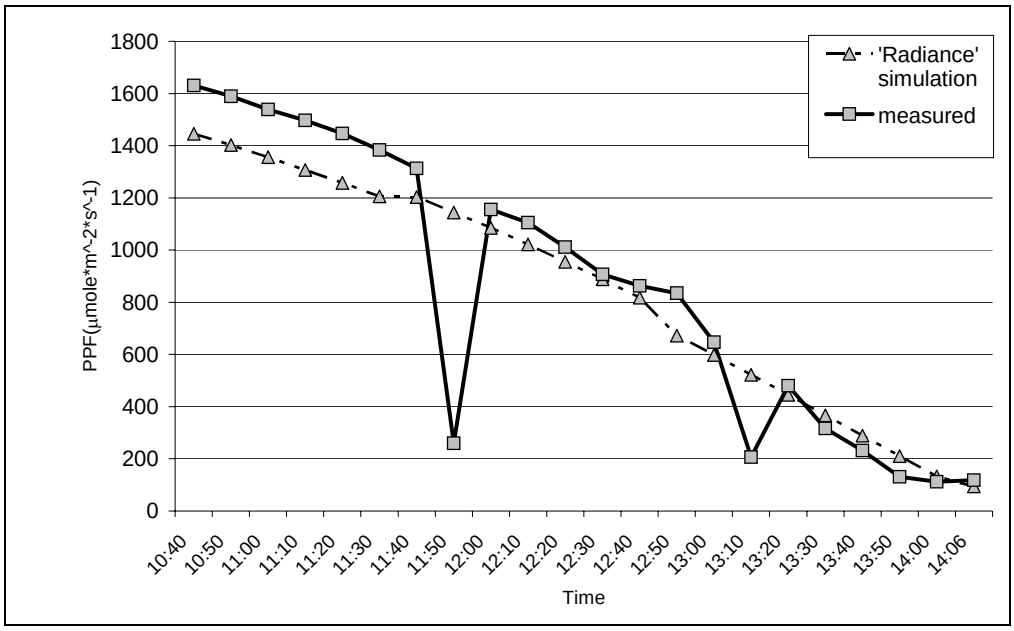

Figure 11 –'Radiance' Simulation and measurements of intercepted light for the 14/9/2003 in 'Shomrat' orchard (cv. Hass).

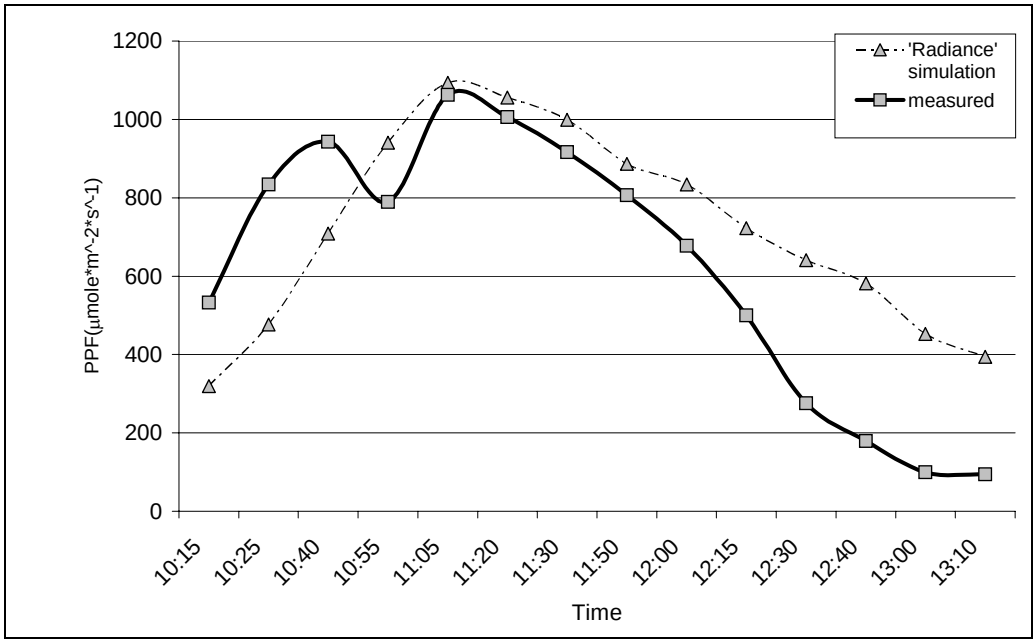

Figure 12 –'Radiance' Simulation and measurements of intercepted light for the 8/6/2004 in 'Shomrat' orchard (cv. Hass).

3.1.2 Simulation results

In simulating the intercepted radiation we used two basic orchard geometries. The first is the trapezoidal hedgerow, defined by the pruning angle of the two sides of the row and by the tree height, and the second is that of high density planting of small trees, represented by cylinders of 1.5 meters in diameter and 2 meters in height. The results presented here are the simulated readings of light sensing nodes on a virtual grid of 10cm x 10cm spacing between the nodes. The light sensing grid is placed on the outer contour of the canopy, aligned with the pruning angle. Readings are taken every hour during daylight on the 15th day of the month from April to October, representing the Israeli growing season. The results are divided into canopy height layers: h<2 m (h<1 m for high density orchard), 2<h<4 m (h>1 m for high density orchard), h>4 m, and the top horizontal face of the canopy. The division into layers was done in order to gain better understanding on the partitioning of the intercepted radiation on the tree outer surface. The two sides of the hedgerow are presented separately only when they differ with respect to intercepted light, i.e. the north and south faces of an east-west planting (the east and west faces of a north-south rows are similar due to the symmetric daily sun trajectories). The results are averaged over the daylight hours and presented as the total average intercepted radiation per hectare per day.

3.1.2.1 Hedgerow orchard

3.1.2.1.1 Tree height –to row width ratio (R)

The non-dimensional tree height to row width ratio (R) is a key factor in planning planting strategies. The common rule-of-thumb is that the tree height should be 80% of the row width. The applicability of this ratio was examined in two ways. First, by keeping the tree model (5.5 m high trapezoidal row) constant and changing the inter-row width from 5 m (ratio of 1.1) to 9 m (ratio of 0.61). Second, by keeping the inter-row width constant at 7 m and changing the tree height by stepwise ‘slicing’ of the upper meter of the tree, starting with a 7.5 m tree (R=1.07), and keeping the pruning angle constant

Figure 13 depicts simulation results of the average intercepted radiation, keeping the tree height constant and Figure 14 shows simulation results of the average intercepted radiation, keeping the row width constant.

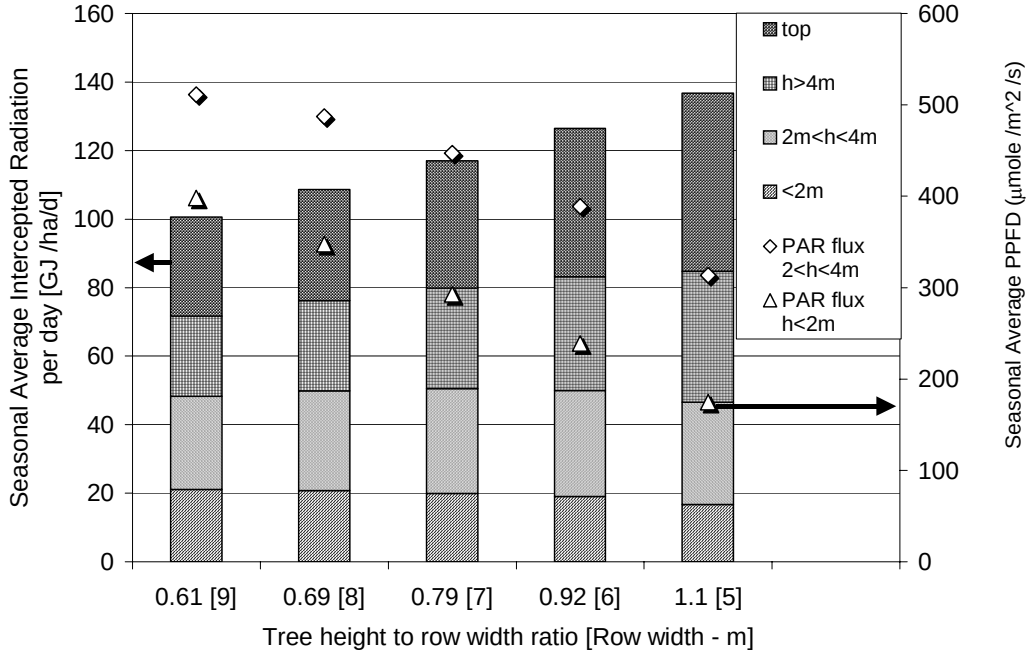

Figure 13 – Average intercepted radiation at various heights as a function of the tree height-to-row width ratio (tree height constant, 5.5m)

Figure 13 shows the average intercepted radiation absorbed at distinct height layers as a function of *R* for a typical 5.5 m tree. As *R* increases (a decrease in the inter-rows width and an increase in the planting density) two opposing effects take place: a very slight decrease in light flux reaching the lower parts of the canopy and an increase in the canopy specific surface area(see table 4). For the top layers (inclined and horizontal surfaces) of the canopy, the simulation results indicate an increase in the average intercepted radiation with the increase in *R*. The computed increase cannot be the result of changes in inter-shading between neighboring trees, which practically does not exist at the canopies' tops. Clearly, this result is due to the increase in the canopy overall surface area as a result of the increase in planting density. Intercepted light reaching the middle layer of the canopy increases by 12.3% when *R* increases from *R*=0.6 to *R*=0.9, and then

decreases with further increase in *R*. Combining the h<2m and the 2-4m height layers yields a local maximum in the average intercepted radiation around *R*=0.8. However, the sensitivity of the intercepted light to changes in the value of *R* is quite small, since increasing of *R* results in a comparable increase in the canopy surface area. For example, an increase in inter row width from 5m (*R*=1.1) to 7m (*R*=0.8) increases by only 7.6% the intercepted light at heights below 4m. Similarly, simulation results indicate that the total light intercepted by the hedgerow canopy increases with the increase in *R,* mainly as a result of the increase in canopy surface area. Note, however, that *R*>1.1 would cause the row to closedown.

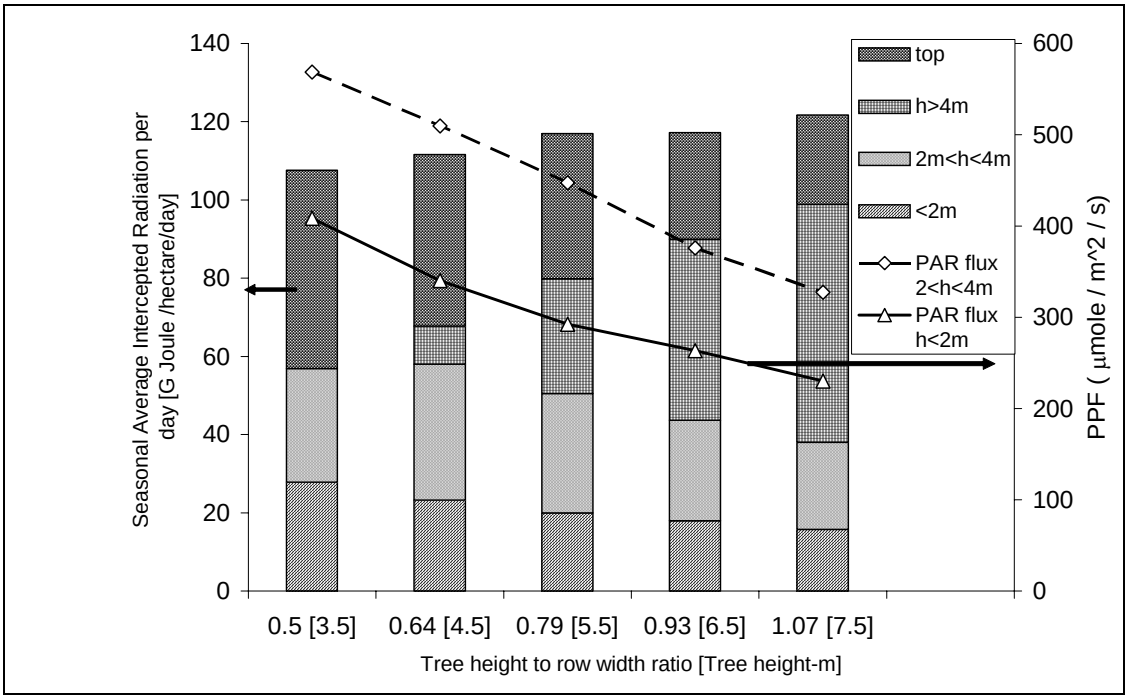

Figure 14 – Average intercepted radiation at various heights as a function of the tree height- to-row width ratio (constant row width of 7m).

Figure 14 describes the average intercepted radiation as a function of the ratio of tree height-to-row width for a constant row width of 7 m and a varying height of the trapezoidal hedgerow model. An increase in the value of *R* from 0.5 to 1.07 represents an overall increase in tree height from 3.5 m to 7.5 m. As the value of *R* increases, the radiation intercepted at the horizontal top surface of the trapezoid decreases due to the

decrease in the surface area. The average radiation intercepted by the canopy at heights above 4 m increases with tree height, mostly due to the increase in the canopy surface area above 4m. In the 2-4 m height layer of the canopy the average intercepted radiation increases with R from R = 0.5 (tree height of 3.5 m) to R = 0.64 (tree height of 4.5 m), simply because of the increase in this layer's envelope area. Than, it gradually decreases as R further increases due to inter row shading. The average intercepted radiation on the bottom 2m of the canopy is maximal for R= 0.5, after which it decreases continuously with the increase in R. A decrease of 21% in the average intercepted radiation was computed when the value of R increased from 0.5 to 1.07. Since there is no change in the envelope area for this layer, it is the change in inter-row shading that is responsible for the decrease in the average intercepted radiation. Therefore, smaller trees intercept more PAR at their bottom 2 m. The total average intercepted radiation increases by 11% when the tree height changes from 3.5m to 7.5m, an increase attributed to the increase in surface area of the upper canopy layers.

To summarize, two opposite effects were demonstrated in our simulations. In general, the total average intercepted radiation increases as the tree height-to-row width ratio increases. The difference was more apparent when the row width was changed, due to the more significant change in the overall surface area per hectare. The average intercepted radiation received by the 0-4 m canopy layer tends to decrease with the increase in R.

The sensitivity of the average intercepted radiation to changing the two parameters that determine the value of R is not symmetrical. Changing the row width creates a larger change in the surface area per hectare then lowering the trees height, since more trees are added per hectare. However, this increase in planting density increases inter-row shading and thus reduces the penetration of light into the lower parts of the canopy. Thus, in order to increase the total intercepted light and to improve its distribution within the canopy a combination of reducing the tree height and increasing the planting density could be an effective strategy.

3.1.2.1.2 Row orientation

Table 5 describes simulation results with respect to partitioning of intercepted light between different height layers and faces of hedgerows with different orientations. As expected, North-South rows show symmetry with respect to the east and west faces of the hedge. In contrast, East-West rows show a distinct difference between the southern and the northern faces of the hedge. While the southern face is illuminated most of the day and is shaded only by the trees in front of it, the northern face is illuminated only in the early morning and the late evening (in the summer), when the sun is low and photosynthesis is less efficient. The differences would have been even larger if winter months were considered, since in Israel the sun path starts at the northeast in the summer months.

Table 5 – Light interception on the various heights and faces in N-S and E-W row orientation.

		Seasonal Average Intercepted Radiation per day [GJ/ha/d]				PPF [μmole /m^2 /s]			
Height Layer↓	Row→ orientation	NS		E-W		NS		E-W	
h>4m		E 14.7	W 14.7	N 4.5	S 13.6				
2<h<4m		E 15.3	W 15.3	N 5.7	S 17.9	E 447.2	W 447.2	N 168.5	S 523.9
h<2m		E 10.0	W 10.0	N 5.3	S 16.3	E 292.4	W 292.4	N 156.7	S 478.7
Top		37.1		37.1					

Table 5 describes the distribution of the seasonal average daily intercepted radiation and average radiation flux between the faces of the row. As expected, the N-S planting results in symmetrical radiation intensities on both the eastern and western faces. The E-W hedge, however, shows a distinct difference in radiation and radiation flux between the well illuminated southern face and the northern face, which is shaded for most of the day. The southern face receives about 68% higher radiation flux.

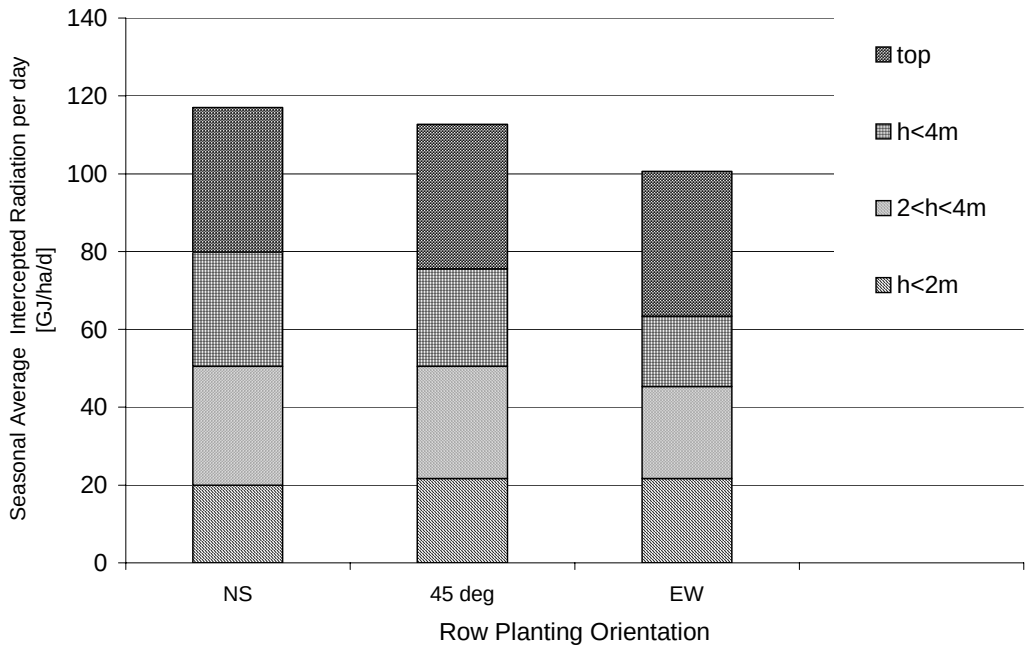

Figure 15 – Average intercepted radiation in various heights of the hedge as a function of row orientation.

Figure 15 shows the average intercepted light at various heights of a trapezoidal hedgerow. The total intercepted light decreases by 4.4% as a result of a change in the orientation by 45^0 from North-South and by 15.7% if the hedgerow orientation is East-West. The decrease in the average intercepted radiation is mainly at the upper and mid canopy layers. Light interception at the lower parts of the hedgerow is practically insensitive to changes in row orientation. Clearly, interception of light at the top of the hedgerow is the same for any orientation.

Therefore, when no other factors such as drainage, winds or slope dictate otherwise, the total average intercepted radiation is significantly higher for North-South (N-S) planting orientation than for East-West (E-W) orientation. While the average intercepted radiation on the east and west faces of a N-S hedge are equal, in an E-W orientation most of the intercepted light falls on the southern face. This inhomogeneous light regime may have significant impacts on growth, branching, and fruit distribution in orchards with E-W rows.

3.1.2.1.3 Pruning angle

The angle at which the sides of the hedgerow are pruned affects the intercepted radiation in two opposite manners. On one hand, as the pruning angle (α) decreases (see Figure 16) the grazing angle between the row and sun approaches 90^{o}, which improves light interception. On the other hand, a larger pruning angle (measured from the horizontal) results in an increase in the hedgerow's roof area, which intercepts radiation all day long.

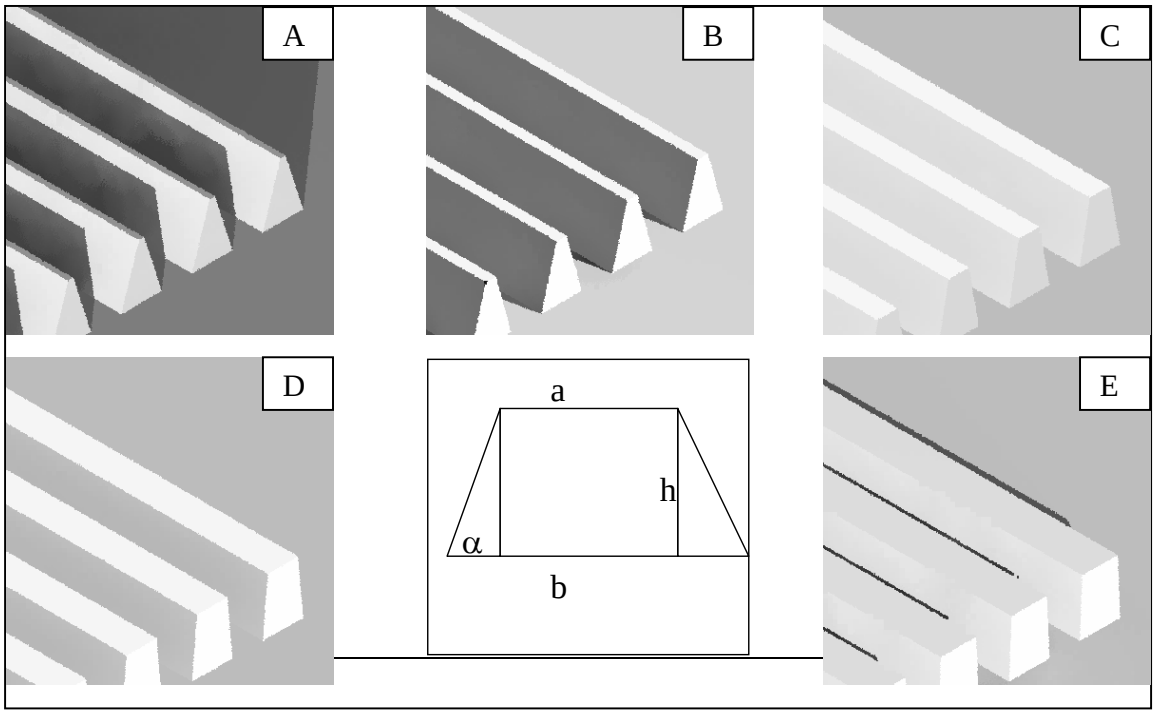

Figure 16 – Basic designs of simulated hedgerow cross sections, $\alpha=72^{0}$ (A), 75^{0} (B), 79^{0} (C), 85^{0} (D), and 87^{0} (E).

Figure 17 describes the simulated results of the intercepted energy flux at different canopy heights as a function of the pruning angle. The results of these simulations demonstrate two opposite effects in response to changes in the pruning angle. Namely, while the total average intercepted radiation increases as the pruning angle goes from 72^{0} to 87^{0}, light intercepted by the lower 0-2 m and 2-4 m layers decreases with an increase in the pruning angle. A 60% increase in light interception by the lower 2 m of

the hedgerow canopy and an increase of 53% in the lower 4 m is predicted as a result of reducing the pruning angle from 87^0 (an almost rectangular shape) to an almost pyramidal shape (pruning angle of 72^0). In contrast, light interception at the hedge roof increases significantly with the increase in α, merely as a result of increasing surface area. At a pruning angle of 87^o, light interception by the top of the hedge is 86% higher than for a pruning angle of 72^o. However, the effect of pruning angle on the canopy total light interception is less apparent. Indeed, as the pruning angle increases from 72^o to 85^o an increase of only 8.1% in the total intercepted light is predicted. Therefore, the effect of the hedgerow's pruning angle on the total average intercepted radiation is small. However, its effect on the distribution of intercepted light is substantial. As the pruning angle becomes sharper the average intercepted radiation at the middle and lower canopy sections increases significantly.

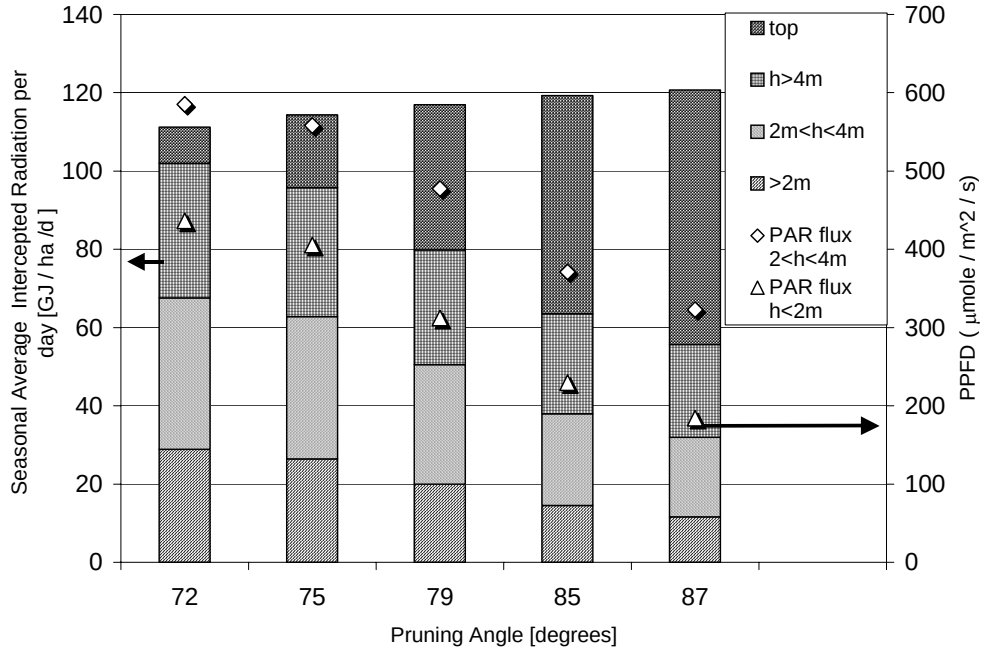

Figure 17 – Average intercepted radiation at various heights as a function of the pruning angle (α).

3.1.2.1.4 Slopes

Although the Israeli Avocado orchards are normally planted on flat land, in many areas in the world (California, Mexico, etc.) Avocado is planted on sloping lands. The positioning

of the rows in respect to the slope creates different patterns of shading, and changes the grazing angles towards the sun.

The effect of the slope on intercepted light was studied using two planting models – hedgerows in parallel to the slope direction and perpendicular to it (Figure 18).

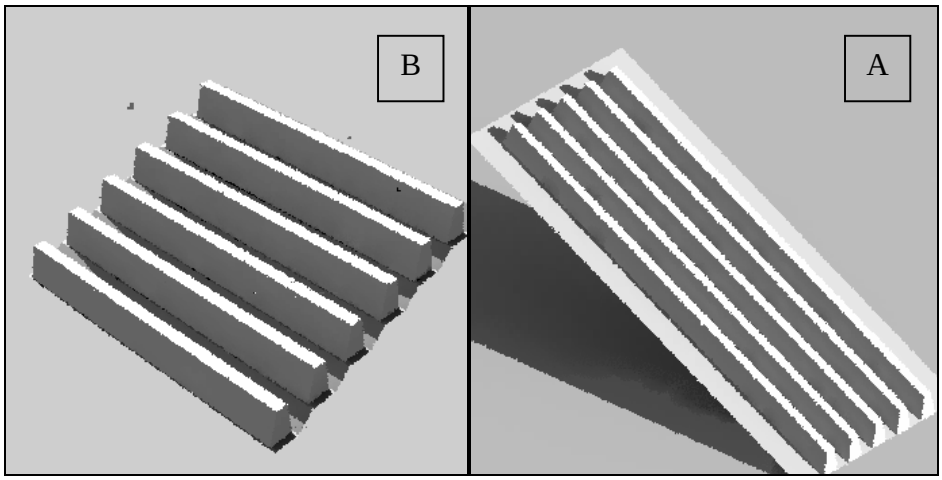

Figure 18 - 'Radiance' simulation of planting strategies on slopes- Rows parallel to the slope (A) and perpendicular to the slope (B)

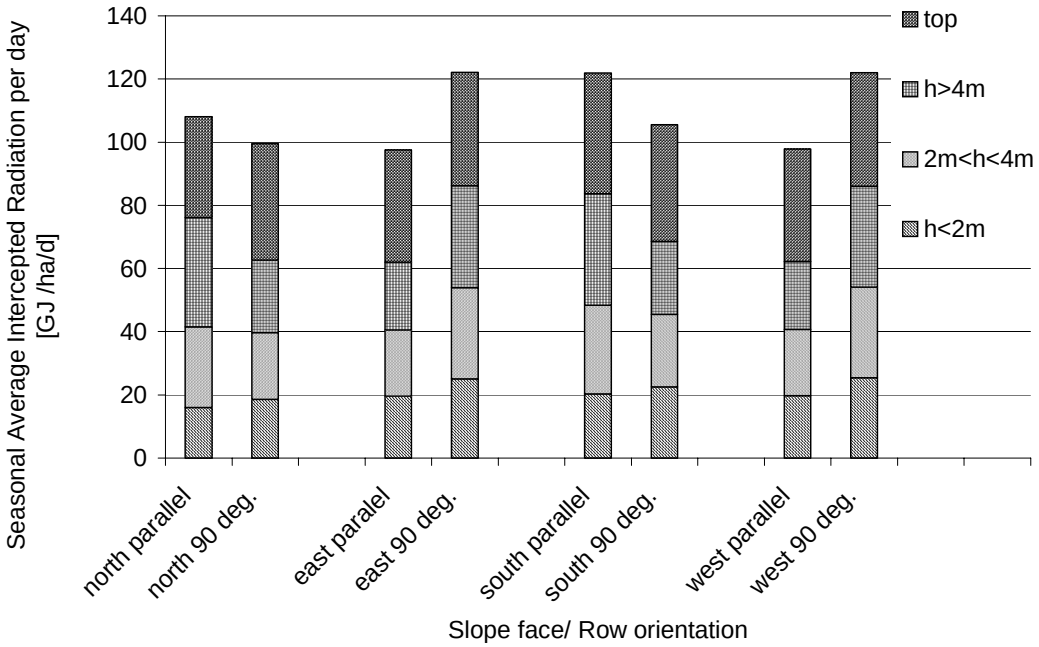

Figure 19 - Intercepted light at various canopy heights for different orientations of a 40% slope and two planting strategies: Rows in parallel to the slope and perpendicular to it.

Figure 19 describes the average intercepted radiation when planting the row in parallel to the slope (A) and perpendicular to it (B), for four slope directions. As seen, there is a distinct difference between the planting strategies. For slopes facing east and west the perpendicular planting strategy is preferable, yielding 20% more total seasonal intercepted radiation. The advantage in the seasonal intercepted radiation is even larger at the various heights, 22% more at the bottom layer, 27% more at the middle layer and 33% more at heights above 4 m. (The total difference is lower since the top intercepts the same amount of radiation).

For a northern slope there is an advantage to the parallel planting strategy, with 8% more light interception compared to the perpendicular planting strategy. Here, the differences between the strategies at the various heights are 13%, 17%, and 33% for the <2 m, 2<h<4 m, and h>4 m layers, respectively. In contrast, at the top there is an advantage of 13% to the perpendicular strategy.

For a southern slope, a parallel planting strategy intercepts 13% more light than when planting perpendicular to the slope. Seasonal light interception in rows along the slope is 10% (bottom), 19% (mid), and 34% (top) higher than in the comparable parts of rows running normal to the slope.

Generally, the effect of planting on sloping lands is similar to that presented for flat-land, where a N-S planting strategy yields better seasonal light interception and better distribution between the sides of the hedgerow. In order to achieve the advantages of a N-S planting on sloping lands, rows should be planted perpendicular to the slopes (configuration B) on east\west slopes and parallel to the slope (configuration A) on north/south slopes. In addition, the difference in seasonal intercepted radiation is larger on the top layer than on the mid layer, but there is no advantage to E-W planting over a N-S planting strategy w.r.t. the bottom layer, as is the case for flat land.

In conclusion, when planting hedgerows on slopes and no other factor dictates otherwise, the general tendency should be aiming at a North-South row direction regardless of the slop orientation.

3.1.2.2 High density orchards

3.1.2.2.1 Tree height-to-row width ratio

Since the height of individual Avocado trees is fairly constant, due to shaping needs, changing the tree height-to-row width ratio (*R*) can be achieved by changing the planting widths. Basic tree geometry of a 2 m high cylinder of a 1.5 m diameter is used for the simulations described in this chapter. In order to simplify the calculations, the cylinder is made out of 8-face polygon (see Figure 20). The virtual measurement grids are placed on 4 of its walls (facing north, west east and south) and the outcome of these simulations is presented as the average between the four faces. Results are presented here, as in the rest of this chapter, as an average seasonal intercepted radiation [G Je/hectare/day].

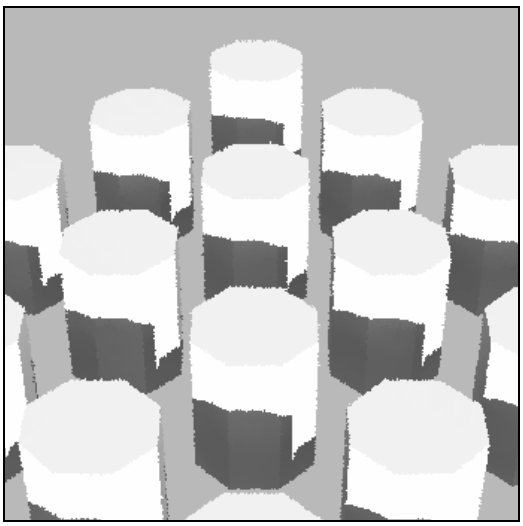

Figure 20 - 'Radiance' simulation of cylindrical representation of the high density orchard.

Figure 21 describes the average intercepted radiation with the change in planting density of cylindrical 2 m high trees. As seen, there is a constant decrease in the total average intercepted radiation per hectare per day as the planting density decreases. Decrease of 25% and 44% in the total average intercepted radiation was simulated as planting widths increased from 2 x 2 m to 2.5 x 2.5 m and 3 x 3 m, respectively (*R* values decreasing from 1 to 0.8 and 0.67).

The simulated intercepted radiation per hectare per day for the lower canopy layer was essentially constant for the planting densities simulated (changes smaller then 10%). These small changes were the result of the compensating effects of greater planting density, i.e., more surface area with increased inter tree shading. For the upper canopy layer of 1-2 m, intercepted radiation increased by 38% with the increase in tree planting density from3x3 m to 2x2 m. Here, the inter tree shading effect was minimal. The intercepted radiation on the top of the cylindrical trees increased substantially with the increase in planting density, solely due to the increase in surface area of the top layer.

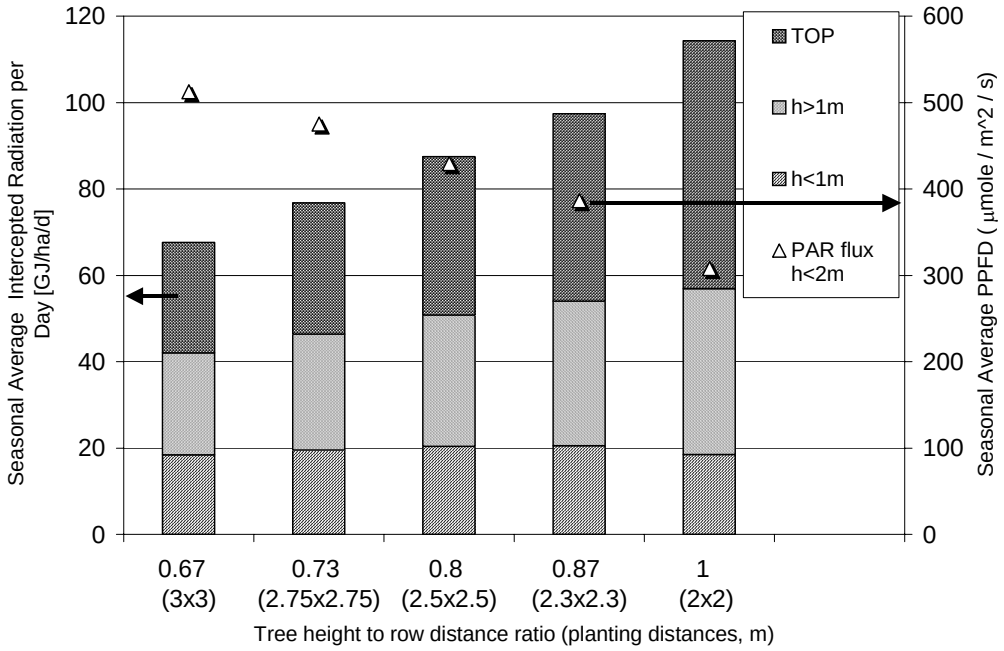

Figure 21 – Average intercepted radiation at various canopy heights for various tree height-to-row width ratios (high density orchard).

3.1.2.2.2 The effect of slopes

To date, most high-density orchards are planted on steep slopes (especially in California). When examining the influence of the slope on light interception two key factors are examined - the slopes angle, which can reach up to 30^0 or more, and the aspect, i.e. the slope's direction. Two typical slopes have been examined, 40% (21.8^0) and 60% (30.9^0)

(see Figure 22). More moderate slopes showed similar results to flat land with almost no difference for different orientations.

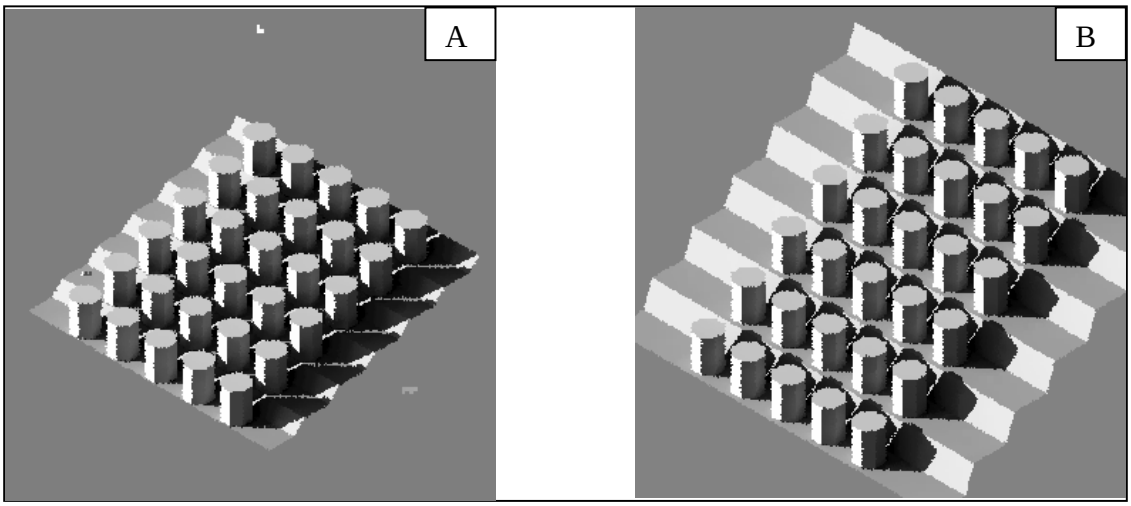

Figure 22 – 'Radiance' simulation of isolated trees planted on slopes: A-40%; B-60%.

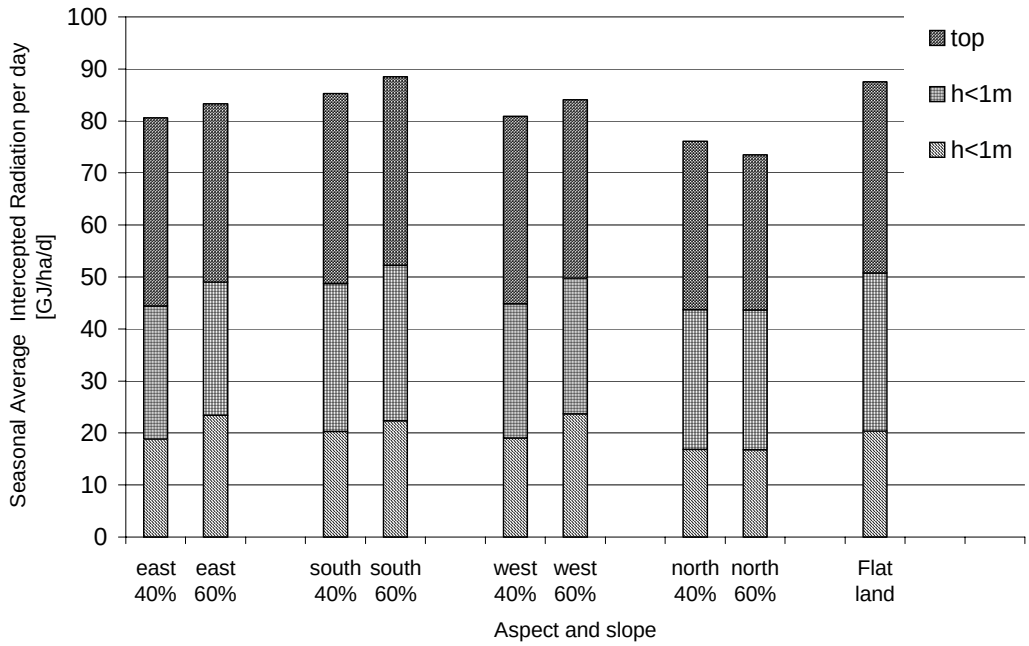

Figure 23 – Intercepted light at various heights of isolated tree orchard on 40% and 60% slopes.

Figure 23 describes the average intercepted radiation by individual-trees of a high density orchard planted on a 40 and 60% slope (in the northern hemisphere). As seen, the southern aspect receives the largest amount of energy at both slopes. The east and west aspects receive similar amount of average intercepted radiation, about 5.4% and 5.9% less then the southern aspect, for the 40 and 60% slopes, respectively. The northern aspect, facing away from the sun, receives 10.7% and 17% less radiation than the southern aspect, for the 40% and 60% slopes, respectively. The southern face receives about the same radiation as in flat land, with merely 2.5% less on a 40% slope and 1.2% more on a 60% slope. On the east, west and southern slopes, the 60% slope yields higher average intercepted radiation then the 40% slope, both at the lower 1m layer and for the total average intercepted radiation. This result is due to the reduced shading between the trees. On the northern slope, the 40% slope yields higher average intercepted radiation then the 60% slope due to reduced shading by the ground.

3.1.2.2.3 Manipulating canopy shape

In the previous sections, we have modeled the high density as cylinders. However, in practice this is not the only shape found in high-density orchards. In the following section we intend to simulate a range of different cone geometries by changing the diameter of the base or the top while maintaining the height of the tree at 2 m. Three geometries were simulated: (1) a cylinder with a 1.5 m diameter and 2m height, (2) a truncated cone with a 1.5 m base diameter and 1 m top diameter, (3) a sharp angled truncated cone with a 1.5 m base diameter and 0.5 m top diameter and (4) a truncated cone with a 2m base diameter and a 1m top diameter (Figure 24).

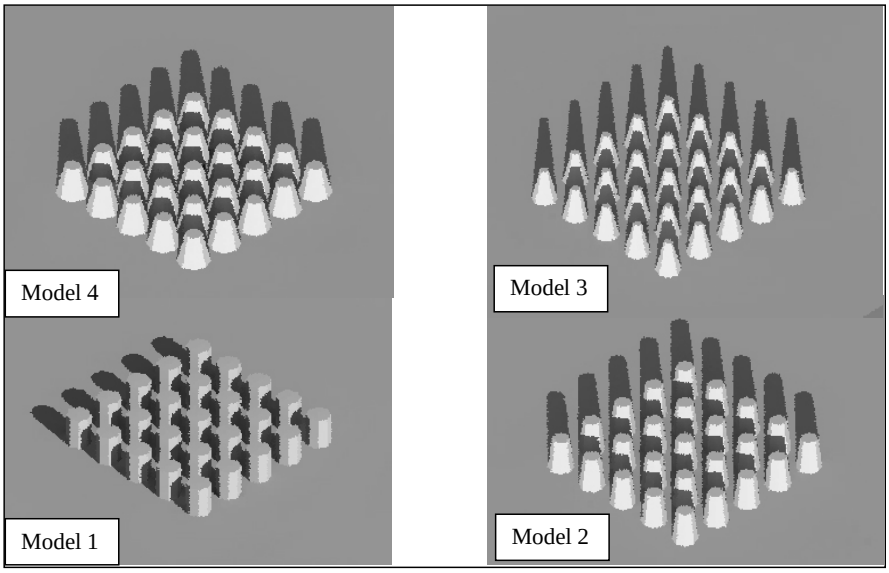

Figure 24 – ‘Radiance’ simulation of isolated trees geometries.

Table 6 – Dimensions of the 2 m high cylinder/cone models simulated.

Model no.	Planting Density [mxm]	Base Diameter [m]	Top Diameter [m]
1	2.5x2.5	1.5	1.5
2	2.5x2.5	1.5	1
3	2.5x2.5	1.5	0.5
4	2.5x2.5	2	1

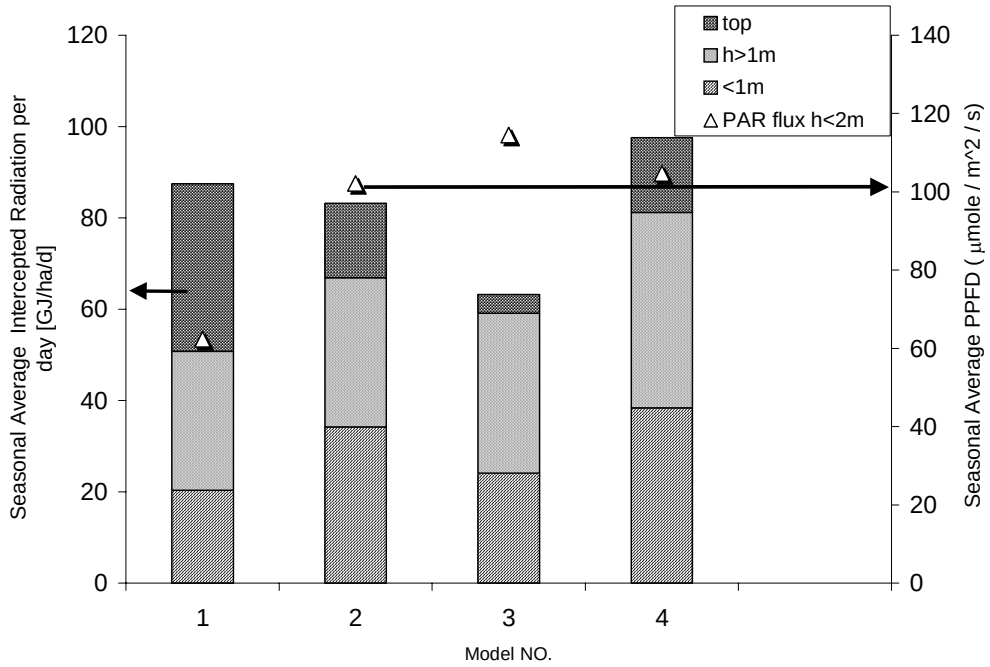

Figure 25 - Intercepted light at various heights and seasonal average PPF in isolated tree orchard for the canopy designs described in table 6.

As seen in Figure 25, changing the tree shape to a cone has opposing effects when the change in shape is merely shrinking the top surface of the cylinder the effect on the total average intercepted radiation is negative, and it decreases by 5% when going from model 1 to model 2 and by 28% when going from model 1 to model 3. This is mainly due to the decrease in the area of the top base. The seasonal average PPF, however, grows as the pruning angle grows. An increase of 64% in PPF was computed when the model changed from model 1 to model 2, and by 84% when going from model 1 to model 3. If the tree base is enlarged w.r.t. model 1 (model 4) the total average intercepted radiation grows by 10% and the distribution of light at the various heights is much better, 44% of the light is intercepted at the bottom 1 meter of the conical tree model while only 23% is intercepted at this layer in a cylindrical treemodel.

3.1.2.3 Light interception by the orchard floor

Part of the radiation reaching the orchard eventually reaches the orchard's floor. This 'wasted' radiation can result in an increased surface temperature and evaporation from

the ground. A common practice in some orchards is to spread reflective materials on the ground between the rows, in order to reflect some of the 'wasted' light reaching it back onto the lower parts of the canopy. It was suggested by Zamet (1998) that a slightly higher surface temperature resulted in an increase in the uptake of nitrogen.

Four models were used in studying the radiation balance beneath the canopy and between the rows. These models are presented in Table 7

Table 7 – Description of models used in the simulation of Figure 26.

Model no.	Morphology	Height (m)	Planting widths (m x m)	Ground coverage By canopy (%)
1	Trapezoidal Hedgerow (N-S planting)	5.5	7x6	57
2	Trapezoidal Hedgerow (E-W planting)	5.5	7x6	57
3	Cylinder (d=1.5 m)	2	2.5x2.5	28

Figure 26 depicts the average intercepted radiation on the floor under the tree canopy and on the ground in the work row. The first thing apparent from this figure is the obvious connection between the ground coverage and the light intercepted in between the rows. As expected, the highest intercepted radiation is predicted for the high-density orchard (model 3), which has only 28% canopy coverage. Radiation intercepted at the ground for the E-W planting strategy is larger than in the N-S planting strategy. This is mainly due to the longer time on which direct sun radiation hits the row (during the morning and afternoon hours). The intercepted radiation reaching the orchard floor under the canopy was essentially the same for models 1, 2 and 3.

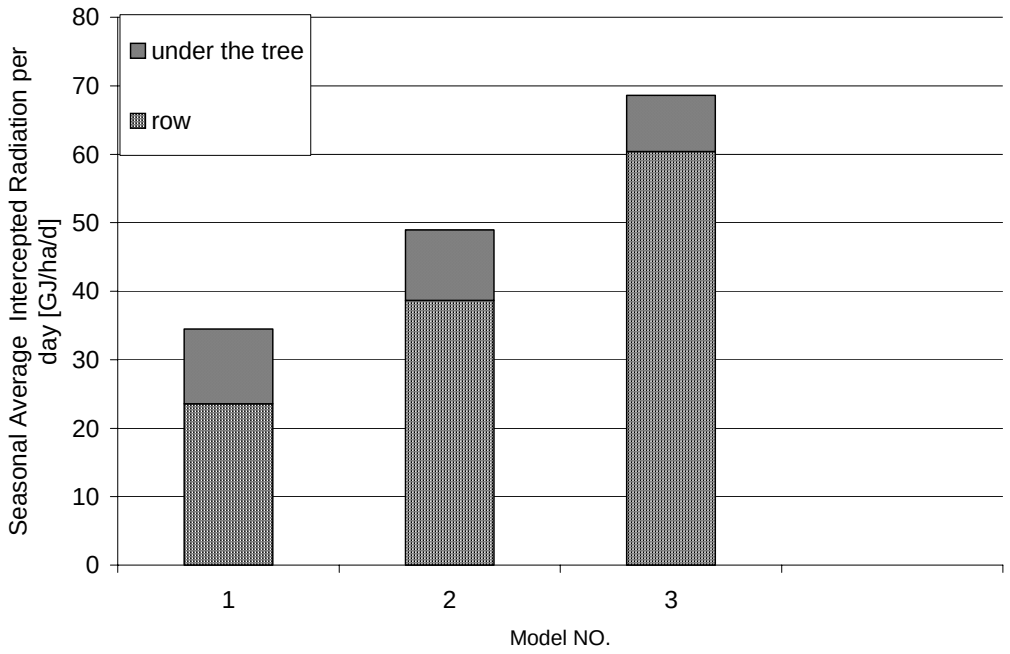

Figure 26 – Average seasonal radiation intercepted by the ground in the row and beneath the tree for three different orchard architectures.

3.1.2.4 Reflective mulches

A possible practice to improve the light regime of the lower parts of the canopy is to spread reflective mulches on the surface between the rows. In order to test the effectiveness of such a practice a simulation of reflective mulches was conducted using our 'Radiance' model. The reflective mulch was made of aluminum sheets (reflectivity of 90%) laid on the alleyways of a N-S trapezoidal hedgerow. Four geometries of reflective mulches were tested, a flat mulch placed directly on the ground ('carpet'), a pipe with 0.75m diameter placed along the center of the alleyway ('pipe 1'), a pipe with 1.5m diameter placed along the center of the alleyway ('pipe 2'), and a half pipe with 1.5m diameter placed along the center of the alleyway ('pipe 3'). The simulated results are presented in Figure 28.

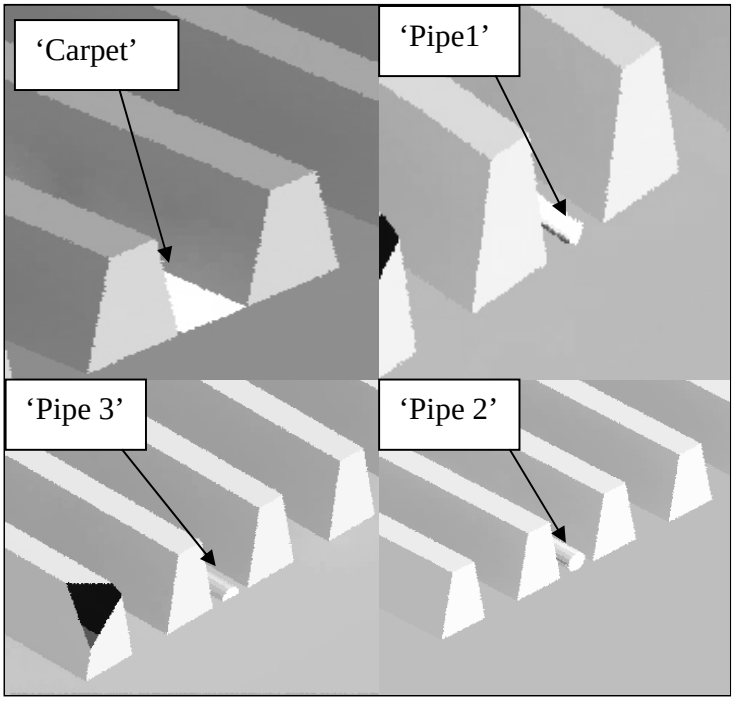

Figure 27 – ‘Radiance’ simulation of the models tested in this section.

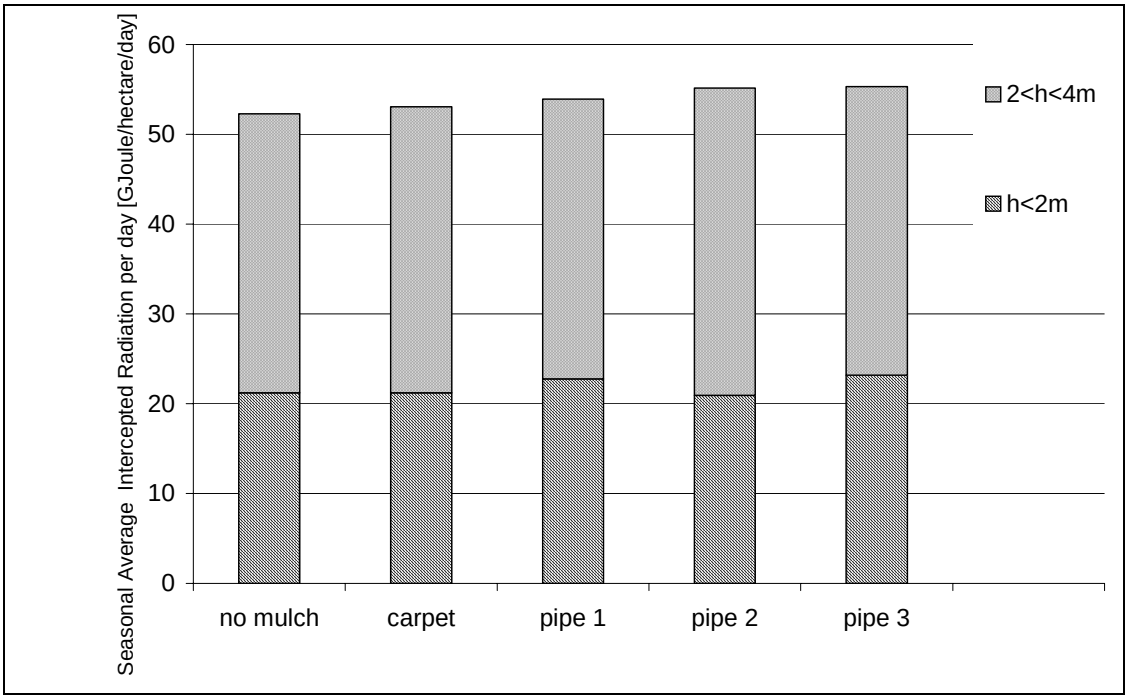

Figure 28 – Average seasonal radiation intercepted at the canopy bottom, with and without reflective mulches.

As can be seen in Figure 28, the ‘carpet’ mulch added nothing to the bottom 2 m layer and 2.5% to the middle layer when compared with the orchard without the mulch. The ‘pipe 1’ mulch added 7.4% to the bottom 2 m-height layer and 0.2% to the layer extending between 2 and 4 m. The ‘pipe 2’ mulch reduced 1.3% of the intercepted light from the bottom 2 m-height layer, probably due to shading caused by the mulch itself. However it added 10% to the intercepted light of the layer extending between 2 and 4 m. The ‘pipe 3’ mulch added 9.3% to the bottom 2 m-height layer and 3.3% to the layer extending between 2 and 4 m. Most of the added intercepted radiation took place around the solar noon. It should be noted that the model represents an ideal situation. In reality, wrinkling, dust and shading by the canopy can reduce the effectiveness of such mulches.

These simulation results show a limited effect on the intercepted radiation, and raise doubts as for the effectiveness of the application of reflective mulches as a radiation improvement practice. Among the models tested, ‘pipe 3’ the half-cylinder lying on the alleyway presented the best simulated outcomes.

3.1.3 Summary

In this chapter we have discussed the influence of various morphological manipulations of the Avocado orchard w.r.t. light interception and its distribution on the canopy surface. It is generally agreed that the economic yield of the Avocado tree is closely related to the intensity and distribution of solar radiation. A major objective of the morphological and geometrical manipulations of the Avocado orchard is to direct a larger proportion of the incoming radiation to the lower parts of the canopy.

The first parameter studied was the effect of the tree height-to-row width ratio, *R*, on the intercepted radiation in Avocado orchard. Figure 13 and 14 suggest that the total average intercepted radiation increases with the increase in *R*. Increasing the value of *R* by increasing the tree height or by decreasing inter row spacing increases the total intercepted radiation. The intercepted radiation reaching the lower parts of the canopy surface (<4m) is not substantially affected by changes in the value of *R* through changing the inter row width. However, when *R* is increased by increasing the tree height the intercepted radiation by the lower parts of the canopy (0-4m) decreases with the increase

in tree height. In both cases, the average intercepted radiation intensity (PPF) decreases as *R* increases.

Thus, for a densely planted short trees could yield an optimal interception of solar radiation in hedgerow orchard, both in terms of total numbers and the distribution to the lower surfaces of the canopy.

The effect of changes in the value of *R* on intercepted radiation and PPF in the high density orchard model is similar to the results presented in Figure 13 for hedgerow at constant height. The total intercepted radiation increases and the average radiation intensity decreases as the tree density increases (see Figure 21)

The effect of row orientation on the intercepted radiation is presented in Figure 15. Clearly, the total intercepted light in a N-S hedgerow planting is higher than in an E-W planting. In addition, in a N-S hedgerow the intercepted radiation is equally partitioned between the eastern and western faces while in an E-W planting most of the radiation is intercepted by the southern side.

The effect of the slope the on intercepted radiation is presented in Figure 19. On eastern and western slopes, planting the row perpendicular to the slope (which corresponds to N-S planting) resulted in higher total intercepted radiation then planting the row in parallel to the slope (corresponding to E-W planting). For southern and northern slopes, planting in parallel to the slope (N-S planting) proved superior to planting perpendicular to the slope (E-W planting).

The effect of pruning angle on intercepted radiation for hedgerows and high density orchard is presented in Figure 17 and Figure 25, respectively. As the pruning angle becomes sharper and the hedgerow shape becomes more pyramidal rather then rectangular (a cone rather then a cylinder for high density orchard), the distribution of light along the canopy surface becomes more uniform, i.e. more light is intercepted at the lower parts of the tree. The total average intercepted radiation decreases as the angle becomes sharper. This is mainly due to the decrease in the surface area of the tree tops.

In order to further study the influence of canopy architecture on intercepted radiation, representative canopy architecture models (hedgerow & high density orchard) were selected. The models are described in Table 8. The intercepted radiation under these canopy models was simulated and results are presented in Figure 29.

Table 8 – Canopy architectures used in Figure 29.

Model no.	Row shape	Tree height	Planting density
1	Trapezoidal hedgerow(narrow alley)	7.5	7x6
2	Trapezoidal hedgerow (N-S plating)	5.5	7x6
3	Trapezoidal hedgerow (72^0 pruning)	5.5	7x6
4	Trapezoidal hedgerow	4	5x3
5	Cylinder single trees(radius=0.75 m)	2	2.5x2.5
6	Cone1 single trees	2	2.5x2.5

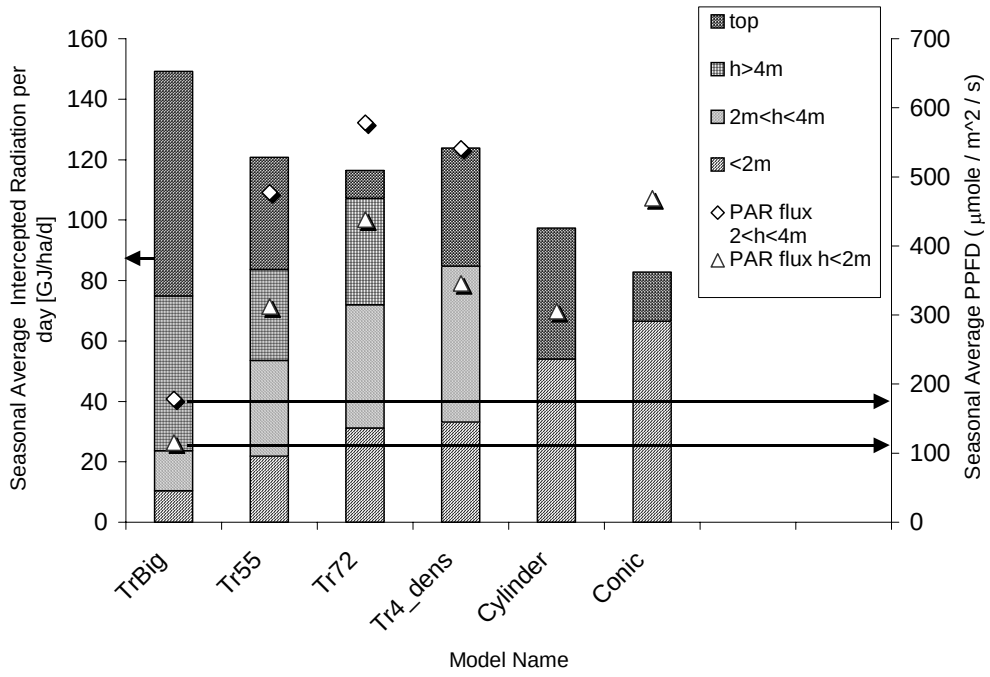

Figure 29 – Intercepted light at various heights of representative models described in table 8.

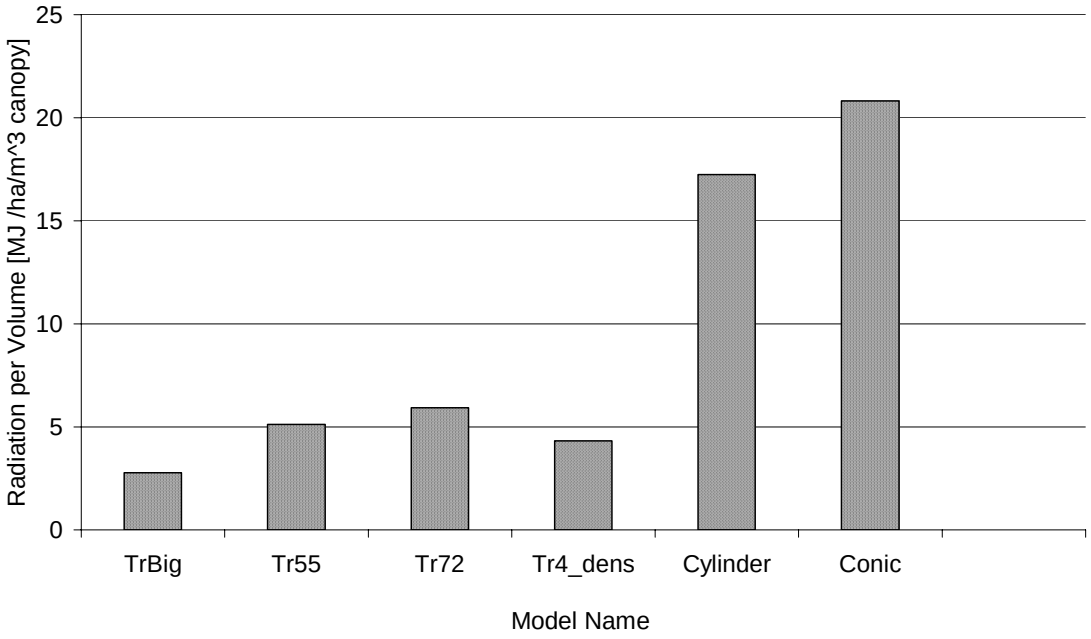

Figure 30– Total specific light intercepted per hectare in the models described in table 9.

Figure 30 depicts the total average intercepted radiation per unit canopy volume. The specific average intercepted radiation can supply a hint as to how much radiation an average cubic meter of canopy recieves. As we can see, smaller trees receive larger amounts of radiation per m^3 of canopy, up to twice or three times more then the large hedgerows. However, this index does not pay significance to the nature of light penetration into the canopy, and for areas which lack sufficient light for photosynthesis.

3.2 Light penetration into the canopy

3.2.1 Experimental results

3.2.1.1 Field measurements of light penetration

Light interception by the canopy is not a sufficient parameter for deciding which orchard planting strategy maximizes 'sun harvesting'. Planting density is certainly a key parameter for maximizing light interception, but since the Avocado canopy is extremely dense intercepted radiation may not penetrate deep into the canopy and many parts of the tree might prove redundant as far as effective photosynthetic process is considered. Some parts of the tree may even be regarded as parasitic, i.e. consuming water, nutrients, and photoassimilates without contributing to primary production.

Light penetration measurements were done in a hedgerow plantation in kibbutz 'Shomrat' where both pruned and unpruned faces were measured. Small single leader trees were measured as well. Additional measurements were done at the beginning of the growing season (June).

The measurements, as described before, covered a 192x15 points cross section grid that was translated into half-tree crossection contour lines using the 'Surfer' v.8 software (Golden Software, Golden, CO.). All together, 96 cross sections were collected and the results presented below are representative samples.

Each contour represents the fraction of the solar radiation that penetrated to that measured simultaneously outside of the tree silhouette (contour spacing is 10%). The dotted line represents 20% of external light, or approximately 500 μEinstein (~100W/m^2). This value is normally considered the threshold for significant photosynthetic activity in Avocado. The outmost tree contour was chosen as the 95% contour, i.e. any grid point with less than 95% of the clear sky radiation is considered 'canopy'. Grid points are transformed into a continuous contour using the 'Natural Neighbor' interpolation method, hence the smooth contours.

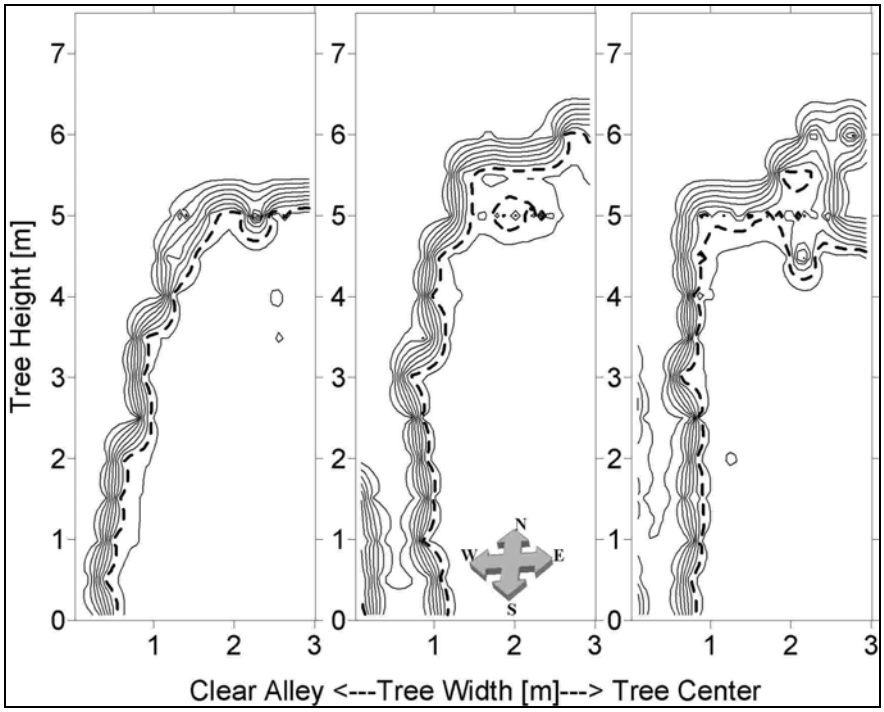

Figure 31 – Iso-luminance contours of half-tree cross sections based on measurements done on the 3/9/2003 in 'Regba' orchard, CV. Hass; pruned hedgerow; three different cross sections from the same row.

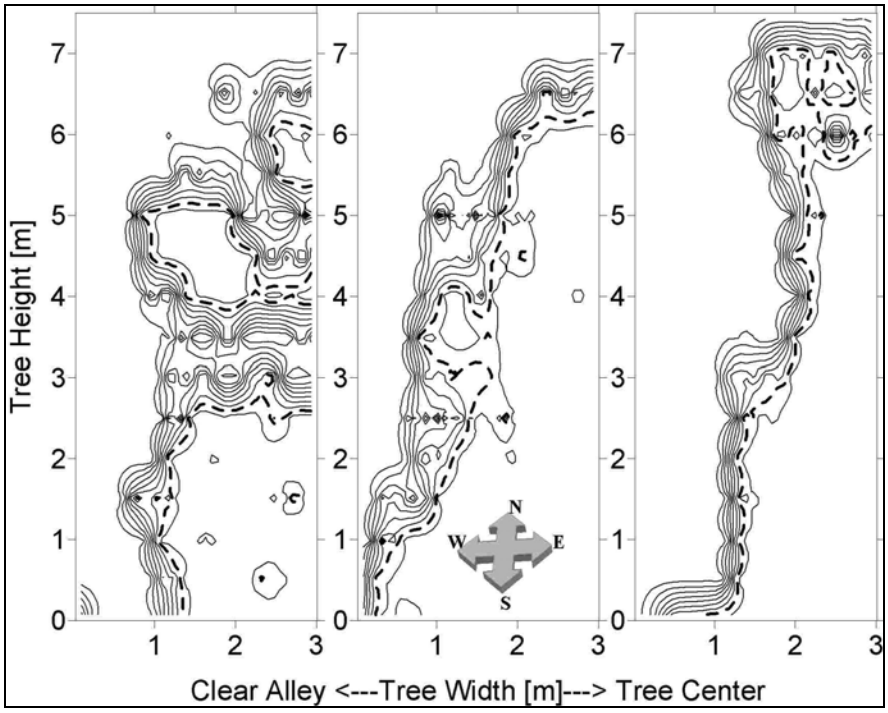

Figure 32 – Iso-luminance contours of half-tree cross section measurements done on the 10/9/2003 in 'Shomrat' orchard, CV. Hass; pruned hedgerow; three different cross sections from the same row.

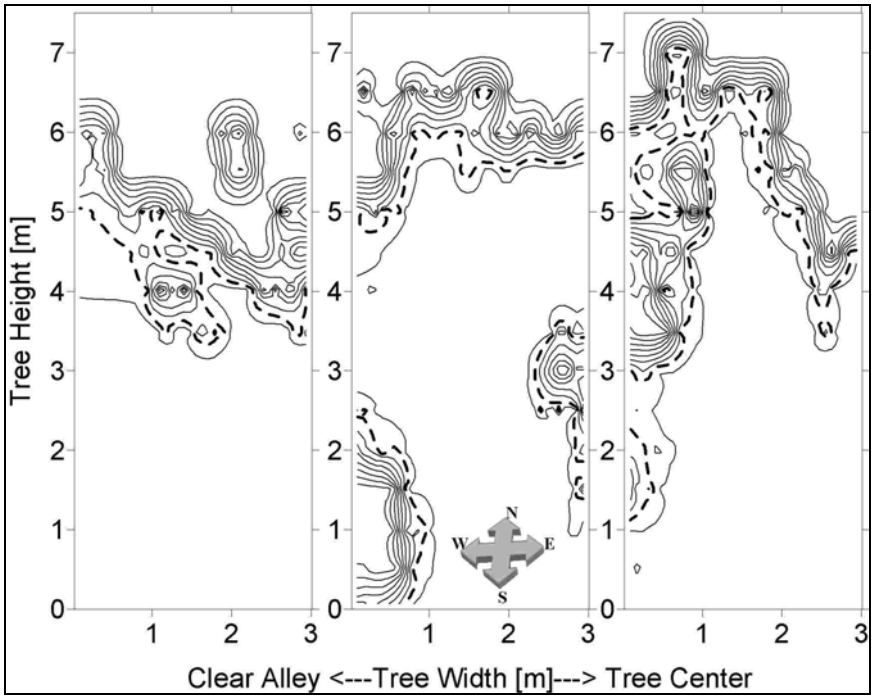

Figure 33– Iso-luminance contours of half-tree cross section measurements done on the 11/9/2003 in 'Shomrat' orchard CV. Hass; unpruned hedgerow; three different cross sections from the same row.

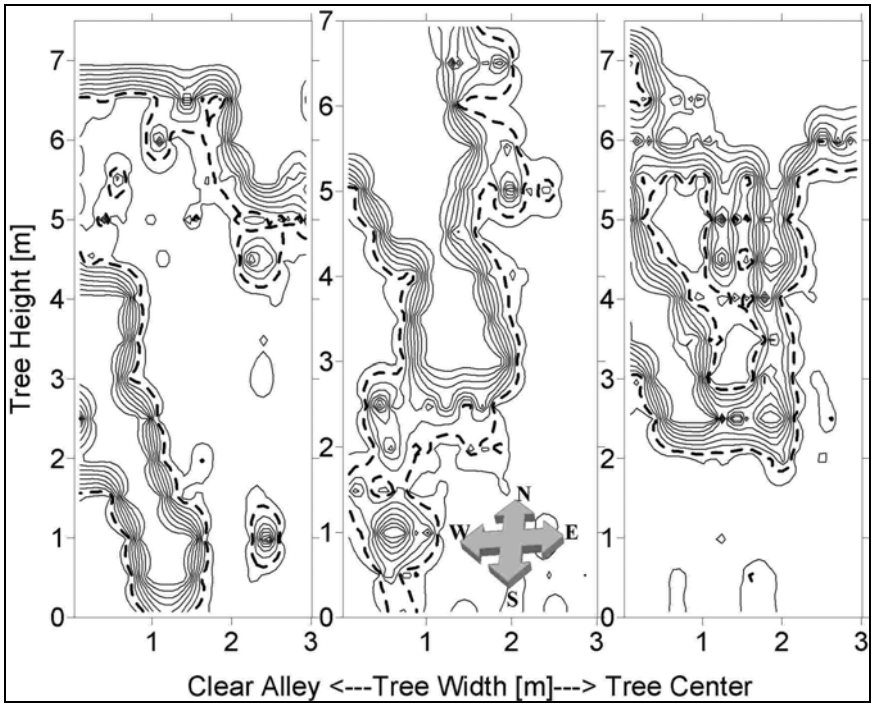

Figure 34 – Iso-luminance contours of half-tree cross section measurements done on the 16/9/2003 in 'Shomrat' orchard, CV. Hass; selective limb removal; three different cross sections from the same row.

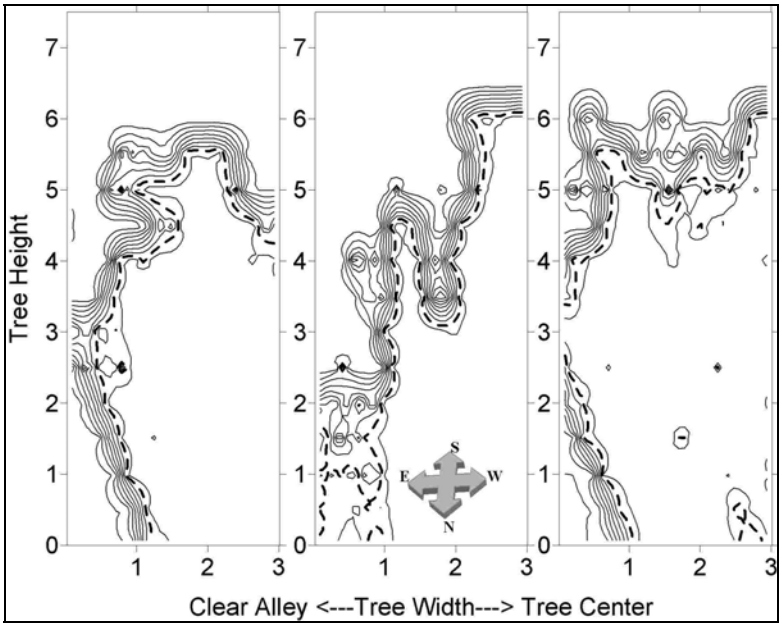

Figure 35 – Iso-luminance contours of half-tree cross section measurements done on the 7/6/2004 in 'Shomrat' orchard; CV. Hass; pruned hedgerow; three different cross sections from the same row.

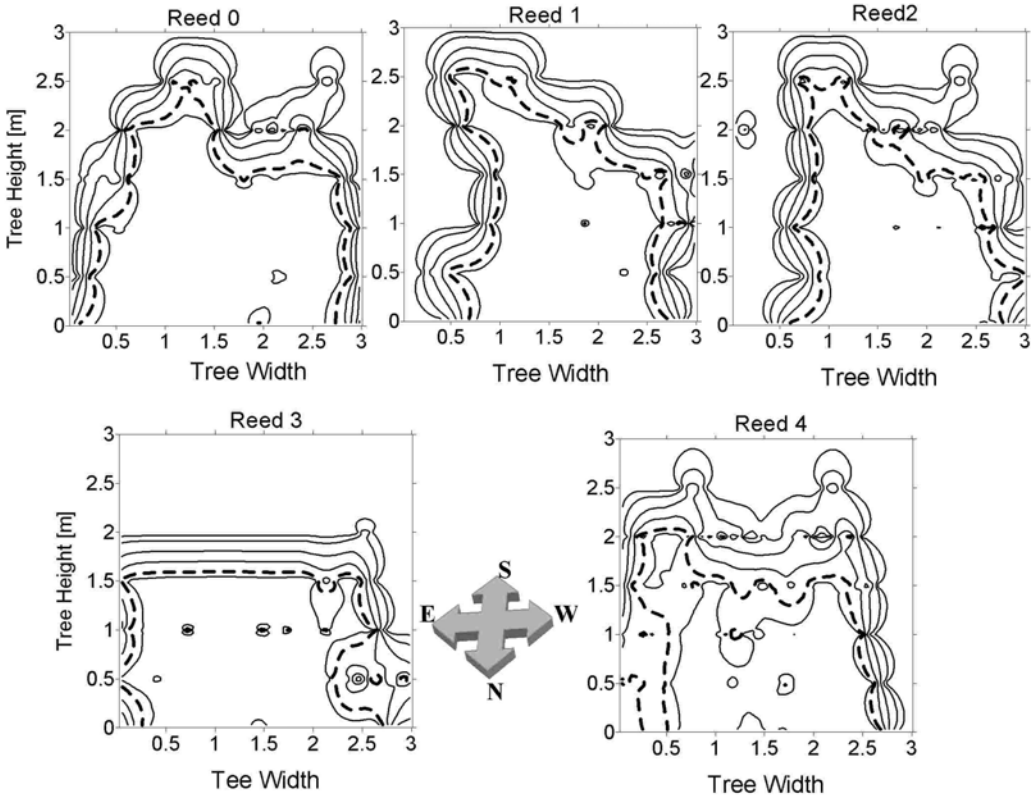

Figure 36 – Iso-luminance contours of full tree cross section measurements done on the 7/6/2004 in 'Shomrat' orchard; CV. Reed; small trees.

Figure 31 - 32 show a typical behavior of light in pruned Avocado hedgerow. The canopy creates a thick uniform mass of leaves along the outer contour of the canopy, causing light to extinct to 20% of its ambient level within a very short width that ranges from 20cm to 1m. The hedge is characterized by a nearly vertical canopy 'wall' – even in cases were the canopy was pruned at a non-vertical angle. Figure 32 demonstrates 'canopy windows' enable light penetration deep into the canopy, creating 'patches' of light in the middle of the canopy.

Figure 33 demonstrates the fate of an unpruned hedge. Not pruning and shaping the row made it a horizontal 'roof', intercepting the entire solar radiation within the canopy's upper meter or so. Since this row is alternately pruned (as part of an independent experiment lead by Dr. Gad Ish-Am), the canopy is not completely blocked and a few 'windows' are present, enabling light penetration into the canopy.

Figure 34 demonstrates the 'selective limb removal' technique, also known as the 'the Israeli method', which basically requires manual removal of large limbs or leaders by an experienced planter. This pruning method results in the formation of 'windows' in the canopy, through which light can penetrate into the canopy and promote juvenility and growth. As can be seen, the trees are not well defined, since trees are not separated by wide rows. Large patches of light within the tree canopy are clearly visible. Note that the limb removal technique results in lowering of the trees, but since this technique hasn't been practiced for many years the trees are still large (>7.5m).

Figure 35 presents results from the same locations as those corresponding to Figures 31-32 but taken a year later and on a different season. Light penetration seems similar. A more rigorous comparison of these results will be presented later.

Figure 36 demonstrates the behavior of light in a small 4 year old 'Reed' cultivar. The trees represent well the 'single leader' trees used in high density planting. Here, too, light penetrates about 0.5 m into the canopy. The tree's apparent inclination to the left reflects the time of measurement, which was slightly after the solar noon (left side represents the east) causing self shading in a few of the cases.

3.2.2 Light penetration along the day

Light penetration measurements at a given cross section were taken at 1 hour intervals between 09:20 and 13:20 on 8/6/2004. The results are presented in Figure 37. The thick line represents the 95% contour at 12:30 – around the solar noon, which is assumed here close to the canopy's outer boundaries. The dotted line is the 100 W/m^2 or (~500μEinstein/m^2/s) contour.

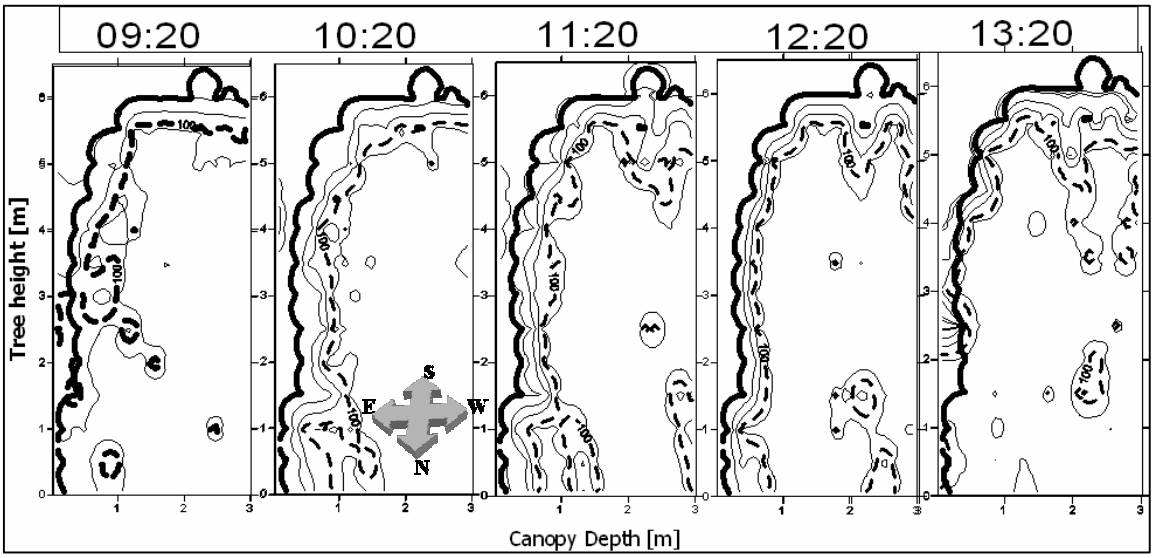

Figure 37 – A diurnal series of contours of light penetration into half-tree cross section based on measurement done on the 8/6/2004 between 09:20 and 13:20 in 'Shomrat' orchard, CV. Hass.

At 09:20 the tree is still shaded by the row to its east, as seen by the shadow outside of the tree canopy boundaries, and light penetration occurs mainly through the top-eastern (top left) faces. At 10:20 and 11:20 the opposite row is barely visible (it is 'peeking' from the left side), hence the entire eastern side of the row is illuminated. At 11:20 – 12:20 the sun is high in the sky and light penetrates mostly from the top. A 'window' in the canopy exists in the top right side, as can be seen by the deep light penetration, and light patches are visible near the ground. At 13:30 the sun moves to the west and the shading that's apparent in the left side is the tree shading upon itself.

A RMSE test between measured and simulated readings, in a manner described in 2.2.4, was preformed and yielded an average RMSE of ~90 W/m^2 or(~22% of external short wave radiation).

3.2.3 Extinction of light in the canopy: experimental results

In order to enable modeling of light penetration into the canopy, the extinction coefficient needs to be found following eq. (3). Assuming logarithmically spaced leave density intervals seems to be supported by the contours presented above, since light penetration at most cross sections seems to be similar. The method, as described in section 2.1.4, included averaging the relative radiation of the central 50 cm of the canopy around the solar noon, thus getting a plot of decreasing light levels along a light path starting at the top of the tree (where the relative radiation equals 1). Measurements were taken at 0.5 m steps into the canopy. The results are presented as a row or a face average, and are fitted with exponential regression.

Table 9 presents experimental data and their matched light extinction coefficient. The agreement between the data and the exponential curve is high in most cases, especially when considering the fact that this is a biological system with much variability. When comparing regressions based on a single cross section and on a row averaged data we can see that the extinction coefficient slightly decreases. The same tendency is apparent when aggregating all the data. This is mainly due to the fact that more incidents of 'light spots' deep in the canopy enter the calculation. Being interested with an average parameter, including deep penetrating light patches seems more representative of actual Avocado canopy.

The extinction coefficients measured on September are somewhat larger then those measured in June (see Table 9), which probably reflects growth. The September measurements that took place after the summer growth presented a higher extinction coefficient (k =1.86) while the June measurements of the 'Hass' and 'Reed' yield lower values (k =1.56 and k =1.52, respectively).

When aggregating the entire data, the results change somewhat (see Figure 38 - Figure **40**). The September measurements that included many more cross sections yields a lower extinction coefficient (k=1.17) while the June measurements of the 'Hass' and

'Reed' yield higher values (k =1.29 and k =1.52, respectively). The lower value of the September calculated extinction coefficient is due to larger number of crossections out of which the extinction coefficient was extracted. The slightly higher value of the small 'Reed' trees is due to their increased vigor that creates a denser canopy.

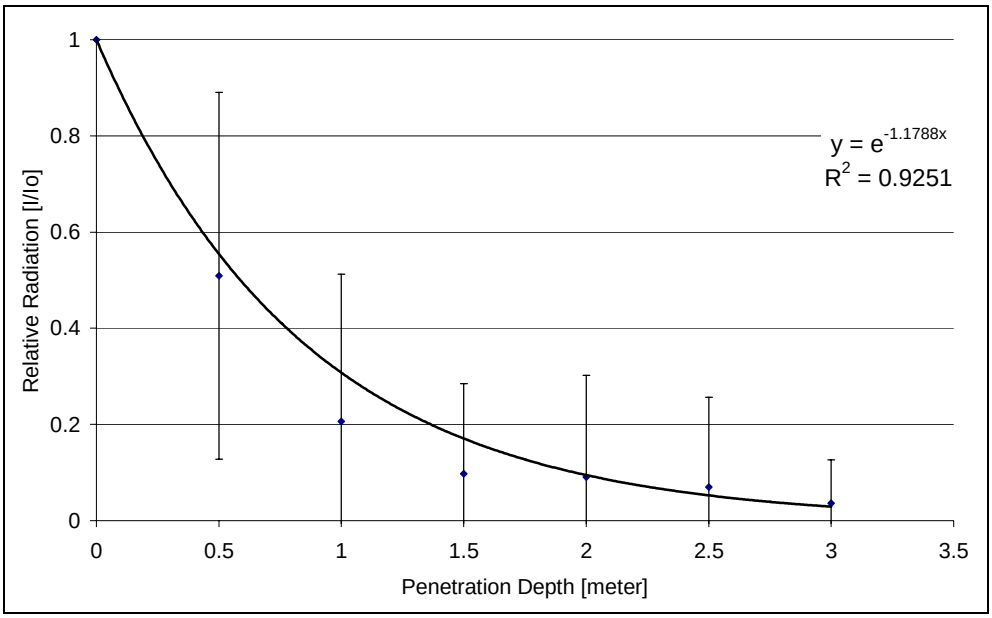

Figure 38 – Relative irradiance in different depth of the canopy as measured on the 3-16/9/2003; 'Shomrat orchard', CV. 'Hass'.

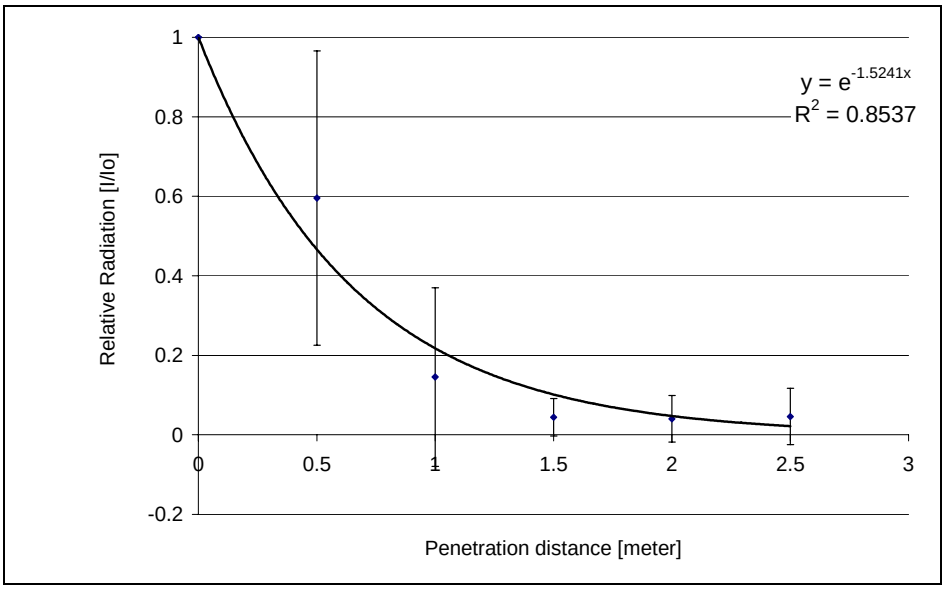

Figure 39- Relative irradiance in different depth of the canopy as measured on the 7/6/2004; 'Shomrat orchard', CV. 'Reed'.

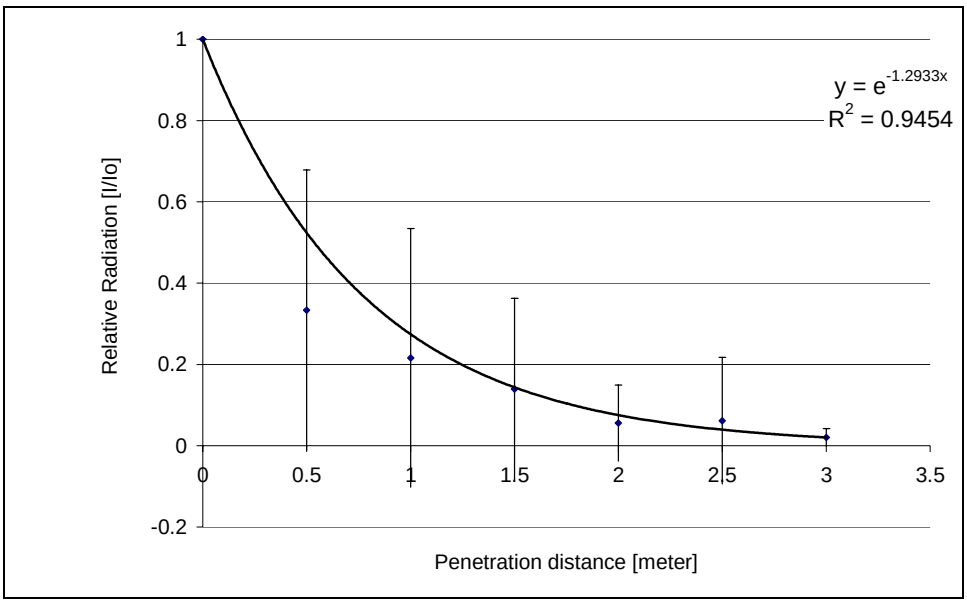

Figure 40 - Relative irradiance in different depth of the canopy as measured on the 7/6/2004; 'Shomrat orchard', CV. 'Hass'.

3.2.4 Assessment of cumulative LAI from the experimental results

Figure 41 depicts the cumulative overlying LAI as computed using eq. 3, from light attenuation within the canopy. The data represent measurements taken at the central 50 cm. of the canopy around the solar noon, averaged over about 40 cross sections. The ELADP value was estimated, using leaf inclination measurements, as 2.3. Light is attenuated rapidly up to a distance 3-4 m from the surface, representing a cumulative average value of about LAI=5 ± 1.1. This result might be slightly lower in reality due to the presence of large woody structure.

Figure 42 depicts the cumulative LAI from 3 different half-cross sections of Avocado trees, as computed using eqs. (3) - (4). As stated before, this method of assessing the cumulative LAI is taken from horticulture and therefore might show valid trends, but can have errors as for absolute values. From Figure 42 we can see that the change in LAI is rapid around the tree canopy envelope. The LAI increases to 4-5 over the course of 2m from the outer canopy envelope, where most of the Avocado canopy is located. These values though might be over estimation due to shading caused by the trunk and major branches.

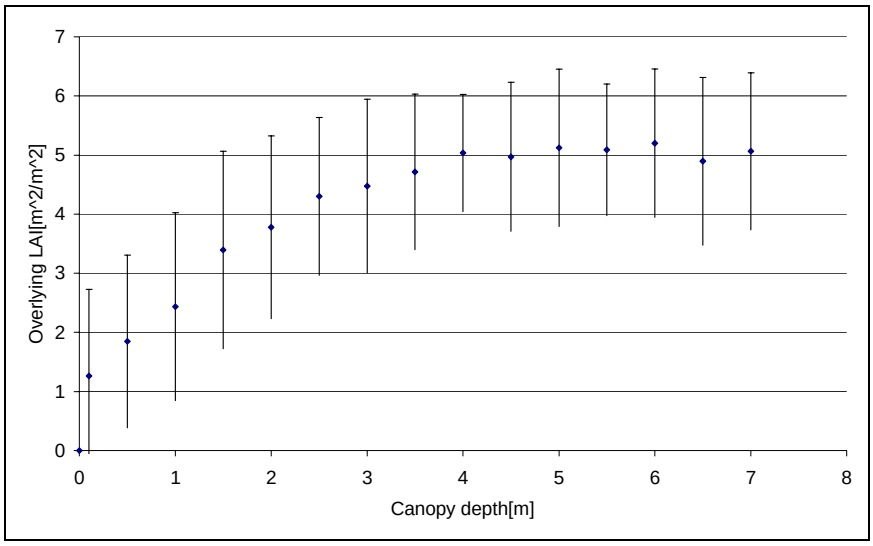

Figure 41 – Average cumulative overlying LAI for different penetration depths, with STDEV.

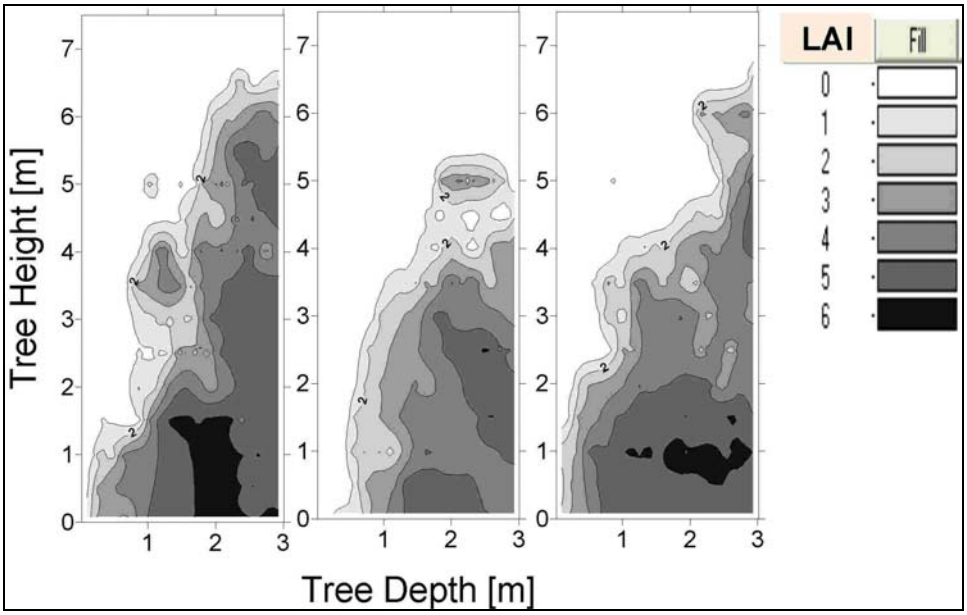

Figure 42 – Cumulative LAI for representative half-tree cross sections.

3.2.5 Computer simulation results

3.2.5.1 Correlating field data with "MIST" extinction parameter

In order to find the appropriate extinction coefficient to be used for the 'MIST' material within 'RADIANCE', the morphological and spatiotemporal location of the orchard were

modeled. A grid mimicking the exact position of the measurement grid was built and simulations were made on this model with changing extinction coefficients. The 'root mean squared error' (RMSE) between the measured and simulated penetrating light was calculated for different extinction coefficients. The minimal error coefficients are presented in Table 9**.**

The main reason for the extinction coefficient minimizing the RMSE between measured and simulated data ($k_{\text{"Radiance"}}$) being smaller then the extinction coefficient computed from the canopy central 50cm.data (k) is the presence of 'light spots' in the depth of the canopy. Since the trees are modeled in 'Radiance' as homogeneous opaque objects (the field measurements only provide us with the outer silhouette of the tree), light extinct from the outer surface into the tree depth and no direct light is found inside the canopy. Therefore the existence of 'light spots' in the actual readings can not be foreseen and their presence will cause a lower simulated $k_{\text{"Radiance"}}$ to have the minimal RMSE. The average discrepancy between the simulated and measured extinction coefficient is less then 25%, and for a biological system, with great variability in branching patterns this discrepancy is acceptable.

Table 9 – light penetration into the canopy. Comparison of measured extinction coefficient ($k_{Physical}$) and the simulated extinction coefficient ($k_{"Radiance"}$).

Date	Cross section	k_l	$k_{"Radiance"}$	Discrepancy [fraction]
08/09/2003	W1	2.08	1	0.52
08/09/2003	W3	2.26	1.5	0.34
08/09/2003	W8	1.94	1.5	0.23
08/09/2003	W9	1.51	1.5	0.01
08/09/2003	e2	2.53	2	0.21
08/09/2003	e3	1.85	2	0.08
08/09/2003	e4	1.75	1	0.43
08/09/2003	e5	0.88	1	0.14
08/09/2003	e6	1.34	1	0.25
08/09/2003	e7	1.07	1	0.07
10/09/2003	e3	1.13	1	0.12
10/09/2003	W2	2.10	2	0.05
07/06/2004	e0	1.4	1.5	0.07
07/06/2004	e5	1.38	1.5	0.09
07/06/2004	w2	2.10	3	0.43
07/06/2004	Fuerte 0	1.30	1	0.23
07/06/2004	Fuerte 1	0.93	1	0.08
07/06/2004	Fuerte 4	1.16	1.5	0.29
07/06/2004	Reed0	1.64	2.5	0.52
07/06/2004	Reed3	1.40	2	0.43
Average				0.23

3.2.6 Modeling the Potentially Productive Canopy Volume (PPCV)

Figure 43 describes the cumulative distribution function of the number of hours the canopy volume per hectare stays above the threshold level for productive photosynthesis. Looking at the graphs representing the test models, it becomes apparent that there is a distinct difference between the curves representing the various hedgerow geometries and the high density orchard. For the hedgerow models, 50% of the canopy volume is potentially productive for 3.5, 2 and 1 hours for models Tr72, Tr4_Dens, and Tr55, respectively. Model TrBig doesn't reach PPCV fraction of 50% even for one hour throughout the growing season. In contrast, the high density models show PPCV fraction of 50% for 7 and 9 hours for the cylindrical and conical models, respectively. This difference may explain the reported high yields in high density orchards, and can suggest that the PPCV fraction and the duration of maintaining high PPCV fraction are good estimates of the system's efficiency.

Comparing Trbig with Tr55 emphasizes the great benefit in opening up the rows and cutting down the tree's height. Cutting down 2 m of the tree height and scaling down the canopy skirt from 6 m to 4 m enable larger fraction of the volume to significantly contribute to the photosynthetic process for longer periods of time. Comparing Tr72 with Tr55 demonstrates the importance of a sharp pruning angle. Changing the pruning angle from ~80^0 to ~70^0 (Tr55 and Tr72) while keeping the height at 5.5 m and the row width constant results in a greater volume at above threshold level of PAR for a longer period of time. Comparing Tr55 and Tr4_dens, which have the same height to row width ratio and the same pruning angle, demonstrates the benefit of lowering the rows height and increasing the planting density. The distribution of potentially productive hours is very similar between the models, but Tr4_dens, with the higher surface area, seems to have higher volume of potentially productive canopy.

Among the hedgerow models, the model with the maximal fraction of potentially productive volume for 1 hour (65%) is Tr72. Model Tr4_dens and Tr55 are slightly behind with ~50% potentially productive volume. TrBig has a significantly lower fraction of potentially productive volume for one hour, 33%.

Both the high density models reach nearly 100% of potentially productive volume, indicating that all the canopy volume is exposed to saturation levels of PAR for

at least 1 hour. All the canopy volume of the conical model is exposed to threshold PAR level for almost 3 hours.

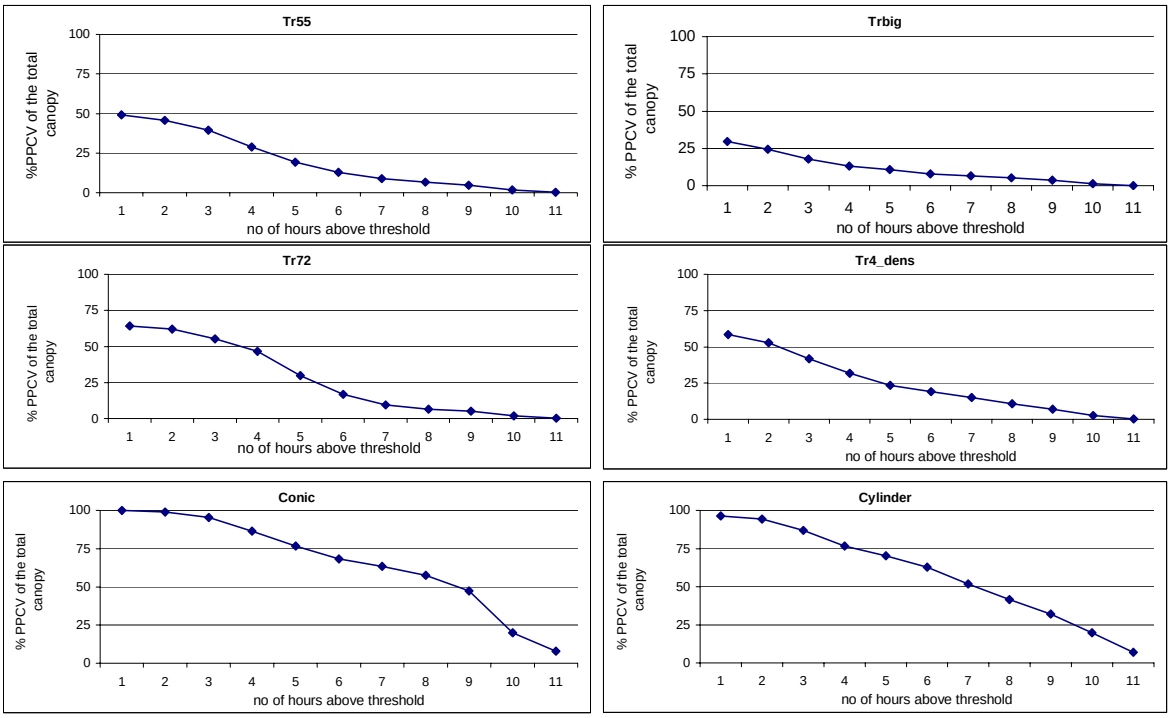

Figure 43- Cumulative probability distribution function of the fraction of potentially productive canopy volume under a range of potentially productive hours for the test models.

3.2.7 Potentially productive volume distribution with canopy height for a range of exposure times

The exposure time to radiation above threshold PAR and the patterns of light penetration into various heights of the canopy were computed. The simulation results presented in this chapter describe the seasonal diurnal average of the potentially productive canopy volume, and its partitioning width the canopy. The results describe the PPCV in terms of average potentially productive volume per hectare at the different height layers. The potentially productive fraction of the total canopy volume is presented in brackets.

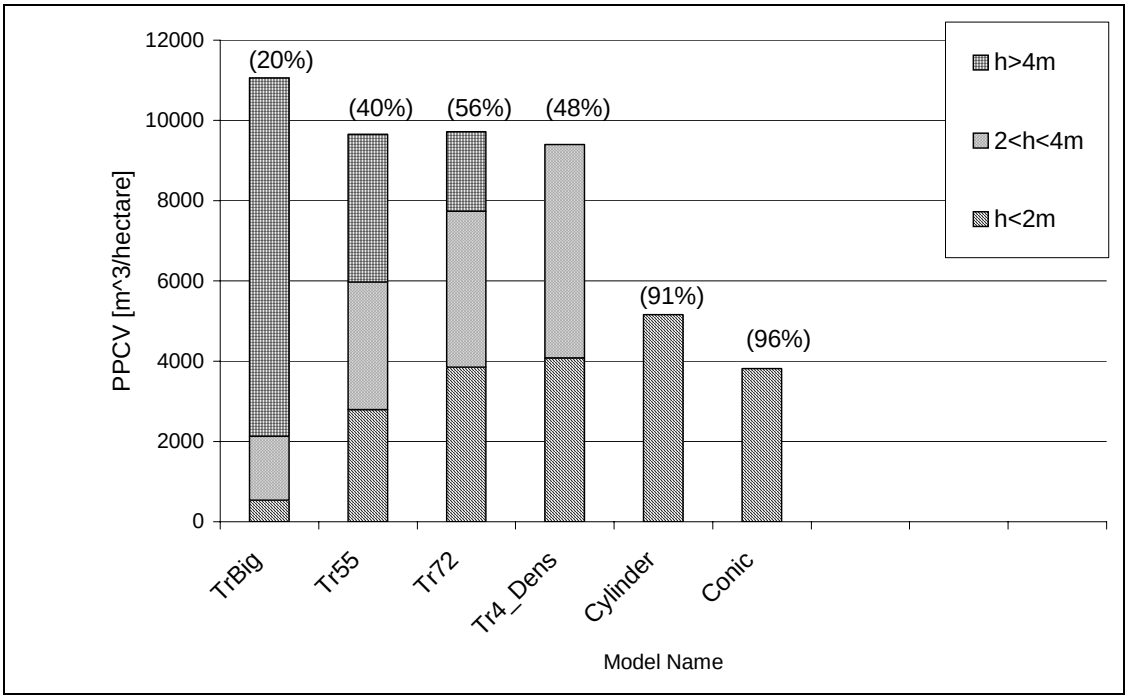

Figure 44 - PPCV per hectare at various canopy heights in selected models. Exposure time is larger than 2 hours/day. The fraction of the potentially productive part out of the total canopy volume appears in brackets.

From Figure 44 it is apparent that the model with the largest canopy volume (TrBig) has also the highest total PPCV, due to its largest total surface area. The total PPCVs of the other three hedgerow models are comparable, due to a similar surface area. The computed total PPCV of both high density models is much lower, around 4000 m^3/ha, due to their small volume.

Another parameter tested is the ratio between the potentially productive and the total tree volume maintained by it expressed as the PPCV fraction. The relative fraction of potentially productive volume out of the total canopy volume is 91% and 96% for the high density orchard (cylindrical and conical, respectively), indicating that most of the canopy volume is exposed to above threshold PAR for more then 2 hours. In contrast, for the three medium-height hedgerow models (Tr55, Tr72, and Tr4_dens) the fraction of potentially productive volume is in the range of 50%. Model TrBig shows the lowest fraction of potentially productive volume, 20%, due to its extreme internal shadowing and large total volume. A comparison between TrBig and Tr55 indicates the importance of maintaining a value of R in the ranges of 0.7-1. Tr55 (R=0.8) seems to have slightly

less total PPCV then TrBig (*R*=1.07), but twice its fraction of PPCV. It also shows a better distribution of the PPCV among the various height layers, demonstrating the benefit gained by maintaining trees with *R* values in the range of 0.7-0.9.

Fixing the pruning angle and *R* while planting a denser orchard of lower trees is beneficial, as canbe seen from a comparison of Tr55 and Tr_4dens. The shorter and denser orchard model is characterized by a higher fraction of PPCV together with improved distribution of the PPCV within the canopy. Comparing Tr55 and Tr72 implies at the importance of the pruning angle. The two models are similar in all parameters except of the pruning angle. Tr72 has a slightly higher total PPCV and a significantly higher fraction of potentially productive volume. The advantage of a large pruning angle is also expressed in the improved PPCV distribution along the canopy height layers. The same conclusions are drawn when comparing the cylindrical and conical models.

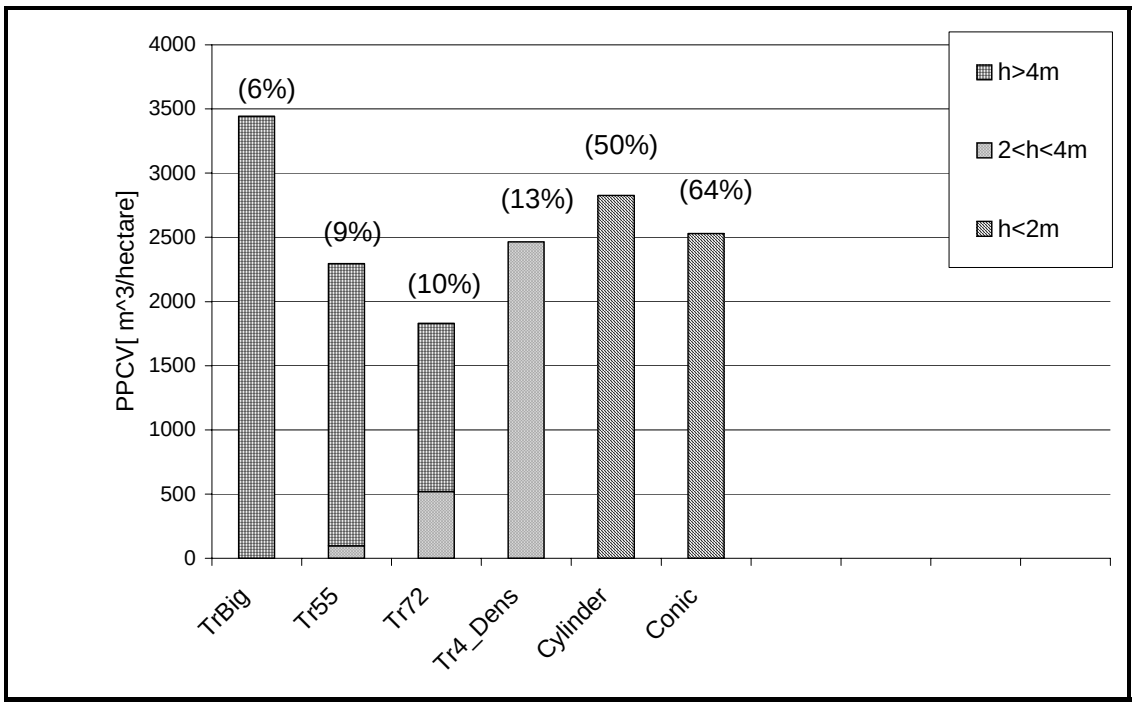

Figure 45 - PPCV per hectare at various canopy heights in selected models. Exposure time is larger than 6hours/day. The potentially productive part of the total canopy volume appears in brackets.

In Figure 45 we can see a total change in trends. The computed total PPCV of both high density models is higher than that of the medium-height hedgerow models. The combination of high surface area and low total volume reveals its real advantage –

maintaining a large portion of the canopy potentially productive for long exposure times. It is apparent that the total value of PPCV for the hedgerow models changes with the volume. The total PPCV is still largest for TrBig. Tr55 is predicted to have higher total PPCV than Tr72 – indicating that for time span of more then 6 hours the total canopy volume influences the PPCV more then the pruning angle.

The high fraction of the potentially productive volume out of the total canopy volume is in the high density orchard indicate that more than a half of the total canopy volume is exposed to above threshold PAR levls for more than 6 hours. In contrast, for the three medium-height hedgerow models (Tr55, Tr72, and Tr4_dens) the fraction of potentially productive volume is in the range of 10%. Model TrBig shows the lowest fraction of potentially productive volume, 6%.

PPCV at the lower 2 m of the canopy exists only in the high density models. The hedgerow models reveal a totally shaded lower canopy. PPCV at the 2-4 m height-layer of the canopy exists only Tr72 (~500 m^3/ha). And in Tr55 (~100 m^3/ha). Note that for Tr4_dens, the 2-4 m layer is the upper most layer of the tree and thus the PPCV at this layer in this model is very high.

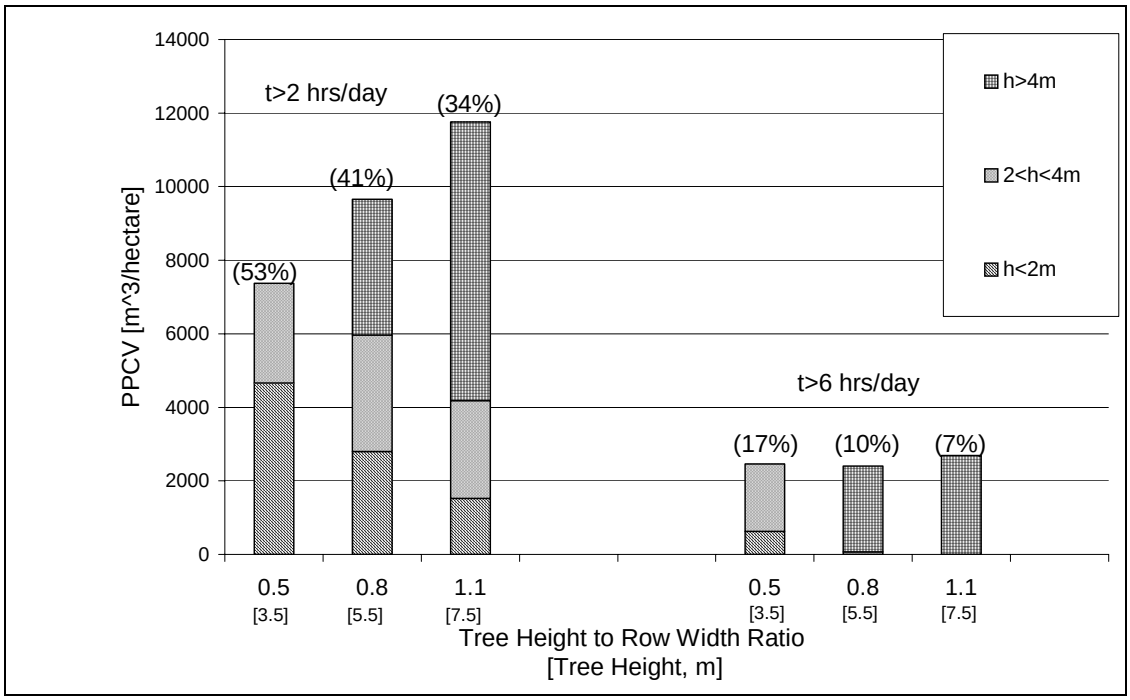

Figure 46 - PPCV per hectare at various canopy heights in models with changing *R* (row width is constant at 7m). Exposure time is larger than 2 hours/day (left) and larger than 6 hours/day (right). The potentially productive part of the total canopy volume appears in brackets.

In Figure 46 the results of simulating the influence of changing *R* (through changes in the tree height) on the PPCV for two exposure periods are presented. Considering exposure periods larger than two hrs/day (left), the total PPCV increases with tree height whereas the opposite is true for the PPCV fraction. The distribution of PPCV at the lower parts of the canopy was the highest for the short tree (low *R*), decreasing gradually with the increase in the tree height (and *R*). In the 7.5 m tree, most of the PPCV is found higher than 4 m above the ground. For exposure periods larger than six hrs/day (right), the total PPCV is much lower, as expected, and is almost independent of tree height. The PPCV fraction is proportionally much higher for the low tree model. In the short tree model, all the PPCV is in the 0-4 m height layer while in the medium and high tree models it is above 4 m from the ground. Clearly, an advantage for the shorter trees exists, especially when long exposures are considered.

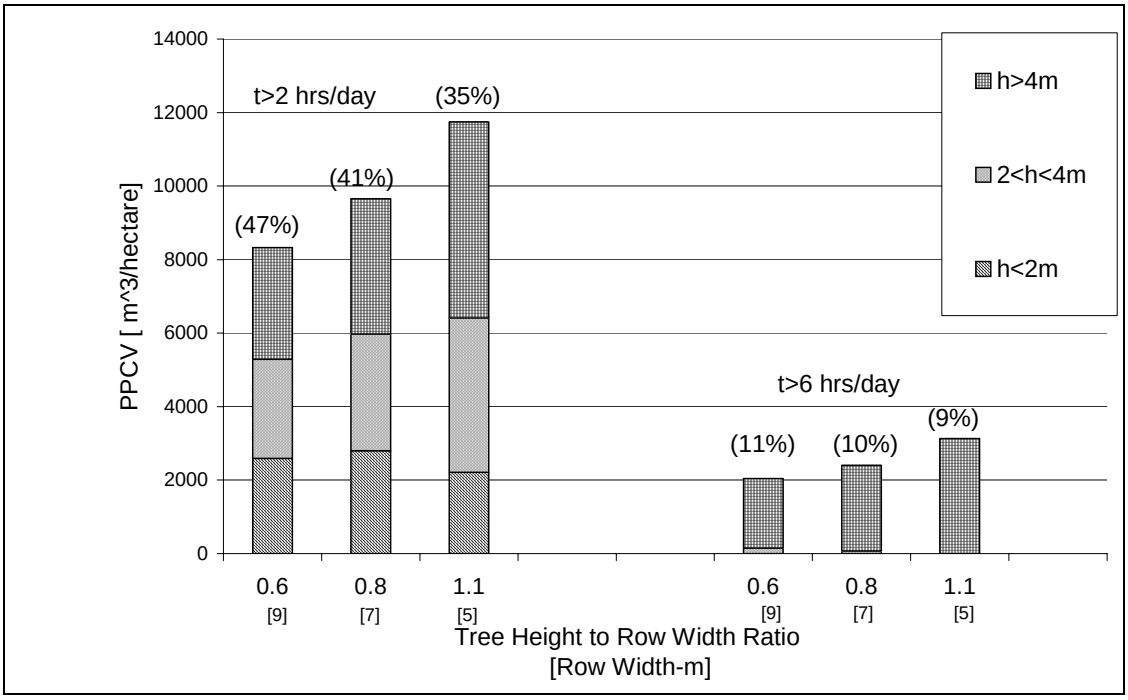

Figure 47 - PPCV per hectare at various canopy heights in models with changing *R* (tree height is constant at 5.5 m). Exposure time is larger than 2 hours/day (left) and larger than 6 hours/day (right). The potentially productive part of the total canopy volume appears in brackets.

In Figure 47 the results of simulating the influence of changing R via changes in the row width on the PPCV for two exposure periods are presented. Considering exposure periods

larger than two hrs/day (left), the total PPCV decreases with the increase in row width (decrease in *R*) and the opposite is true for the PPCV fraction. The distribution of the PPCV at the lower parts of the canopy is marginally effected by the change in the row width. This results from the opposite effects of the decreasing canopy volume (per hectare) and the reduced shading due to opening the rows.

For exposure periods larger than 6 hrs/day (right), the total PPCV is significantly lower, and slightly decreases for increased row width. The PPCV fraction is essentially independent of variations in the row width. All the PPCV in the three models examined was above the 4m height layer. In terms of total PPCV, these simulation results indicate a clear advantage for dense planting (higher *R*) for any exposure period.

Examining the results presented in Figure 46 and Figure 47 in terms of the PPCV distribution within the canopy, dense planting (narrow rows) of smaller trees seem to be clearly advantageous for both long and short exposure periods.

3.2.8 The dynamics of the PPCV along the day

Figure 48 and 49 depict the diurnal penetration of the PAR into the hedgerow models into the high density orchard respectively. Model Tr72, representing the hedgerow models, is characterized by symmetry in the penetrating radiation between the morning hours (on the eastern face) and the afternoon hours (on the western face of the row). The top of the canopy receives radiation most of the day. This is due to the fact that the hedgerow is oriented in a N-S direction. Light penetration into the canopy at the inter-row faces of the hedge is the largest at 10:30 and at 14:30, when the sun-grazing angle is optimal for light interception of this model. Radiation penetration is maximal at the top of the canopy during the solar noon. The dotted line represents the model PPCV (the 500 μEinstein/m^2/s contour).

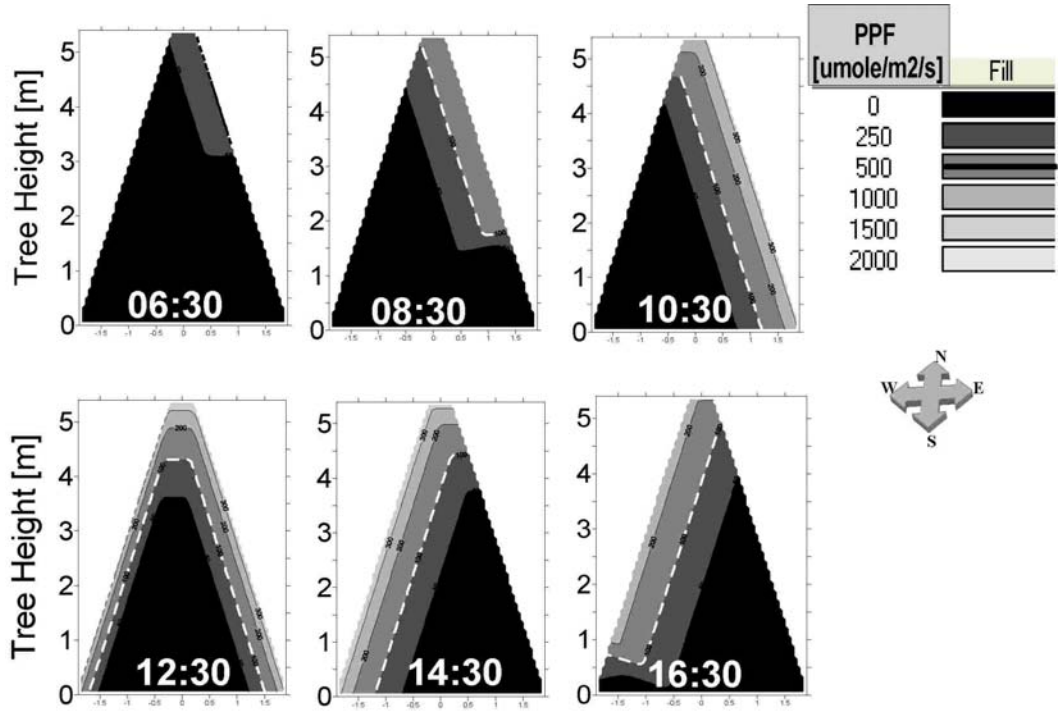

Figure 48 – Simulation of diurnal changes in the extinction of solar radiation within the canopy of model Tr72.

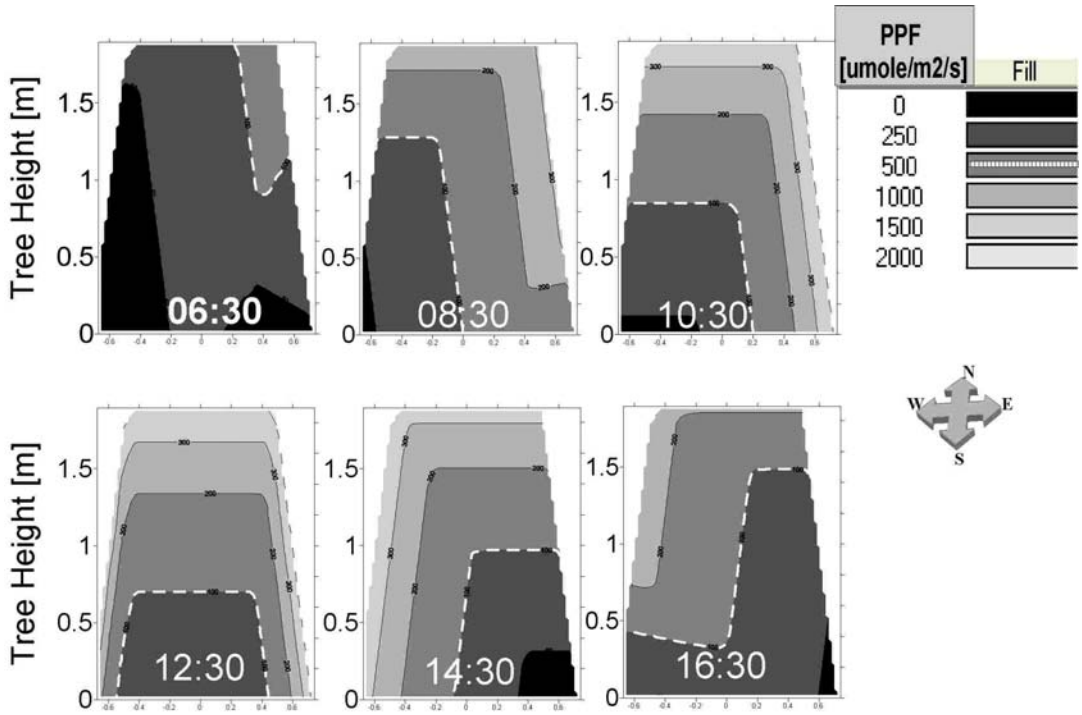

Figure 49 - Simulation of diurnal changes in the extinction of solar radiation within the canopy of the conical high density model.

Examining the simulated results for the individual conical tree model, the influence of the diurnal solar movement is apparent. In the early morning hours the western side is shaded and in the late afternoon the eastern side is shaded. However, because of the small diameter of the tree, 1.5m at the bottom and 1m at the top, solar radiation can penetrate deep into the tree volume. The broken line representing the PPCV contour encircles only a small core of the tree. During noon hours, the non-PPCV contour recedes to a small volume at the bottom of the tree.

Figure 49 shows that for a N-S hedgerow, light penetration into the canopy is symmetrical around the solar noon. Maximal PPCV occurs at 10:30 and 14:30, where the tree surface is at the optimal grazing angle, and not at the solar noon, where the radiation intensity is maximal. For an E-W hedgerow, light penetrates the canopy mainly around noon and only through the southern face. For most of the daylight hours, most of the penetrating radiation is through the top of the canopy.

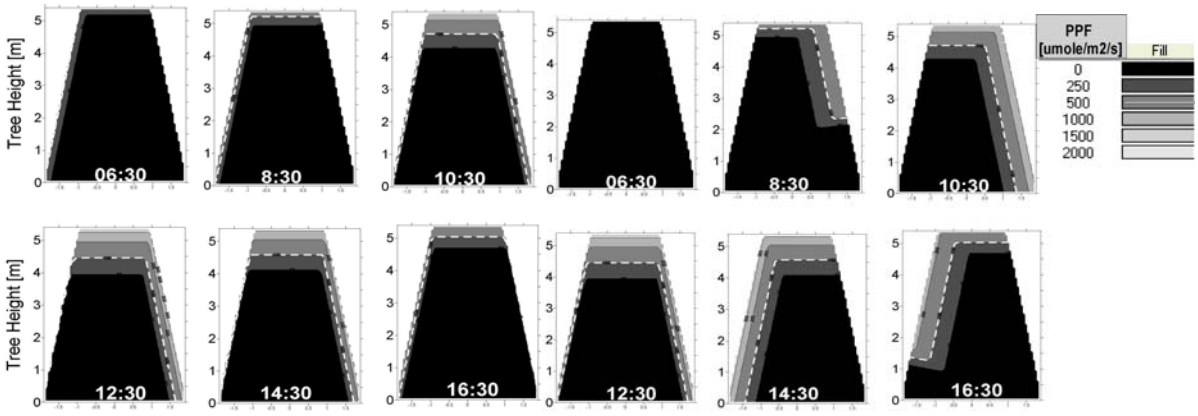

Figure 49- The effect of hedgerow orientation on simulated diurnal changes in the extinction of solar radiation within the canopy. The simulation is for model Tr55, a N-S hedgerow (right), and an E-W hedgerow (left).

3.2.9 Exposure duration of PPCV

Figure 50 reveals the exposure duration of different parts of the canopy to PAR above the threshold level. It appears that the canopy volume that is potentially productive for long periods of time (larger than 4 hours) in TrBig is located only in the upper most 1 m of the tree. Comparing TrBig and Tr55, we can see that by lowering the tree height and enlarging the work row exposure for long periods of time (PPCV) expands to the middle part of the tree outer surface. The lowering of the PPCV near the tree envelope is also apparent in model Tr4_dens, which has the same height to row width ratio and the same pruning angle as Tr55, but represent an orchard with narrower rows. Pruning the hedge to a sharper angle (Tr72) is accompanied by a PPCV that extends down to the bottom of the canopy outer 'skirt'. For the high density models, the PPCV both occupies most of the canopy volume and last for longer hours. Deeper penetration of light into the core of the canopy is apparent for the conical model compared to the cylindrical model.

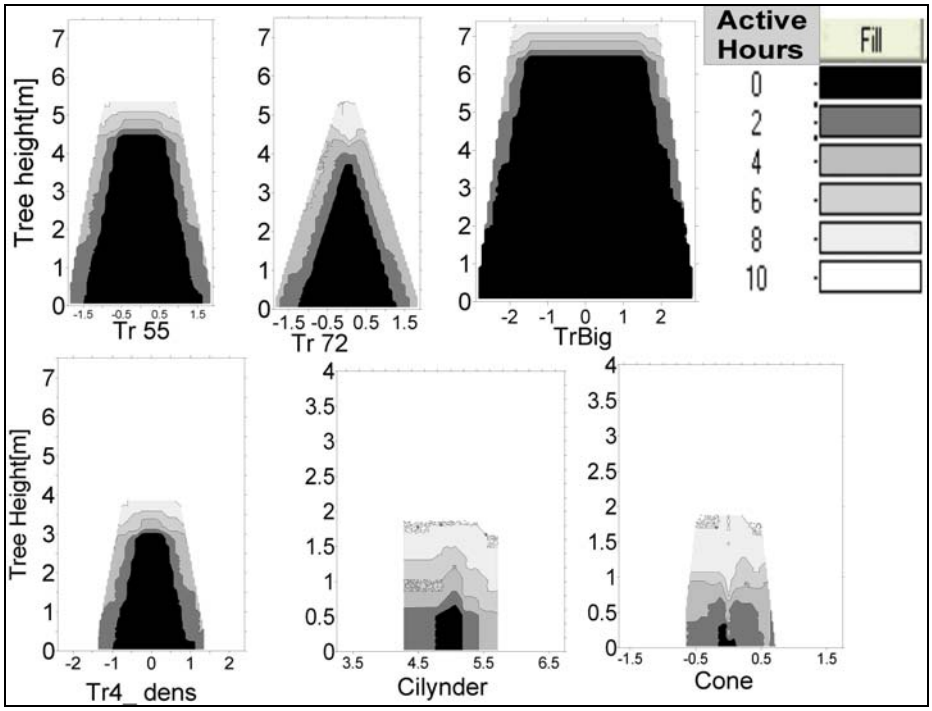

Figure 50 - Seasonally averaged daily exposure for PAR above the threshold level in selected models.

3.2.10 Summary

Simulation results of the dynamics of the potentially productive canopy volume (PPCV) make it possible to better understand and control the parameters that govern light penetration into the Avocado canopy. Table 10 presents main geometrical and simulated radiation parameters. In the four hedgerow models examined, PPCV in the range of ~10,000 m^3/ha is predicted for at least 2 hours. For the high density models, comparable PPCV values are in the range of 4000-5000 m^3/ha. PPCV for at least 4 hours is predicted to decrease drastically, to 5500-6000 m^3/ha, in the hedgerow models. However, for the high density models, the PPCV for at least 4 hours decreases only slightly, to 3500-4000 m^3/ha. For exposure times longer then 6 hours the PPCV continues to decreases (3450 m^3/ha for TrBig model and ca. 1800-2450 m^3/ha for the other hedgerow models). At the same time a PPCV value of about 2500 m^3/ha has been computed for the high density models. Under these conditions, the PPCV of the high density orchard was higher than for the medium-height hedgerow models.

In general, we can conclude that the practices contributing to increased total penetrating radiation and its distribution to the bottom of the canopy in hedgerows are (1) lowering of the tree height, (2) dense planting, and (3) angled pruning. When comparing the hedgerow and high-density practices we can see an advantage to hedgerow plantation when short exposure times are considered. This advantage diminishes when longer exposures are accounted for. The fraction of the PPCV out of the total canopy volume follows the pattern of the PPCV. For the medium-height hedgerow models the PPCV fraction decreases from 50%, for exposure time of at least 2 hours, to 30%, for exposure time of at least 4 hours, and to only 10% for exposure time of at least 6 hours. For the high density models, the PPCV fraction decrease from 90-95% to 70-84% and 50-64% for exposure times of 2, 4, and 6 hours, respectively. For the TrBig model the comparable values are 20% for exposure time of at least 2 hours, 8% for exposure time of at least 4 hours, and to 6% for exposure time of at least 6 hours. These results indicate a much higher efficiency of the high-density models over the hedgerow models. This advantage is maintained over all the time periods inspected. The practices of lowering the tree height, planting densely, and angled pruning prove beneficial in this case as well. These conclusions are supported by Figure 50, predicting the PPCV to be located at the top of

the canopy and at its upper – outer envelope in hedgerow models, as oppose to the PPCV being located throughout the canopy in the high density models.

It is reasonable to assume that due to the high energetic requirements for the process of fruit bearing in Avocado, fruits would be located in canopy volumes exposed to above threshold PAR for relatively long daily hours. Based on our simulation results, in hedgerow trees such regions are found at the top of the tree (for TrBig model) and in the upper half of the canopy envelope (for the medium-height tree models). In the high density models the PPCV fraction exposed for 4-6 hours is in the range of 50-80%, suggesting that most of the canopy is exposed to above threshold PAR for such periods. Accordingly, in a high density orchard one would expect to find the Avocado fruit to be located throughout the canopy volume.

Examining the envelope surface area to volume ratio (S/V) reveals an agreement between high ratio and high PPCV fraction. Among the hedgerow models, these with a S/V ratio with values around 1 (Tr72, Tr4_Dens) had a higher PPCV fraction. The high density models have S/V ratios of around 3 and a considerably higher PPCV fraction than the hedgerow models.

Table 10 – Properties of simulated models.

Model	Surface Area [m^2/ha]	Volume [m^3/ha]	$\frac{\text{Surface Area}}{\text{Volume}}$ (S/V)	PPCV t>2hrs (% Potentially productive of total canopy) [Potentially productive_m^3/ha]	PPCV t>6hrs (% Potentially productive of total canopy) [Potentially productive_m^3/ha]
Tr55	18,865	23,744	0.79	9660 (40%)	2290(9%)
Tr72	17,237	17,463	0.99	9720 (55%)	1830(10%)
TrBig	27,332	53,570	0.51	11060(21%)	3440(6%)
Tr4_dens	19,300	18,000	1.07	9400 (52%)	2460(13%)
Cylinder	15,988	5,655	2.83	5160 (91%)	2830(50%)
Cone	13,480	3,980	3.39	3814 (96%)	2530(64%)

4 Summary

In this work a new model for mimicking the solar radiation balance of an Avocado orchard was developed. The model utilizes the state of the art software 'Radiance' (LBNL labs, Berkley, CA) and a specific code developed for tracing solar radiation dynamics. The major advantages of the model are:

- The ability to account for complex three dimensional geometries, thus making it possible to simulate close to real orchard designs.
- The ability to compare simulation results to actual field measurements, thus enabling a validation-calibration process for the model.
- The ability to trace not only the intercepted solar radiation, but by incorporation of a carefully designed semi transparent material to simulate the extinction of light as it penetrates into the canopy.
- The ability to position a virtual measurement grid enables getting a very high resolution and detailed picture of the spatial distribution of radiation intensities.
- The software being an 'open-source' code enabled us to add custom modules, such as the time-variation of the sun pathway during the day and along the season.

The limitation in using 'Radiance' is the use of optical parameters, rather then biological parameters, for the orchard trees, which requires that all the biological parameters (e.g. the LAI) be "translated" to optical parameters (e.g. the extinction coefficient).

The first aspect of optical behavior examined was the interception of PAR by the outer envelope of the canopy as a function of a range of agrotechnical practices. This parameter is used in models reported in the literature as the main decision parameter for selection or comparison between models with different geometries, planting density, etc.
The simulated total intercepted radiation represents the net solar energy reaching the canopy, and gives an indication of the canopy's gross photosynthetic potential. While the maximal amount of energy intercepted by the canopy is limited, its distribution along the canopy envelope could be influenced by some agrotechnical practices. The top of the canopy receives excessive amounts of energy, while its lower parts generally receive deficient amounts of energy. The effectiveness of a range of agrotechnical practices was evaluated using the new model in terms of their ability to direct substantial amounts of energy towards the lower layers of the canopy envelope. Simulation results indicate that

the range of agrotechnical practices examined (i.e., varying *R*, the pruning angle, etc.) has, as expected, a limited effect on the total energy intercepted by the canopy. However, some of these practices result in significant improvement in solar energy distribution (at the lower surfaces of the canopy) and therefore on the envelope-average radiation intensity.

A basic assumption in the present model is that it is possible to represent the extinction of radiation in the canopy as a process that decreases exponentially with distance, and therefore could be represented by one extinction coefficient. The dense and uniform nature of the Avocado canopy, as our field measurements indicated, justifies this assumption. Once fitted with this coefficient, diurnal simulations of radiation penetration into the canopy are possible. The concept of potentially productive canopy volume (PPCV) was introduced in order to estimate the part of the canopy volume that acts as a source, rather than a sink, to photosynthetic products. The PPCV was defined as the canopy volume receiving an energy flux above a threshold level. The latter was taken from photosynthetic response curves of isolated Avocado leaves and trees. The photosynthetic efficiency of the canopy was evaluated using two parameters:

- The percentage of the canopy potentially productive volume as a fraction of the total canopy volume.
- The distribution of PPCV within the canopy.

The effectiveness of the various agrotechnical practices was examined both in terms of their contribution to the photosynthetic efficiency and in terms of their influence on exposure durations to solar radiation above the threshold value at distinct canopy regions. The diurnal changes in the PPCV location within the canopy is used in order to identify parts of the canopy which are radiation deficient during various hours of the day.

The effectiveness of the agrotechnical processes on both the intercepted and the penetrated solar radiation was evaluated using six orchard models, representing hedgerow and high density practices.

The main conclusions from these simulations are:

Tree Height to row width ratio –

This important parameter in orchard planning was simulated by independently changing the tree height and the row width. Decreasing tree height from 7.5 m to 5.5 m and 3.5 m proved beneficial in terms of a significant increase in the daily interception and in the radiation intensity at the lower parts of the canopy envelope, with only a small decrease in the total intercepted radiation. The total PPCV exposed for more than 2 hrs/day decreased with decreasing the tree height although larger fractions of it reach in the lower parts of the canopy. An increase in the PPCV fraction (tree efficiency) is also evident. For the longer exposure period (t>6 hrs/day), the lower hedgerow(tree height of 3.5 m) has the same total PPCV as the higher hedgerow (tree height of 7.5 m) along with a higher PPCV fraction, indication for higher efficiency.

Decreasing the row width (and thus increasing the number of trees per hectare) increases the total intercepted radiation but does not change significantly the total intercepted radiation at the 0-4 m height layer. This insensitivity of the intercepted radiation at the lower layers stems from the counter influence of the increase in the surface area and the decrease in the radiation intensity due to increased inter row shading. When examining the effects of row spacing on the PPCV, for exposure periods longer than 2 hrs/day the total PPCV decreases with the increase in row width (decrease in *R*) while the opposite is true for the PPCV fraction. The distribution of the PPCV at the lower parts of the canopy was marginally influenced by the change in the row width. This results from the opposite effects of decreasing both the canopy volume and the inter-tree shading when the row width increases. For exposure periods longer than 6 hrs/day the total PPCV slightly decreases with the increase in row width whereas the PPCV fraction is essentially independent of row width. For the three models examined all of the PPCV was located above the 4 m height layer.

Comparing models Tr4_dens and Tr55, both having *R*~0.8 and the same pruning angle, the lower trees and the smaller row width in the Tr4_dens orchard result in an increased total daily intercepted radiation, an increased total daily radiation at the lower parts of the tree, and an increased radiation intensity at the lower canopy layers. When examining the

total PPCV and the fraction of the potentially productive volume in these models the trend is similar and an advantage for the smaller and denser model is apparent.

Planting orientation –

The known advantage of N-S hedgerow planting over E-W hedgerow planting was demonstrated. N-S hedgerows have symmetrical distribution of radiation on their eastern and western faces, while for E-W hedgerows the southern face intercepts much more radiation then the northern face. A higher total intercepted radiation per hectare and higher radiation intensities were computed for N-S hedgerows. N-S hedgerows also show higher total PPCV that is better distributed on the two row faces. N-S planting is superior when planting on slopes as well.

Pruning angle –

Simulation results for a range of pruning angles (pyramid to rectangle) showed that sharper angles (pyramidal cross section) increase the intensity of radiation received by the canopy and improve the distribution of total daily radiation within the canopy. Nonetheless, it is accompanied by a small reduction in the levels of total daily intercepted radiation. With respect to PPCV, the pyramidal model (Tr72) proved superior in terms of total potentially productive volume for short exposure period (t>2 hrs/day) but its small volume is a disadvantage when longer exposure periods are examined.

High density orchards –

This new practice in Avocado growing was tested over a range of models and planting densities. The tree height to row width ratio has principally the same trends as in the hedgerow models. The total intercepted radiation increases and the radiation intensity decreases as the planting density grows. Shaping the tree as a cone rather then a cylinder proved advantageous in increasing the radiation intensity but decreased the total intercepted radiation. The high density models seem to intercept less total radiation than most of the hedgerow models, due to lower ground coverage, but all of the radiation is intercepted at the 0-2 m height layer.

When examining the PPCV parameters, the high density models are expected to have smaller total PPCV than the hedgerow models for short exposure period (t>2 hrs/day),

but almost all of their volume receives radiation above the threshold level. For longer exposure periods the total PPCV of the high density models is the same as that of the hedgerow models, but the PPCV fraction is 5-6 times larger. These results indicate that the high density models are highly efficient w.r.t. photosynthetically produced matter.

4.1 Required further research

This thesis gives rise to a few research topics needed in order to improve the model and enable a more valid orchard planning policy. These topics include:

- Quantitative research evaluating the actual contribution of the PPCV and the demands of the 'parasitic' volumes in terms of photoassimilates, water nutrients, etc.
- Further investigation of the extinction of light as it penetrates the Avocado canopy, quantitative research as for its dynamics around the year and in various cultivars.
- Further research regarding the Avocado canopy leaves density, LAI and its distribution, leaf inclination distribution, and the bi-directional reflectance distribution function (BRDF).
- Better understanding of the energetic contribution of the 'potentially productive' canopy and the requirements of the non-productive canopy in order to enable full energetic balance.

5 Appendix

5.1 Reflectivity data

Table 11 – Canopy and ground reflectance as measured in September 2003 and June 2004 in 'Shomrat orchard'.

Test no.	Canopy	Ground
1	0.076	0.053
2	0.067	0.079
3	0.021	0.077
4	0.031	
5	0.101	
6	0.095	
7	0.176	
Average	0.081 +/-0.051	0.070 +/- 0.014

5.2 Fruit counting data

Table 12 – Fruit counts at various height layers for different treatments.

			Height Layer			
Date	Pruning method		h>4m	4>h>2m	h<2m	Total
11/2003	Changing Asymmetric (EAST)	average	12.7	21.0	21.1	54.8
		STDEV	22.3	33.9	36.9	92.0
	Changing Asymmetric (WEST)	average	25.0	17.6	12.9	53.0
		STDEV	36.5	19.1	14.2	53.8
	Fixed Asymmetric	average	7.3	18.0	8.5	33.8
		STDEV	7.9	26.3	18.0	39.0
	Israeli method	average	42.7	46.5	25.1	135.0
		STDEV	52.7	61.6	34.4	129.0
11/2004	Changing Asymmetric (EAST)	average	123.8	93.3	37.3	254.4
		STDEV	92.8	81.3	37.0	144.5
	Changing Asymmetric (WEST)	average	117.0	88.9	58.1	264.0
		STDEV	86.4	76.3	44.1	192.1
	Fixed Asymmetric	average	29.0	36.2	37.3	102.5
		STDEV	39.6	30.6	43.6	87.5
	Israeli method	average	21.6	20.0	6.7	48.4
		STDEV	31.0	22.2	35.4	50.7

5.3 Additional half tree contours

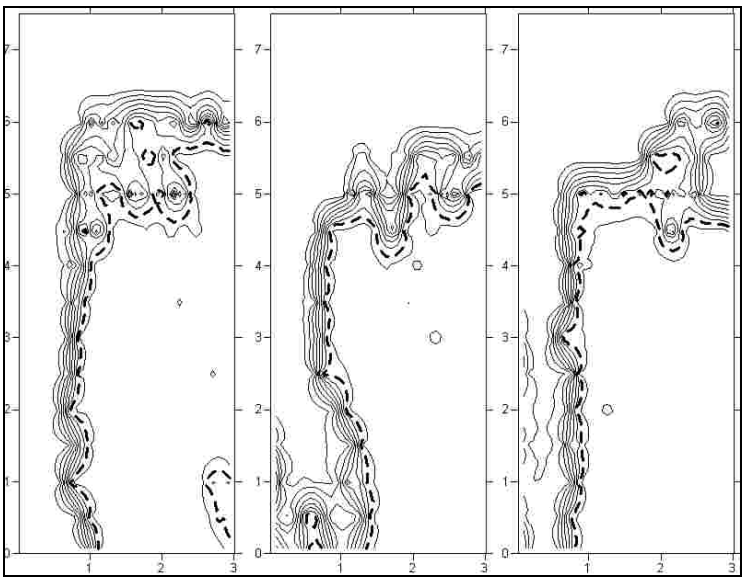

Figure 51– Contours of half-tree cross sections based on measurements done on the 7/9/2003 in ‘Shomrat’ orchard; CV. Hass; pruned hedgerow; three different cross sections from the same row.

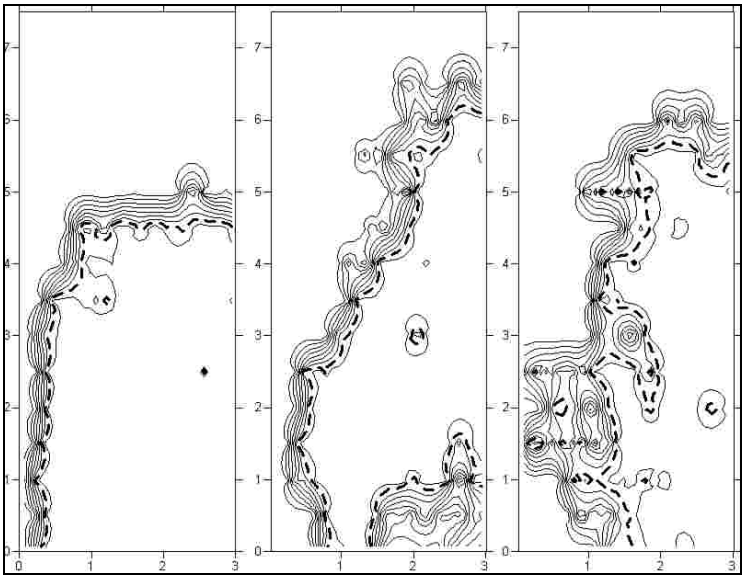

Figure 52 - Contours of half-tree cross section measurements done on the 8/9/2003 in ‘Shomrat’ orchard; CV. Hass; pruned hedgerow; three different cross sections from the same row.

5.4 ELADP Data

Table 13 – Leaf inclination data (horizontal (Nh) and vertically inclined (Nv) leave number) used to estimate ELADP. Readings taken at 'Shomrat orchard'

Tree no.	Nh	Nv	ELADP
1	10	3	5.2
2	3	2	2.4
3	5	2	3.9
4	4	2	3.1
5	9	13	1.1
6	14	3	7.3
7	4	7	0.9
8	6	11	0.9
9	7	13	0.8
10	7	10	1.1
11	8	6	2.1
12	10	6	2.6
13	6	8	1.2
14	6	4	2.4
15	11	9	1.9
16	7	8	1.4
17	7	6	1.8
18	21	13	2.5
19	10	6	2.6
20	6	6	1.6
21	15	16	1.5
22	5	5	1.6
23	6	5	1.9
24	11	6	2.9
25	15	11	2.1
26	21	12	2.7
AVERAGE			2.3
STDEV			1.4

5.5 Daily radiation penetration curves

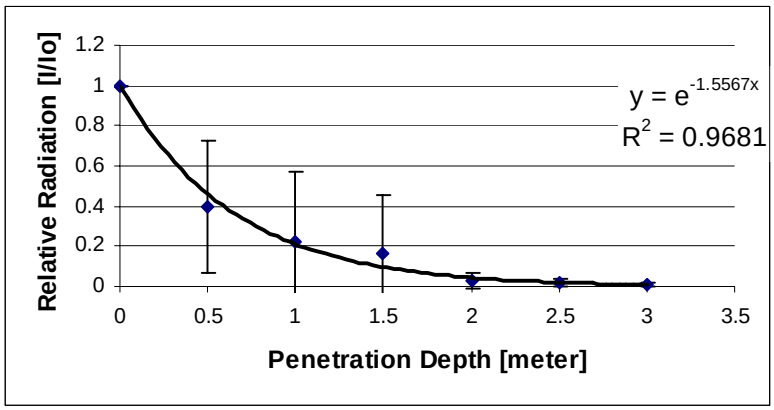

Figure 53- Relative irradiance in different depth of the canopy as measured on the 3/9/2003; 'Shomrat orchard', CV. 'Hass'.

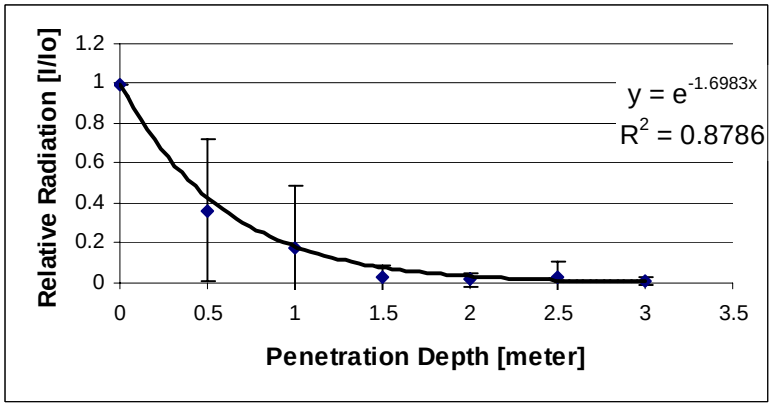

Figure 54- Relative irradiance in different depth of the canopy as measured on the 3/9/2003; 'Shomrat orchard', CV. 'Hass'.

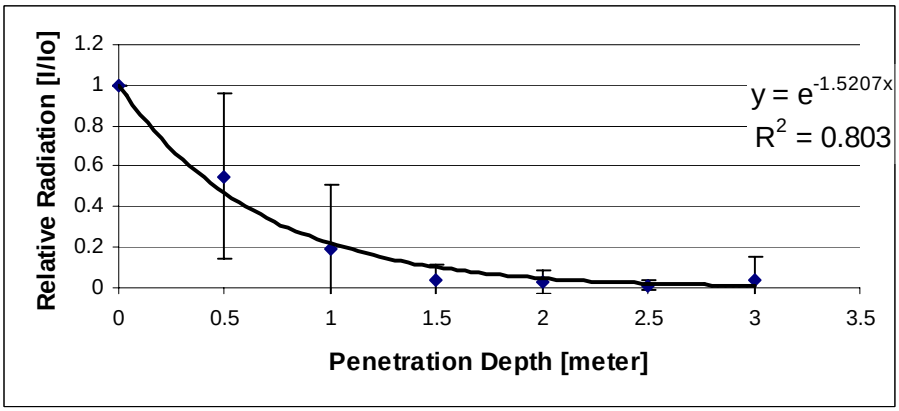

Figure 55- Relative irradiance in different depth of the canopy as measured on the 7/9/2003; 'Shomrat orchard', CV. 'Hass'.

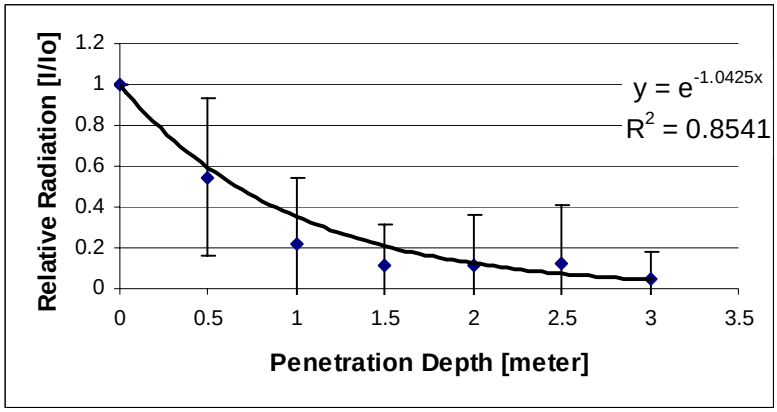

Figure 56- Relative irradiance in different depth of the canopy as measured on the 8/9/2003; 'Shomrat orchard', CV. 'Hass'.

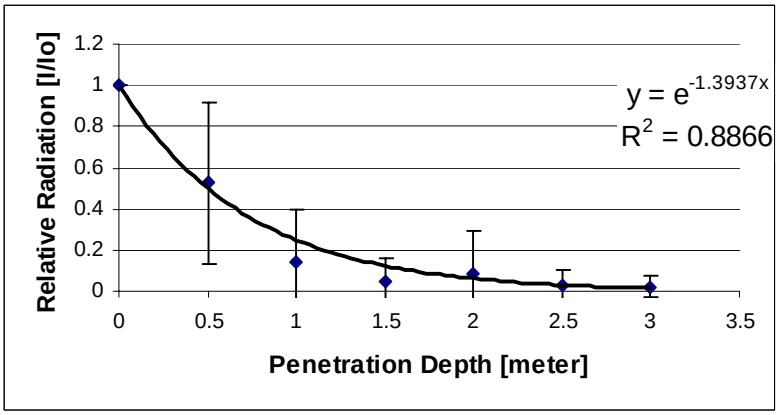

Figure 57- Relative irradiance in different depth of the canopy as measured on the 8/9/2003; 'Shomrat orchard' , CV. 'Hass'.

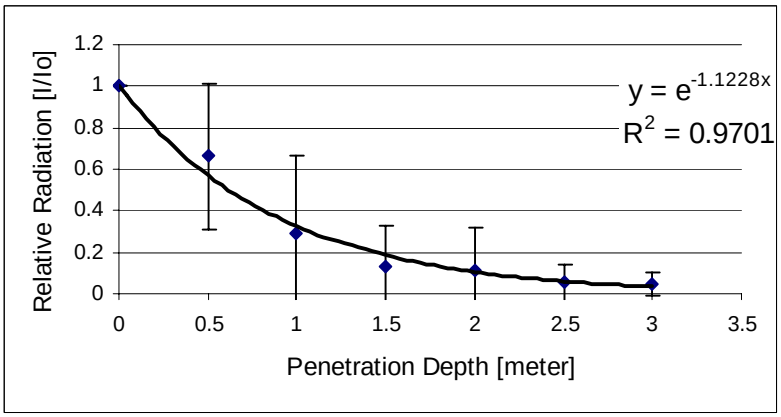

Figure 58- Relative irradiance in different depth of the canopy as measured on the 10/9/2003; 'Shomrat orchard' , CV. 'Hass'.

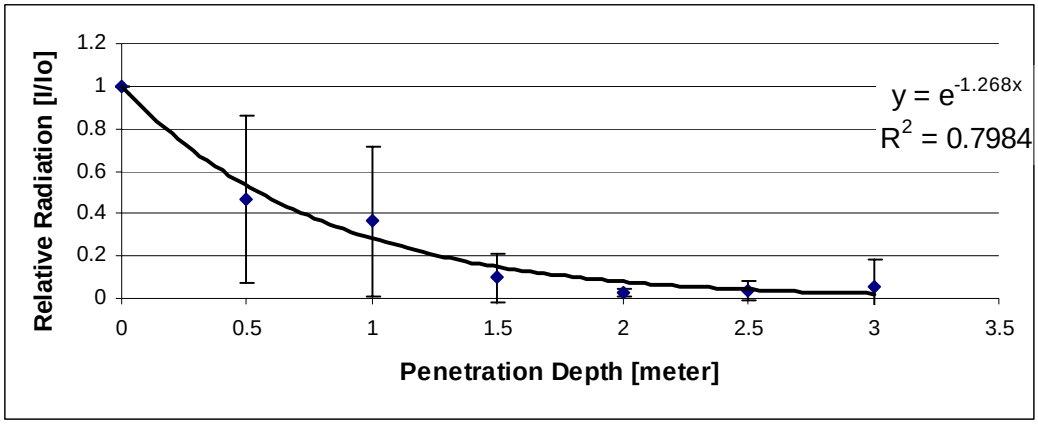

Figure 59 - Relative irradiance in different depth of the canopy as measured on the 16/9/2003; 'Shomrat orchard' , CV. 'Hass'.

5.6 Avocado photosynthetic response curves found in the literature

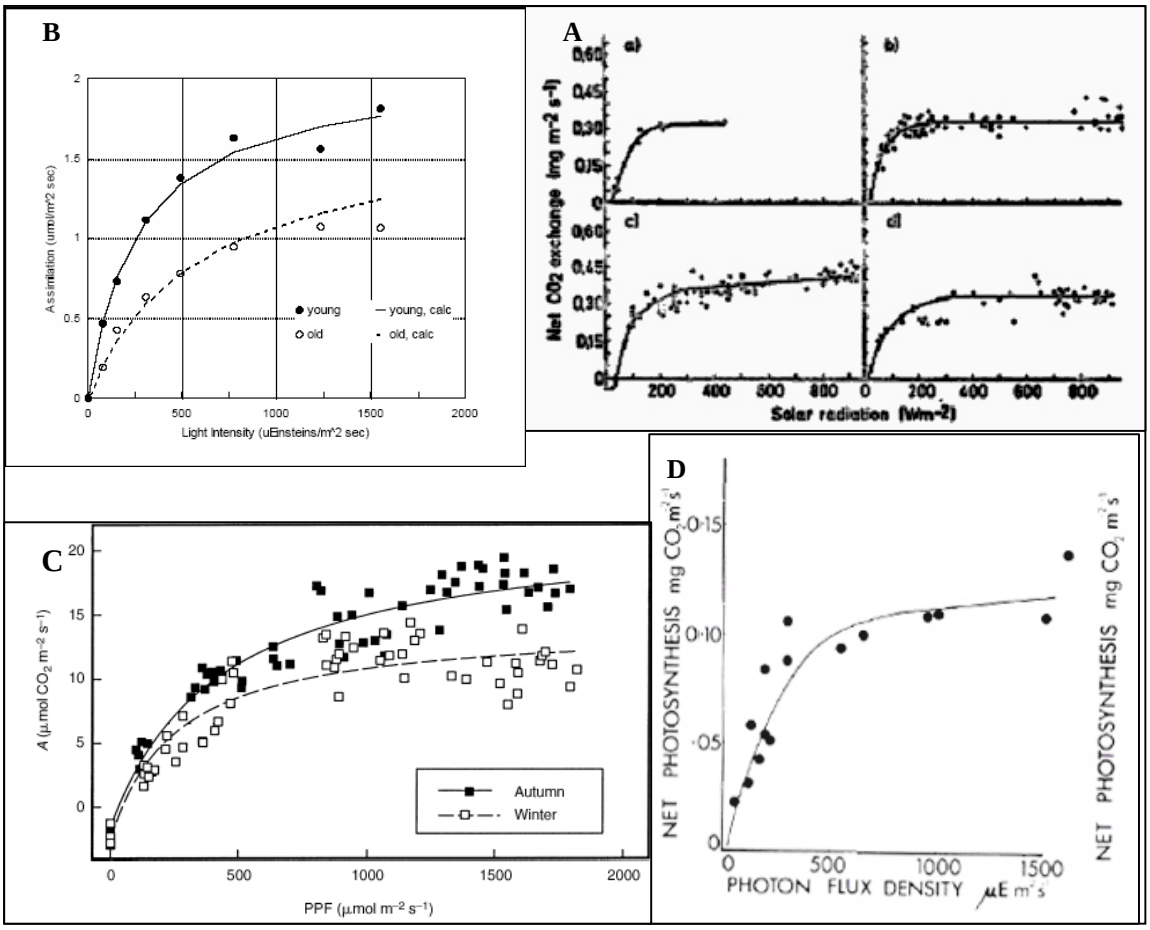

Figure 60- Photosynthetic response curves found in the literature. A-(Bower, 1978); B-(Heath et al., 2003)C-(Schaffer and Whiley, 2002); D- (Scholefield et al., 1980).

References

Adato, I. 1990. Effects of paclobutrazol on Avocado (Persea americana Mill.) cv. Fuerte. Scientia Hortic. 45:105-115.

Annandale , J. G., N. Z. Jovanovic , and G. S. Campbell. 2004. Two dimensional solar radiation interception model for hedgerow fruit trees. Agricultural and Forest Meteorology 121:207-225.

Barritt, B. 1989. Influence of orchard system on canopy development, light interception and production of third year granny apple trees. acta Horticulturae 243:121-130.

Barritt, B., C. Rom, J. Konishi, and M. Dilley. 1991. Light level influences spur quality and canopy development and light interception influences fruit production in apple. hortscience 26:993-999.

Bender, G. S., and B. A. Faber. 1999. Improving avocaodo productivity. Revista Chapingo Serie Horticultura 5:155-158.

Bergh , B. O., and E. Lahav 1996. Tree and tropical fruits. Pages 113-166 *in* J. N. Moore editor. Fruit Breeding. John Wiley & Sons.

Bower, J. P. 1978. The effects of shade and water relations in the Avocado cv. Edranol. S. Afr. Avocado Growers' Assoc. Res. Rpt. 2:59-61.

Cain , J. C. 1972. Hedgerow orchard design for most efficient interception of solar radiation .Effects of tree size ,shape ,spacing and row direction. Search Agr. 2:1-14.

Campbell, G. S. 1986. Extinction coefficients for radiation in plant canopies using an ellipsoidal inclination angle distribution. Agricultural Forest Meteorology 36:317-321.

Cohen, S., M. Fuchs, S. Moreshet, and Y. Cohen. 1987. The distribution of leaf area, radiation, photosynthesis and transpiration in a shamouti orange hedgerow orchard. Agricultural and Forest Meteorology 40:123-144.

Crane , J. H., B. Schaffer , and T. L. Davenport 1992. Rejuvenation of a mature, non-productive 'lula' and 'booth8' Avocado grove by topping and tree removal. Proc. Fla. State Hort. Soc. 105:282-285.

Friday, J., and J. Fownes. 2001. a simulation model for hedgerow light interception and growth. Agricultural and Forest Meteorology 108:29-43.

Genard, M., F. Baret, and D. Simon. 2000. A 3D peach canopy model used to evaluate the effect of tree architecture and density on photosynthesis at a range of scales. Ecological Modelling 128:197-209.

Heath, R. L., M. L. Arpaia , and M. V. Mickelbart. 2001. Avocado tree physiology- understanding the basis of productivity. california Avocado comission.

Heath, R. L., M. L. Arpaia , and M. V. Mickelbart. 2003. Avocado tree physiology- understanding the basis of productivity. california Avocado comission.

Heinicke, D. R. 1963. The micro climate of fruit trees. Proc. Amer. Soc. Hort. Sci. 83:1-11.

Hofshi, R. 1998. Dreaming in Reality. California Avocado Society Yearbook 82:137-154.

Hofshi , R. 1999a. High-Density Avocado Planting - An Argument for Replanting Trees. Subtropical Fruit News 7:9-13.
Hofshi , R. 1999b. Some economic reasons to canopy managemant. Pages 45-48 *in* H. R., editor. Avocado Brainstorming.
Jackson , J. E. 1980. light interception and utilization by orchard systems. Hort Reviews 2:208-267.
Jackson, J. E., and J. W. Palmer. 1972. Interception of light by model hedgerow orchards in relation to latitude, time of year and hedgerow configuration and orientation. J. of Applied Ecology 9:341-357.
Kohne, J. S., and S. Kremer-Kohne. 1987. Vegetative growth and fruit retention in Avocado as affected by a new plant growth regulator (Paclobutrazol). South African Avocado Growers' Association Yearbook 10:64-66.
Kohne , J. S., and S. Kremer-Kohne 1990. Results of a high density Avocado planting. South African Avocado Growers' Association Yearbook 13:31-32.
Lahav , E., B. Gefen , and D. Zemet 1971. Ttreatments and factors influencing the size of "Hass" Avocados (1968-1970). 699, Volcani Center, Orchard Division.
Meron, M., S. Cohen, and G. Melman. 2001. Tree shape and volume measurement by light interception and aerial photogrammetry. Transactions of the ASAE 43(2):475-481.
Monsi, M., and T. Saeki. 1953. Uber den lichtfaktor in den pflanzengesellschaften und seine bedentung, fur die stoffproduktion. Japan J. Bot. 14:22-52.
Monteith, J. 1973. Principles of environmental physics. E. Arnold pub.
Myneni, R., J. Ross, and g. Asrar. 1989. a review of the theory of photon transport in leaf canopies. Agricultural and Forest Meteorology 45:1-153.
Palmer, J. 1977. diurnal light interception and computer model of light interception by hedgerow apple orchards. Journal of Appllied Ecology 14:601-614.
Palmer, J. 1980. computed effects of spacing on light interception and distribution within hedgerow trees in relation to productivity. acta Horticulturae 114:80-88.
Palmer, J., and J. Jackson. 1977. Seasonal light interception and canopy development in hedgerow and bed system apple orchards. Journal of Appllied Ecology 14:539-549.
Potter, E., D. Wood, and C. Nicholl. 1996. Delta-T Devices Limited.Sun Scan Version 1.05 User Manual.
Razeto, B., L. Jose, and T. Fichet. 1992. Close Planting of Avocado. Pages 273-279 *in* Proc. of Second World Avocado Congress.
Ross, J. 1981. the radiation regime and architecture of plant stands. Dr. w junk publishers.
Schaffer , B., and A. W. whiley 2002. environmental phisyology. Pages 135-160 *in* The Avocado. CABI.
Schaffer, B., and A. W. Whiley. 2003. Environmental regulation of photosynthesis in Avocado trees-a mini review. *in* proceedings of V World Avocado Congress.

Scholefield, P. B., J. J. Walcott, P. E. Kriedemann , and A. Ramadansan. 1980. Some environmental effects on photosynthesis and water relations of Avocado leaves. Calif. Avocado Soc. Yrbk. 64:93-105.

Snijder, B., J. M. Mathumbu, and P. J. C. Stassen. 2000. Planning and managing new Avocado orchards. South African Avocado Growers' Association Yearbook 23:33-35.

Stassen , P. J. C. 1999. Planning and managing more intensive Avocado orchards. Pages 60-62 *in* R. Hofshi editor. Proceedings of Avocado Brainstorming.

Stassen , P. J. C., B. Snijder , and Z. J. Bard 1999. Results obtained by pruning overcrowded Avocado orchards. Revista Chapingo Serie Horticultura 5:165-171.

Thorp , T. G., and B. Stowell 2001. Pruning Height and Selective Limb Removal Affect Yield of Large 'Hass'Avocado Trees. Hortscience 36(4):699–702.

Thorpe , G. 1999. Avocado canopies: a New Zealand perspective. Subtropical fruit news 7:8-9.

Ward, G., and R. Shakespeare. 1998. Rendering With Radiance : The Art and Science of Lighting Visualization. BookSurge Publishing.

Ward, G. J. 1994. The radiance lighting simulation and rendering system. Pages 459-472 *in* Computer Graphics, Annual Conference Series. ACM SIGGRAPH.

Whiley , A. W. 2002. Crop managemant. Pages 231-258 *in* B. N. wolstenholme editor. The Avocado: Botany ,Production And Uses.

Whiley , w. 1994. Ecophysiological studies and tree manipulation for maximization of yield potential in Avocado (Persea americana Mill.). PhD Thesis University of Natal.

Wolstenholme , B. N. 1987. Theoretical and applied aspects of Avocado yield as affected by energy budgets and carbon partitioning. South African Avocado Growers' Association Yearbook 10:58-61.

Wolstenholme, B. N., and A. W. Whiley. 1995. Strategies for maximaising Avocado productivity: an overview. Pages 61-70 *in* Proceedings of The World Avocado Congress III.

Wolstenholme, B. N., and A. W. Whiley. 1999. Ecophysiology of the Avocado (Persea americana Mill.) tree as a basis for pre-harvest management. Revista Chapingo Serie Horticultura 5.

Woolf , A. B., I. B. Ferguson , L. C. Requejo-Tapia , and L. Boyd 1999. Impact of Sun exposure on harvest quality of 'Hass' Avocado fruit. Revista Chapingo Serie Horticultura 5:353-358.

Wunsche, J., A. Lasko, and T. Robinson. 1996. The bases of productivity in apple production systems: the role of light interception by different shoot types. journal of american society for horticulture science 121:886-893.

Zamet, D. N. 1998. On our awareness of the climatic affects of Avocado yields. California Avocado Society Yearbook 82:161-164.

Zilberstaine , M., and E. Kalusky 1999. Improving Avocado orchard yield through the use of pruning and griddling. Subtropical Fruit News 7:7-8.